

1-1-2013

Investigation Of Dopamine Dynamics In Bdnf+/- Mice Using In Vivo Microdialysis And Electrochemical Analysis Of Purine And Monoamine Molecules Using A Boron-Doped Diamond Electrode

Johnna A. Birbeck
Wayne State University,

Follow this and additional works at: http://digitalcommons.wayne.edu/oa_dissertations

Recommended Citation

Birbeck, Johnna A., "Investigation Of Dopamine Dynamics In Bdnf+/- Mice Using In Vivo Microdialysis And Electrochemical Analysis Of Purine And Monoamine Molecules Using A Boron-Doped Diamond Electrode" (2013). *Wayne State University Dissertations*. Paper 750.

**INVESTIGATION OF DOPAMINE DYNAMICS IN BDNF^{+/-} MICE USING *IN VIVO* MICRODIALYSIS
AND
ELECTROCHEMICAL ANALYSIS OF PURINE AND MONOAMINE
MOLECULES USING A BORON-DOPED DIAMOND ELECTRODE**

by

JOHNNA ANN BIRBECK

DISSERTATION

Submitted to the Graduate School

of Wayne State University,

Detroit, Michigan

in partial fulfillment of the requirements

for the degree of

DOCTOR OF PHILOSOPHY

2013

MAJOR: CHEMISTRY (Analytical)

Approved by:

Advisor

Date

DEDICATION

This work is dedicated to my parents William and Lori Courneya, my sisters Rachel Hale and Samantha Courneya, my husband Rob Birbeck, and also to the loved ones who passed before seeing me complete my work Grandma Judith Greenwood, Uncle Brendt Greenwood, Aunt Beverly Courneya, and Grandma Charlotte Courneya. Thank you for your continued support, encouragement, compassion, and love.

ACKNOWLEDGEMENTS

I would first and foremost like to thank my advisor Dr. Tiffany Mathews, for all of her advice, support, and guidance. She helped mold me into the scientist that I have become, encouraged me to try new experiments without fear, and never lost faith in me. She went above and beyond her duties as a mentor to make my time here at Wayne State University a success. To my undergraduate advisor, Dr. Judy Westrick, who believed in me from the start and encouraged me to not only get a bachelor's degree in chemistry, but to also go to graduate school. I wouldn't be here if it wasn't for her. And to my dissertation committee, Dr. Sarah Trimpin, Dr. John Santa Lucia, and Dr. Scott Bowen, thank you for your advice, comments, and support which greatly impacted my research, making it stronger and more complete.

I would graciously like to thank my lab members Dr. Kelly Bosse, Dr. Francis Maina, Dr. Madiha Khalid, for all of your help in collaboration with the BDNF projects in order to gain a more comprehensive understanding for each project. To Dr. Madiha Khalid, thank you for all of the encouragement and support as we traveled this journey together. And to my current lab members Brooke and Aaron, and past Dr. Jamie Carroll, Dr. Rabab Aoun, Stella, Katie, Chris, Joe, Michelle, Stephanie, and Doug who always kept the lab fun, interesting, and full of good times and memories.

Most importantly, I would like to thank my parents, William and Lori, and my sisters Rachel and Samantha for always being supportive and encouraging me through this journey. And lastly to my husband, Rob, thank you for listening to my presentations, your help in reading my many manuscripts for clarity, and for being my rock when I needed it most. I couldn't have done this without you. I love you always and forever.

TABLE OF CONTENTS

Dedication.....	ii
Acknowledgments.....	iii
List of Tables.....	ix
List of Figures.....	x
Abbreviations.....	xii
Contributions.....	xv
CHAPTER 1: Introduction and Overview.....	1
1.1 Neurochemistry.....	1
1.1.1 Neurotransmission.....	1
1.1.2 Dopamine.....	2
1.1.3 Adenosine.....	6
1.1.4 Dopamine and adenosine system interactions.....	10
1.1.5 Brain-derived neurotrophic factor.....	11
1.1.6 Brain-derived neurotrophic factor, the dopamine system, gender and age.....	12
1.2 Neurochemical techniques.....	13
1.2.1 Microdialysis.....	13
1.2.2 Electrochemical detection.....	18
1.2.3 Slice fast scan cyclic voltammetry.....	21
1.2.4 Locomotor activity.....	23
1.3 Research objectives.....	24

1.3.1 Objective 1: Characterization of the dopamine system in female BDNF ^{+/-} mice.....	24
1.3.2 Objective 2: Characterization of the dopamine system in aged BDNF ^{+/-} mice.....	25
1.3.3 Objective 3: Method development for the simultaneous detection of purine and monoamine molecules using a boron-doped diamond electrode.....	26
CHAPTER 2: Materials and Methods.....	28
2.1 Chemicals.....	28
2.2 Animals.....	28
2.3 Genotyping.....	29
2.4 In vivo microdialysis.....	32
2.4.1 Surgery.....	32
2.4.2 Microdialysis experiments.....	33
2.5 Slice fast scan cyclic voltammetry.....	35
2.6 Tissue content.....	37
2.7 HPLC and electrochemical detection.....	37
2.7.1 Detection of neurotransmitters using a porous carbon working electrode.....	37
2.7.2 Detection of neurotransmitters using a boron-doped diamond working electrode.....	38
2.8 Locomotor activity.....	39
2.9 Statistical analysis.....	40

CHAPTER 3: Potentiated striatal dopamine release leads to female BDNF ^{+/-} mice	
hyperdopaminergia.....	42
3.1 Introduction.....	42
3.2 Results and Discussion.....	43
3.2.1 Elevated basal striatal DA levels in female BDNF ^{+/-} mice.....	43
3.2.2 DA metabolites are not different across genotypes.....	45
3.2.3 Slice FSCV: DA release is elevated in the female BDNF ^{+/-} mice.....	46
3.2.4 Stimulated DA release via microdialysis is potentiated in the female BDNF ^{+/-} mice.....	48
3.2.5 Methamphetamine-stimulated DA release via microdialysis is potentiated in the female BDNF ^{+/-} mice.....	49
3.3 Conclusions.....	52
3.4 Materials and Methods.....	53
3.4.1 Mice.....	53
3.4.2 Microdialysis: Surgery and Experimentation.....	53
3.4.3 Slice fast scan cyclic voltammetry.....	55
3.4.4 Statistical Analysis.....	56
CHAPTER 4: Normalized striatal dopamine dynamics in aged BDNF deficient mice....	58
4.1 Introduction.....	58
4.2 Methods.....	60
4.2.1 Animals.....	60
4.2.2 Microdialysis.....	61

4.2.3 Slice voltammetry.....	62
4.2.4 Locomotor activity.....	65
4.2.5 Statistical analysis.....	65
4.3 Results.....	66
4.4 Discussion.....	74
CHAPTER 5: Simultaneous detection of monoamine and purine molecules using a boron-doped diamond electrode.....	
5.1 Introduction.....	82
5.2 Materials and Methods.....	85
5.2.1 Chemicals.....	85
5.2.2 Analytical parameters.....	85
5.2.3 Tissue content.....	86
5.3 Results and Discussion.....	87
5.3.1 Electrode Characterization.....	87
5.3.2 Mobile Phase Parameters.....	88
5.3.3 Hydrodynamic Voltammogram.....	89
5.3.4 Linearity.....	90
5.3.5 Limits of Detection and Quantification.....	92
5.3.6 Precision and Accuracy.....	93
5.3.7 Analysis of Monoamine and Purine Neurotransmitters.....	94
5.4 Conclusions.....	100
CHAPTER 6: Conclusions and Future Directions.....	
6.1 Characterization of striatal dopamine dynamics in female BDNF ^{+/-} mice....	102

6.2 Characterization of a lifelong reduction of brain-derived neurotrophic factor effects on the dopaminergic system in aged BDNF ^{+/-} mice.....	103
6.3 Simultaneous detection of dopamine and adenosine using HPLC with electrochemical detection using a boron-doped diamond electrode.....	107
References.....	110
Abstract.....	135
Autobiographical Statement.....	137

LIST OF TABLES

Table 4.1 Striatal DA dynamics compared between young (3 month) and aged (18 month) mice.....	75
Table 5.1 Figures of merit for the simultaneous detection of dopamine (DA) and adenosine (Ado) using high-performance liquid chromatography (HPLC) with boron-doped diamond (BDD) electrode.....	93
Table 5.2 Comparison of BDD electrode and carbon electrode for the detection of monoamine and purine molecules.....	97
Table 5.3 Comparison of tissue content from literature.....	99

LIST OF FIGURES

Figure 1.1 Dopamine (DA) synthesis and metabolism.....	4
Figure 1.2 The DA synapse.....	5
Figure 1.3 DA and Adenosine (Ado) synapse.....	8
Figure 1.4 Synthesis of Ado from ATP.....	9
Figure 1.5 Generation of Ado from S-adenosylhomocysteine.....	10
Figure 1.6 Schematic of a concentric microdialysis probe.....	14
Figure 1.7 Representative setup for <i>in vivo</i> microdialysis sample collection.....	18
Figure 1.8 Oxidation and reduction of DA.....	22
Figure 1.9 Schematic of a locomotor activity chamber.....	24
Figure 2.1 Representative gel electrophoresis image of genotypic identification for wildtype and BDNF ^{+/-} mice.....	32
Figure 2.2 Structure of methamphetamine (METH).....	34
Figure 3.1 Extracellular DA concentration as measured by zero-net flux.....	45
Figure 3.2 Extracellular DA metabolite levels as measured my microdialysis.....	46
Figure 3.3 DA release and uptake in the CPu of female mice as measured by slice fast scan cyclic voltammetry (FSCV).....	47
Figure 3.4 High potassium (K ⁺) stimulated DA release from the CPu.....	48
Figure 3.5 Methamphetamine (METH) stimulated striatal DA release.....	51
Figure 4.1 Monthly weights of wildtype and BDNF ^{+/-} mice.....	67
Figure 4.2 Homecage locomotor activity for wildtype and BDNF ^{+/-} mice.....	68
Figure 4.3 DA zero-net flux results in aged wildtype and BDNF ^{+/-} mice.....	69
Figure 4.4 Extracellular levels of DA and its metabolites in aged mice.....	70
Figure 4.5 Slice FSCV results of presynaptic striatal DA dynamics in aged mice.....	73

Figure 4.6 Influence of METH on striatal DA dynamics and locomotor behavior in aged mice.....	74
Figure 5.1 Schematic amperometric cell design for the boron-doped diamond electrode (BDD) and SEM image of the BDD surface.....	88
Figure 5.2 Hydrodynamic voltammogram of DA and Ado.....	90
Figure 5.3 Linear calibration curve for the oxidation of Ado and DA.....	91
Figure 5.4 Representative standard chromatogram and striatal tissue content chromatogram.....	95

ABBREVIATIONS

3-MT	3-methoxytyramine
5-HIAA	5-hydroxyindoleacetic acid
5-HT	serotonin
AADC	L-aromatic amino acid decarboxylase
aCSF	artificial cerebral spinal fluid
ADHA	attention deficit hyperactivity disorder
Ado	adenosine
ADP	adenosine diphosphate
AMP	adenosine monophosphate
ANOVA	analysis of variance
ATP	adenosine triphosphate
BDD	boron-doped diamond
BDNF	brain-derived neurotrophic factor
BDNF ^{+/-}	brain-derived neurotrophic factor heterozygous
BDNF ^{-/-}	brain-derived neurotrophic factor knockout
bp	base pairs
cAMP	cyclic adenosine monophosphate
COMT	catechol-o-methyltransferase
CPu	caudate-putamen
DA	dopamine
DAT	dopamine transporter
dNTP	deoxyribonucleotide triphosphate
dATP	2'-deoxyadenosine triphosphate
dCTP	2'-deoxycytidine triphosphate

dGTP	2'-deoxyguanosine triphosphate
DNA	deoxyribonucleic acid
dTTP	deoxythymidine triphosphate
DOPAC	3,4-dihydroxyphenylacetic acid
E _d	extraction fraction
EDTA	ethylenediaminetetraacetic acid
ENT	equilibrative nucleoside transporters
<i>f</i>	frequency
FC	frontal cortex
FSCV	fast scan cyclic voltammetry
GABA	γ-aminobutyric acid
GDNF	glial derived neurotrophic factor
GPCR	G protein-coupled receptor
HPLC	high-performance liquid chromatography
HVA	homovanillic acid
i.p.	intraperitoneal
IR	infrared
kDA	kilo Dalton
K _m	Michaelis-Menton constant
K _i	inhibition constant
L-DOPA	L-3,4-dihydroxyphenylalanine
MAO	monoamine oxidase
METH	methamphetamine
MPP ⁺	1-methyl-4-phenylpyridinium
MPTP	1-methyl-4-phenyl-1, 2, 3, 6-tetrahydropyridine

mRNA	messenger ribonucleic acid
NAc	nucleus accumbens
NDA	naphthalene-2,3-dicarboxaldehyde
NE	norepinephrine
NGF	nerve growth factor
NT	neurotrophin
NT-4	neurotrophin 4
OPA	o-phthalaldehyde
p	pulse
PCR	polymerase chain reaction
Ras	GTP binding protein
rcf	relative centrifugal force
ROS	reactive oxygen species
RNA	ribonucleic acid
SEM	standard error of the mean
SN	substantia nigra
TE	tris-EDTA
TH	tyrosine hydroxylase
TrkB	tyrosine kinase B
UV	ultraviolet
VMAT	vesicular monoamine transporter
VNUT	vesicular nucleotide transporter
V_{max}	maximum velocity
VTA	ventral tegmental area
WT	wildtype

CONTRIBUTIONS

Chapter 2: Materials and Methods

For all experiments throughout this dissertation that utilized brain-derived neurotrophic factor (BDNF) heterozygous mice and wildtype mice, in-house breeding, weaning, genotypic identifications were required. The procedures for the breeding, weaning, and genotypic analysis were performed by Kelly E. Bosse, Ph.D. and Brooke Neman. Assistance with these procedures was provided by Katie Logan, Parvejz Khan, Natasha Bohin, Andrezj Czaja, Christopher Rogalla, Michelle Colombo, Stephanie Godden, and myself. Experiments and analysis that involved slice fast scan cyclic voltammetry (FSCV) were conducted by Francis K. Maina, Ph.D. (aged mice), or Madiha Khalid, Ph.D. (female mice). I performed all experiments and analysis that involved *in vivo* microdialysis or locomotor activity.

Chapter 3: Potentiated striatal dopamine release leads to female BDNF^{+/-} mice hyperdopaminergia

In this chapter, all work done with slice voltammetry experimentation and analysis was conducted by Madiha Khalid, Ph.D. I performed all microdialysis experiments and analysis. I also performed all of the required literature search and manuscript writing, which was submitted to *ACS Chemical Neuroscience*.

Chapter 4: Normalized striatal dopamine dynamics in aged BDNF deficient mice

Francis K. Maina, Ph.D. conducted all slice FSCV experiments and analysis for the aged BDNF^{+/-} mice and their wildtype littermates. I performed all microdialysis, and locomotor activity experiments and analysis. Further help with analysis for methamphetamine locomotor activity was provided by Scott E. Bowen, Ph.D. Literature

search and manuscript writing was also conducted by myself, and is in revision to *The Neurobiology of Aging*.

Chapter 5: Simultaneous detection of monoamine and purine molecules using a boron-doped diamond electrode

I performed all mobile phase configurations, analytical parameters, tissue content analysis, as well as figures of merit calculations for this chapter. Furthermore, I wrote and performed the literature search for the manuscript which was accepted to *Analytical Chemistry*.

CHAPTER 1

Introduction and Overview

1.1 Neurochemistry

1.1.1 Neurotransmission

The brain is a complex and organized structure containing greater than 100 billion neurons, with each neuron having its own unique structure and function. Neurons are complex, with no one neuron being the same and each one being asymmetric. Although all neurons are unique from one another, they all consist of the same three major components: cell body, axon, and dendrites. The cell body, also known as the soma, is the smallest part of the neuron in terms of area and contains the nucleus and other cytoplasmic organelles. The cell body is responsible for synthesizing and processing proteins. The axon of a neuron extends out from the cell body as a thin tubular outgrowth, and it is responsible for conducting electrical impulses to the terminals. Finally, the dendrites are multiple fine outgrowths (much smaller than the axon) off of the cell body, and serve as reception sites for other synaptic contacts from nearby neurons.

The small gap (~5–10 nm) between neurons, known as the synaptic cleft, allows for chemical messengers (neurotransmitters) to diffuse across the synapse for chemical communication to occur between the neurons. Upon release from the presynaptic terminal, neurotransmitters diffuse across the synaptic cleft, bind to specific receptors on the pre- or postsynaptic terminal, and are either metabolized by enzymes, or are taken back up into presynaptic neuron by its specific transporter. For a molecule to be defined as a neurotransmitter it must meet four conditions, 1) synthesis of the molecule

in a neuron, 2) neuronal release that modulates and affects other nearby neurons, 3) exogenous application of the molecule mimics the action of the released molecule, and 4) mechanism for the removal of the molecule from the action site. The molecules that meet these conditions are known as classical neurotransmitters, and examples of the most commonly studied are the monoamines dopamine (DA), norepinephrine (NE), and serotonin (5-HT), and the amino acids glutamate and gamma-aminobutyric acid (GABA). Recently, other molecules have been classified as 'atypical' neurotransmitters because they do not meet the conditions that define classical neurotransmitters. Chemical molecules defined as 'atypical' neurotransmitters include purines adenosine (Ado) and adenosine triphosphate (ATP), and gases nitric oxide and carbon monoxide.

1.1.2 Dopamine

DA is a member of the monoamine neurotransmitter family, which includes the molecules epinephrine, NE, 5-HT, and histamine. DA is one of the most studied neurotransmitters within the brain because of its role in memory, motor behavior, motivation, reward pathways, and learning as well as playing a key role in neurological diseases and disorders such as attention deficit hyperactivity disorder (ADHD), addiction, schizophrenia, Parkinson's disease, and Huntington's disease (1-5). In the brain, DA cell bodies are located in two specific regions, the substantia nigra (SN) and the ventral tegmental area (VTA), and their axons terminate to various anterior areas of the brain. The three dominant dopaminergic pathways are the nigrostriatal, mesolimbic, and mesocortical pathways. The nigrostriatal pathway projects DA from the cell bodies in the SN to the caudate-putamen (CPu). The mesolimbic pathway carries DA from the VTA to the nucleus accumbens (NAc). Lastly, the mesocortical pathway transports DA

from the VTA to the frontal cortex. The nigrostriatal pathway is the key pathway for learning and motor control, while the mesolimbic pathway is known for its involvement in reward, motivation, as well emotions such as pleasure and aggression (2, 6).

DA is synthesized in the neuron from L-tyrosine in a two-step process (Figure 1.1). L-Tyrosine is hydroxylated by tyrosine hydroxylase (TH), the rate-limiting step, to form L-dihydroxyphenylalanine (L-DOPA), which is converted to DA by L-aromatic amino acid decarboxylase (AADC). After the formation of DA, it is packaged into storage vesicles by the vesicular monoamine transporter (VMAT), making DA readily available for rapid release in response to an action potential. Upon release into the synaptic cleft, DA has a variety of fates that include binding to DA pre- and postsynaptic receptors, being recycled via the DA transporter (DAT), or diffusing out of the synaptic cleft into the extracellular space. The DA transporter is a 12-transmembrane protein that brings DA back into the neuron through an energy dependent mechanism requiring co-transport of two Na^+ ions and one extracellular Cl^- ion. The presence of the DAT on a neuron indicates that the neuron is a dopaminergic neuron. Once DA is in the cytosol, DA is repackaged by VMAT into vesicles where it is readily available for release (Figure 1.2)

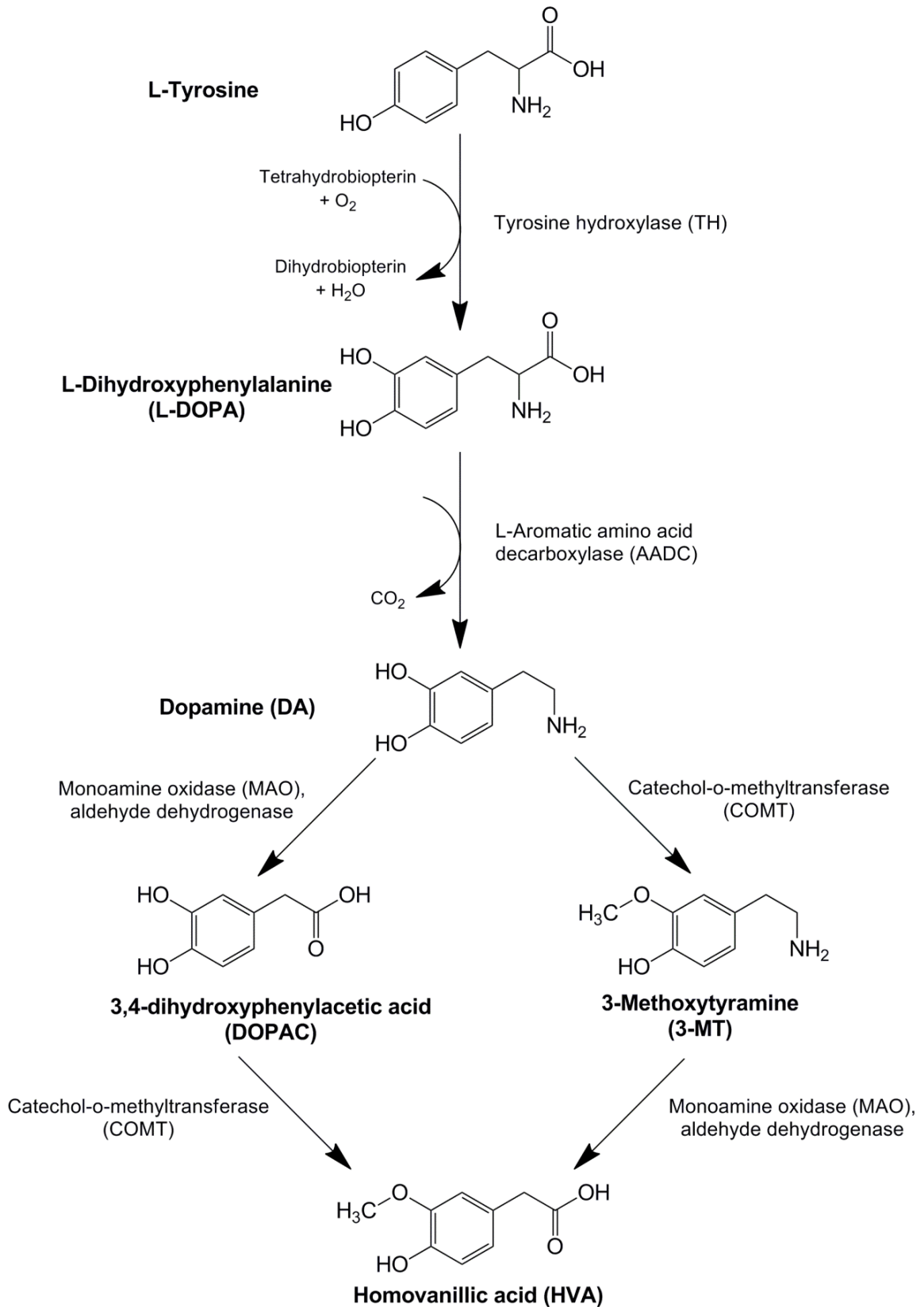


Figure 1.1 DA synthesis and metabolism.

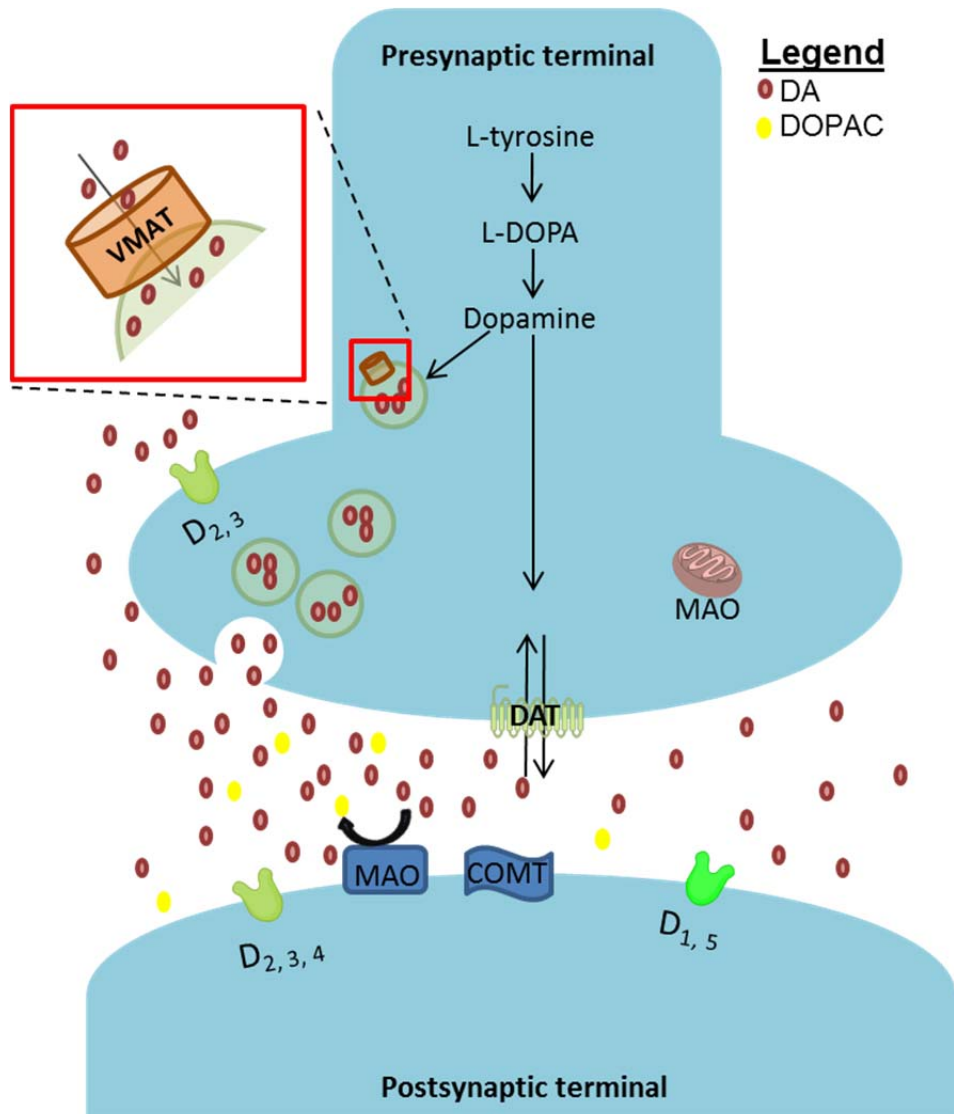


Figure 1.2 The DA synapse. DA is synthesized in the presynaptic terminal where it is packaged into vesicles by VMAT. Upon an action potential DA is released from the vesicles into the extracellular space where it can be metabolized by MAO or COMT, be brought back into the presynaptic terminal by DAT, act upon DA pre- and postsynaptic DA receptors, or diffuse out of the synaptic terminal.

Metabolism of DA is one method for decreasing extracellular DA, and the enzymes that are responsible for DA metabolism are monoamine oxidase (MAO) and catechol-*o*-methyltransferase (COMT). MAO degrades DA by cleaving the amine group and adding a carboxylic acid group in its place, while COMT methylates the hydroxyl group meta to the ethylamine group. When DA is metabolized in a stepwise fashion,

MAO degrades DA to 3, 4-dihydroxyphenylacetic acid (DOPAC), and then COMT acts upon DOPAC to form homovanillic acid (HVA) (Figure 1.1). Alternatively, COMT acts directly on DA to form 3-methoxytyramine (3-MT), which MAO can degrade to HVA (Figure 1.1).

Upon DA release into the synaptic cleft, the primary role of DA is to send a chemical message from one neuron (presynaptic) to a receiving neuron (postsynaptic). To date, there are five known DA receptors that belong to a family of seven transmembrane G-protein coupled receptors (GPCRs). These DA receptors are separated into two groups: DA D₁-like receptors and the D₂-like receptors. The D₁-like receptors include receptors D₁ and D₅ and are coupled to the stimulatory G_s protein that stimulates adenylyl cyclase, which activates signals to second messengers such as cyclic adenosine monophosphate (cAMP). The D₂-like family includes D₂, D₃, and D₄ receptors that are coupled to the inhibitory G_{i/o} protein, inhibiting adenylyl cyclase. When DA receptors are located on a presynaptic DA neuron, they are referred to as autoreceptors. In essence, DA autoreceptors are constantly monitoring the extracellular environment and depending on the extracellular DA levels, activation of the autoreceptor can either induce or inhibit DA release. For instance, activation of DA D₂-like receptors has been known to decrease the release of DA from the presynaptic terminal by a feedback inhibition mechanism (7, 8).

1.1.3 Adenosine

Although classical neurotransmitters were defined strictly as acetylcholine, monoamines, and amino acids, improvements on detection technologies through instrumentation development has led to the discovery of numerous other biologically

relevant molecules and measured on a routine basis. Neurotransmitters that do not fall into the classical neurotransmitter group are referred to as atypical neurotransmitters. Members of the purine family have long been recognized as important biological molecules, particularly in the role of energy metabolism. Adenosine (Ado) has long been considered a neuromodulator and most recently has been described as an atypical neurotransmitter (2). Ado is a member of the purine family, which includes molecules such as adenosine monophosphate (AMP), adenosine diphosphate (ADP), and adenosine triphosphate (ATP). Molecules within the purinergic system are often characterized as intracellular signaling molecules or as the primary building blocks to RNA and DNA. As a result few techniques have been developed for sensitive quantification of these molecules, particularly in terms of their extracellular concentration (9). Despite the classification as predominantly intracellular molecules, there is increasing evidence that many of these purine molecules, such as Ado, are key extracellular signaling molecules (10-12). As an intracellular and extracellular signaling molecule, determining Ado's extracellular concentration is critical to understanding how Ado behaves as an extracellular signaling molecule.

A debate throughout the literature is *exactly* how Ado is released from the neuronal cells. One mechanism of extracellular Ado release into the synaptic cleft is by the fast conversion of ATP to Ado. Cytosolic ATP is packaged into vesicles by the vesicular nucleotide transporter (VNUT: Figure 1.3) in a similar fashion as classical neurotransmitters (e.g. DA) (13). Upon neuronal stimulation, ATP is released from the neuron into the synaptic cleft where ecto-nucleotidases degrade ATP to produce ADP, and henceforth degrade ADP to AMP. AMP is degraded by ecto-5'-nucleotidase to

generate Ado (Figure 1.4). Whether intra- or extracellularly, the breakdown of ATP to Ado is proposed to be completed in less than one second (2). Additionally, a small portion of Ado is also generated through the metabolism of S-adenosylhomocysteine (Figures 1.3 and 1.5) (14-17). Cytosolic Ado is then released into extracellular space by equilibrative nucleoside transporters (ENTs).

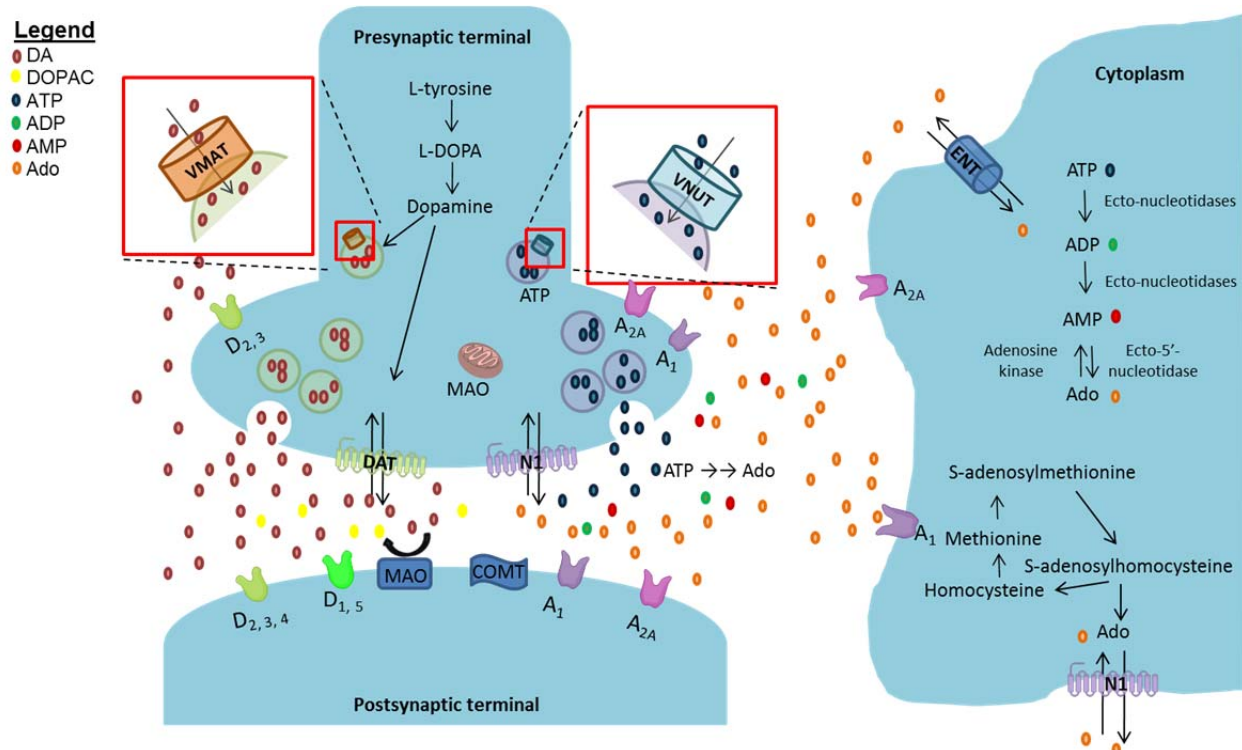


Figure 1.3 The DA and Ado synapse. ATP in the presynaptic neuron is packaged into vesicles via the VNUT, and is released by an action potential into the synaptic cleft. Once ATP reaches the extracellular space, ecto-nucleotidases degrade ATP to Ado. Intracellular Ado is formed by two mechanisms, degradation of ATP to Ado, and by the degradation of S-adenosylhomocysteine.

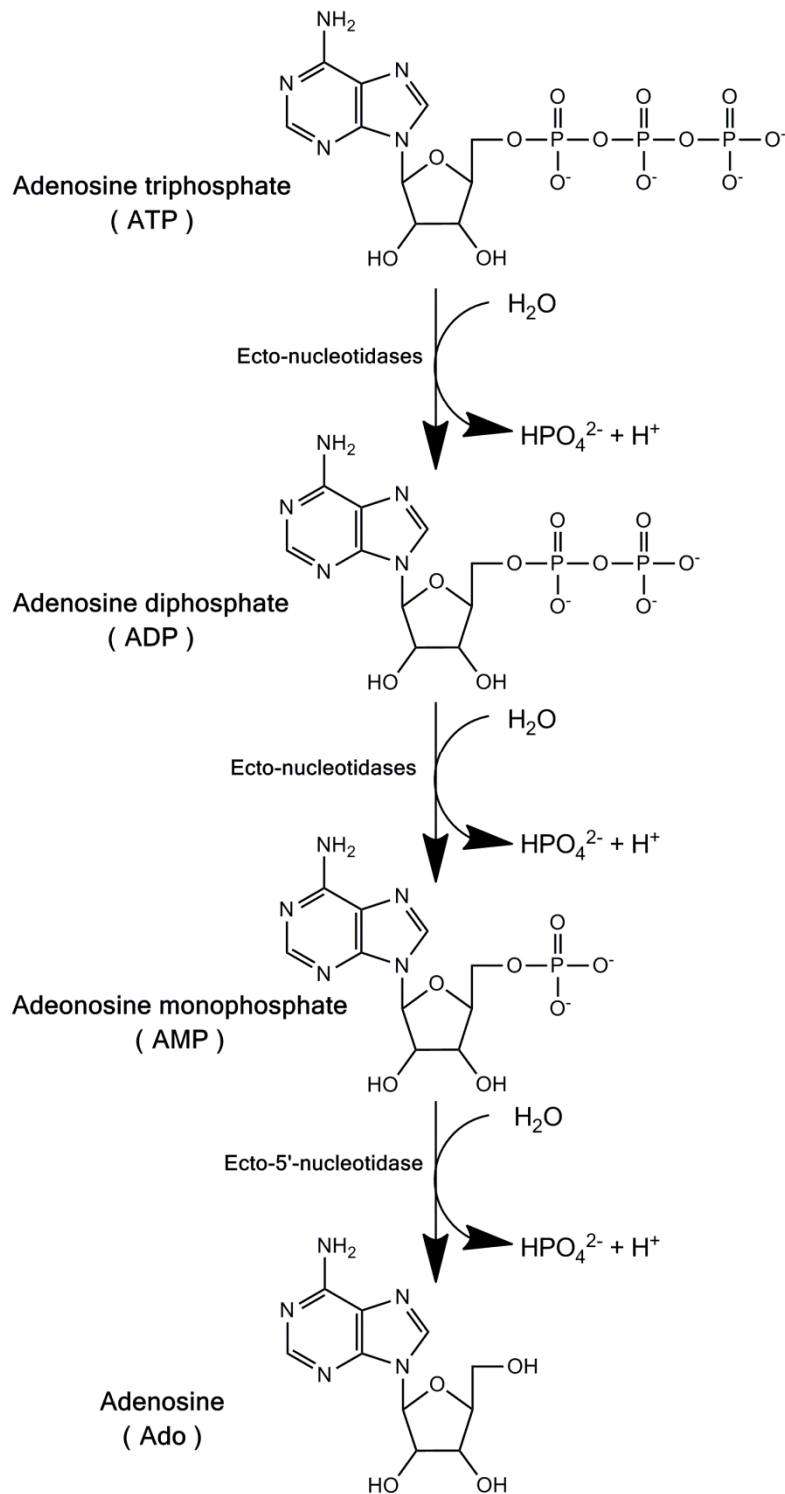


Figure 1.4 Synthesis of Ado from ATP. ATP and ADP are degraded by ecto-nucleotidases or by hydrolysis with water to form ADP or AMP, respectively. The conversion of Ado is achieved by AMP being degraded by ecto-5' nucleotidase.

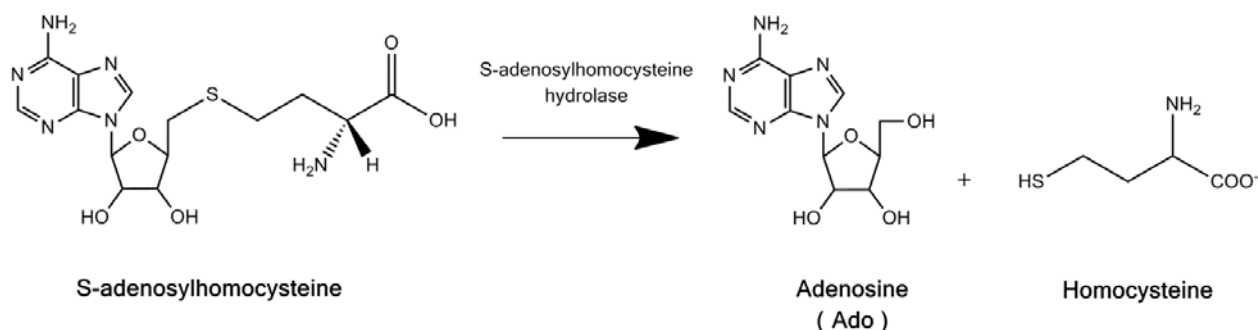


Figure 1.5 Generation of Ado from S-adenosylhomocysteine. S-adenosylhomocysteine is hydrolyzed by S-adenosylhomocysteine hydrolase to form Ado and homocysteine.

1.1.4 Dopamine and adenosine system interactions

The DA and Ado systems appear to be similarly intertwined with respect to their receptors. DA has two families of receptors; D₁-like and D₂-like, while purine P1 receptors (also known as Ado receptors) have at least four distinct subtypes: A₁, A_{2A}, A_{2B}, and A₃. Ado A₁ (coupled to G_i) and A_{2A} (coupled to G_s) receptors are ubiquitous throughout the brain. The largest densities of A_{2A} receptors are concentrated in the dorsal striatum and NAc, which are highly innervated via the DA system. In the dorsal striatal complex, the D₂ and A_{2A} receptors have reciprocal interactions (2, 18). For example, A_{2A} agonists appear to inhibit the D₂ receptor and invoke behaviors similar to D₂ antagonists (2). The ability of purine receptors to evoke DA-like behaviors has prompted the investigation of specific A_{2A} antagonist as possible therapeutic treatment for Parkinson's disease (2). Parkinson's disease is characterized by a loss of more than 80% of dopaminergic neurons. Dopaminergic therapies are used to treat Parkinson's disease such as treatment DA precursor L-DOPA, which attempts to restore dopaminergic function. However, there are limitations to L-DOPA treatment such as dyskinesia, hallucinations, on-off effects, and treatment with L-DOPA becomes less efficacious the longer it is administered (19). As a result, researchers are trying to

discover alternative therapies such as modulating the dopaminergic system indirectly through other neurotransmitter systems. A_{2A} antagonists reverse the motor effects associated with Parkinson's disease, and appear to do so without dyskinesia, a predominant side effect from L-DOPA treatment (20).

1.1.5 Brain-derived neurotrophic factor

The classical belief was that neurons communicate with one another by small molecules like neurotransmitters. However, within the last few decades it has been recognized there are numerous molecules that can influence neurons such as gases like carbon dioxide or nitric oxide or proteins such as neurotrophic factors. Neurotrophins are known for their trophic properties of supporting neuronal cell growth, differentiation, and survival. Brain-derived neurotrophic factor (BDNF), a 27 kDa protein, was first discovered in 1982, and belongs to the neurotrophic family, which includes the neurotrophins nerve growth factor (NGF), neurotrophin-3, neurotrophin-4 (NT-4), and glial-derived neurotrophic factor (GDNF) (21). Of these neurotrophic factors, BDNF is most abundant in the brain and appears to be essential in the early development of the brain (22, 23). BDNF mediates its signaling through its receptor tyrosine kinase B (TrkB), and the TrkB receptors are expressed in DA rich regions such as the striatum, SN, and VTA (24). To better understand BDNF's role in the brain, BDNF knockout mice were developed, but mice that completely lack (BDNF^{-/-}) cannot survive 21 days after birth, highlighting the importance of BDNF in species survival (22, 25). BDNF heterozygous (BDNF^{+/-}) mice developed by Ernfors and colleagues have a 50 % reduction in both BDNF protein and mRNA levels, and have no phenotypic differences when compared to their wildtype littermates (25).

1.1.6 Brain-derived neurotrophic factor, the dopamine system, gender, and aging

With ~13% of the American population over the age of 65, it is becoming increasingly important to understand the aging process and the diseases that are associated with having a higher incidence in the elderly population such as Parkinson's and Alzheimer's disease (2010 Census). Since Parkinson's disease mainly affects the dopaminergic system, considerable attention has been given to DA. It is well known that other molecules or proteins may contribute to or play a role in the development and progression of Parkinson's disease. Besides DA, one molecule that has garnered particular attention with respect to Parkinson's disease is BDNF. Postmortem studies in Parkinson's disease patients brain cultures show that BDNF mRNA expression is significantly reduced in DA neurons in the SN pars compacta (26). Other postmortem studies corroborate this reduction in mRNA expression as BDNF protein levels are decreased in the striatum of Parkinson's disease patients compared to non-Parkinson's patients (27). One of the main reasons for interest in BDNF expression and levels with Parkinson's patients lies with its interactions with DA. Many studies have alluded to BDNFs importance in protecting the dopaminergic system since exogenously applied BDNF is protective prior to a neurotoxic insult. Thus, BDNF administration maintains the viability of DA neurons in the striatum (26, 28-30). For example, an *in vivo* infusion of BDNF increases DA release and enhances DA turnover (31, 32). While a reduction in endogenous BDNF correlates to a decrease in DA D₃ receptor expression in DA rich brain regions such as the NAc and CPu (33). Furthermore, autoradiography from postmortem Parkinson's disease tissue showed a reduction in DA D₃ receptor expression (34). Taken together, there appears to be a complex relationship between

BDNF and DA, and a dysregulation in one or both systems may increase susceptibility to Parkinson's disease.

The risks of developing a particular neurological disease and/or disorder appear to be different in men and women. For example, men are ~1.5 times more likely to develop Parkinson's disease compared to women (35). These susceptibility differences in developing a particular neurological condition with respect to gender have been linked to a dysregulation of DA and BDNF, as well as estrogen (36-38). Unfortunately, to date few animal studies have fully characterized the effect of low endogenous BDNF levels on the DA system with respect to gender hormones such as estrogen and testosterone.

1.2 Neurochemical techniques

1.2.1 Microdialysis

Microdialysis is an *in vivo* sampling technique based on diffusion where extracellular neurotransmitters diffuse down their concentration gradient towards the microdialysis probe. Once the extracellular neurotransmitters are collected, the next step is to analyze them to determine their extracellular levels in a given brain region. There are numerous geometries of microdialysis probes, which are often chosen depending on the tissue that will be sampled. For neurochemical measurements, concentric probes are most commonly used since they are small in length (1–2 mm) and diameter (240–350 μm), allowing for them to be easily, and accurately placed into a specific brain region of interest for analysis (39, 40). The perfusate, which is a physiological buffer resembling the fluid in the extracellular space (artificial cerebral spinal fluid, aCSF) is perfused continuously through the inlet of the probe (Figure 1.6).

Dialysate samples are collected from the outlet line where the dialysate sample contains the neurotransmitters of interest. The microdialysis probe is made of a semi-permeable membrane that allows small molecules (< 6 kDa in our experiments) to flow down their concentration gradients and into the probe.

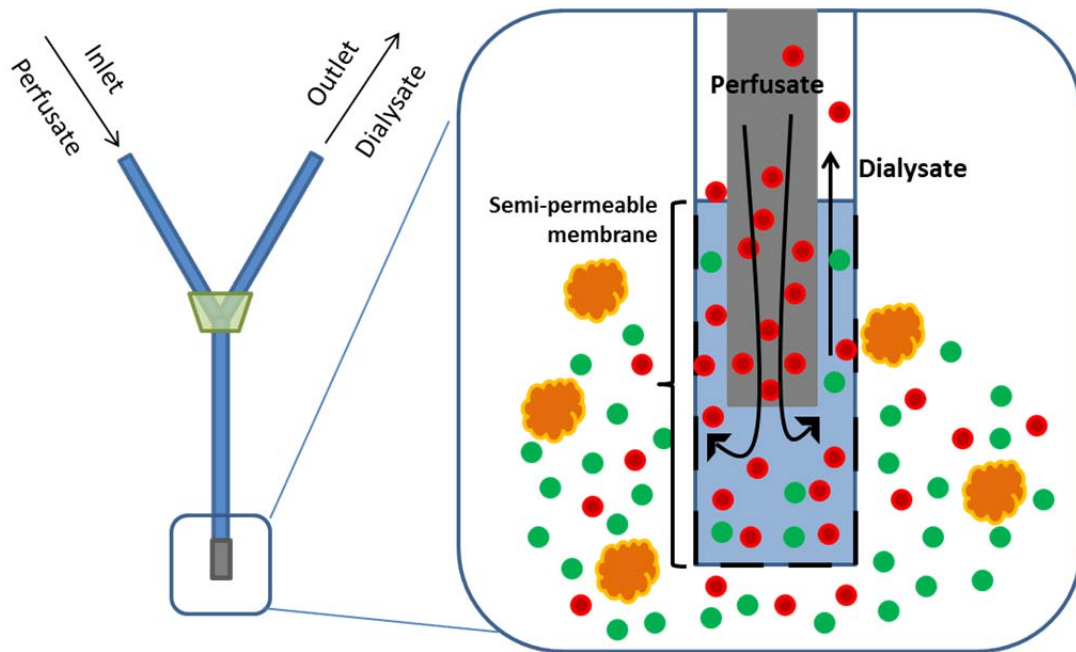


Figure 1.6 Schematic of a concentric microdialysis probe with enlarged image of semi-permeable membrane.

There are numerous methodological experiments that can be performed with the microdialysis probe that ultimately depends on the type of data the researcher is interested in collecting. The most common method using a microdialysis probe is known as conventional microdialysis, where the experimenter examines the dialysate directly with no modification to the sampling technique (41). However, a limitation of the conventional method is that it underestimates the extracellular neurotransmitter levels. This is because the microdialysis probe is not recovering 100% of the analyte of interest from the brain, only a small percentage. Recovery from the microdialysis probe is influenced by multiple parameters such as perfusion flow rate, sample volume, and

temporal resolution capabilities. Recovery is defined as relative recovery or absolute recovery, where relative recovery is the concentration of the analyte in the dialysis sample divided by the concentration of the sample media, while absolute recovery pertains to the total analyte mass during the collection period (42). For example, recovery can be altered as a result of changes in flow rate, where the flow rate increases, the sample volume increases, while the time required to collect the sample is reduced. However, when increasing the flow rate, the relative recovery of the analyte is significantly reduced, which is a result of depleting the analyte of interest in the extracellular space near the dialysis probe, while the absolute recovery increases. Since the analyte in the extracellular space is being swept away at a greater rate, there is not adequate enough time to replenish the analyte of interest, and thus reducing the relative recovery. Yet, reducing the flow rate has its own limitations such as longer collection times making analysis slower and decreased temporal resolution. Therefore, a balance between flow rate and adequate sample volume for the analytical detection technique must be made while providing a reasonable amount of time to collect a physiologically relevant sample.

Retrodialysis is an alternative microdialysis method that uses the probe to deliver an analyte or drug to the brain region of interest. The method of zero-net flux is a retrodialysis method that delivers various known quantities of an analyte of interest (e.g. DA), thus enabling one to estimate 'true' basal levels. The zero-net flux method uses linear regression analysis with the measurements from amount of DA entering the probe (DA_{in}) and the amount of DA leaving the probe (DA_{out}), and the point where the flux of DA leaving and entering the probe is deemed the point at which there is zero-net

diffusion across the probe and mathematically this is observed when the line crosses the x -axis. The point at where no diffusion is occurring through the probe indicates the 'true' concentration (or basal, where it has been corrected) at which the analyte is found in that specific region. Microdialysis itself is an analytical technique that separated molecules based on molecular weight, where molecules less than a particular cut-off weight can easily pass through the probe, while those with a larger molecular weight are excluded. However, microdialysis by itself does not quantitate the neurotransmitter levels in a sample. Therefore, the type of instrumental analysis is key for the proper separation, and detection of neurotransmitters from a dialysis sample. Analysis of dialysate samples begins with a separation component using high-performance liquid chromatography (HPLC) or capillary electrophoresis and then detected either by electrochemical detection, mass spectrometry (MS), or fluorescence detection (42).

An advantage of microdialysis sampling is its ability to collect a diverse number of analytes from the brain, and when coupled to the appropriate analytical method can separate and detect specific neurotransmitters and achieve high sensitivity and selectivity. However, as with all methods, there are limitations with using microdialysis such as spatial and temporal resolution. Spatial resolution of the dialysis probe is dependent on the probe's size. In this set of work, a probe with a length of 2 mm and a diameter of 240 μm was used. Since the brain is a heterogeneous structure with discrete anatomical brain regions, the size of the microdialysis probe limits which regions can be sampled. In order to achieve desirable spatial resolution in a mouse brain, the microdialysis probe must be small enough to sample a region of interest, which can be less than 0.5 mm^3 (42). In the work throughout this dissertation,

commercially available probes are used, which limits miniaturizing the probe to examine specific sub-regions that may be too small to sample from with a commercially available probe. There would be numerous advantages if microdialysis probes could be further miniaturized. Currently, the Kennedy group is fabricating sampling probes with of the following dimensions: 70 μm wide by 85 μm thick by 11 mm long, which would decrease the amount of tissue damage, and may be suitable for other types of analysis such as dialysis samples from cells in a culture (43). The second parameter that can be improve is temporal resolution, which is the time it takes to collect the dialysate sample volume from the brain and can be adjusted by varying the flow rate of the perfusate. Fast flow rates can increase the amount of samples collected, but as state previously can deplete the surroundings of the analyte of interest. Slow flow rates increase sample collection time, so a delicate balance must be met.

Prior to the microdialysis experiment, mice undergo surgery to implant a guide cannula targeting the brain region of interest (e.g. CPu or NAc), and upon recovery (3–4 hours later) from surgery a microdialysis probe is implanted and flow of aCSF commences through syringe pumps. An equilibration period of 12–16 hours occurs before any sampling takes place. Low flow rates of 0.5–2.0 $\mu\text{L}/\text{min}$ are used for delivering the aCSF to the brain as well as sampling from the brain. Microdialysis allows samples to be collected from an intact system since the mice are allowed to freely move within their container (Figure 1.7). Samples are collected every 10–20 min, and are separated off-line by manual injection of the samples onto the HPLC coupled to electrochemical detection.

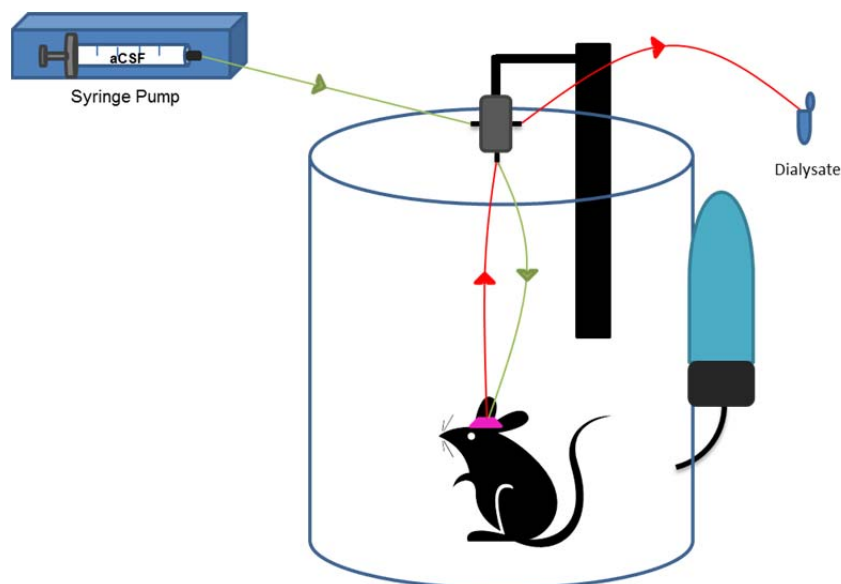


Figure 1.7 A representative setup for *in vivo* microdialysis sample collection. After microdialysis surgery, the mouse is placed in a small cage where he/she has free access to food and water. The syringe pump is continuously perfusing aCSF through the microdialysis inlet at a low flow rate (inlet lines are represented by green lines). The dialysate sample containing the neurotransmitters of interest is collected through the red lines into a microcentrifuge tube. The inlet and outlet lines are connected to a swivel that allows the mouse free movement in his/her cage.

1.2.2 Electrochemical detection

The most common method used for distinguishing neurotransmitters from one another is using HPLC, while the detection method used is typically dependent of the class of neurotransmitter being analyzed. For example, monoamines are typically detected with electrochemical detection, while amino acids are detected with fluorescence or UV, purines with UV, and peptides with MS (44-47). In this dissertation, the focus lies on monoamine and purine molecules, both of which are known to be electrochemically active.

Electrochemical detection is based on a molecules ability to be oxidized or reduced. The electrode materials used for the oxidation/reduction of specific molecules can be gold, silver, platinum, carbon, or boron-doped diamond (BDD). When using these electrodes as the detection element with an HPLC, the design of these

electrochemical cells can be coulometric or amperometric. In a coulometric cell design, a porous type electrode (which is most commonly carbon) oxidizes 100% of the analyte since the analyte passes directly through the electrode. With an amperometric cell design, a disc type electrode is utilized, and only ~10% of the analyte is oxidized because the solution typically approaches the electrode surface at a 90° angle. For coulometric cells, the advantage and disadvantage lie in the fact that the electrode oxidizes 100% of the analyte, and for some samples, complete oxidation of the mobile phase or matrix passing through the electrochemical cell can create large background noise making it difficult to quantify the analyte. Since amperometric cells oxidize a small percentage of the mobile phase matrix, they are less likely to experience large background noise. Disadvantages with the amperometric cell design lie with the sensitivity of the detection of an analyte. Depending on the surface material of the electrode, it is possible that a sample containing a low concentration of the analyte of interest may not be detected because not enough of the sample matrix comes in contact with the electrode surface. To mediate this, cross-flow geometries of the cell design are taken into consideration, and a cross-flow design in which the sample passes perpendicular across the working electrode is the preferred choice in order to achieve a uniform potential across the electrode surface.

An advantage of using electrochemical detection to detect neurotransmitters is that only a few families have electroactive compounds such as the monoamines, amino acids (through derivatization steps), and purines. Electrochemical detection provides the sensitivity and selectivity to measure neurotransmitters in relatively low concentrations ranging in the low pM to high nM. Typically for monoamine analysis, a carbon electrode

surface is used while for the detection of purine molecules, which generally have high oxidation potentials ($> +1000$ mV versus Ag/AgCl reference) a BDD electrode is utilized (48). Carbon electrodes are not used to detect purine molecules because they often cannot reach the high potentials to detect the purine molecules, when higher potentials are used they cause a large increase in the amount of background noise and eventually oxidize the carbon electrode surface (49). The BDD electrode is a relatively new electrode material, and is currently only commercially available as an amperometric cell design (50). Advantages of using the BDD electrode is its higher working potential range, decreased background noise, electrochemical stability due to diamond surface coordination, insensitivity to dissolved oxygen, and is less susceptible to electrode fouling (51, 52).

For separation and detection of monoamines from microdialysis dialysates, samples were collected and manually injected onto the HPLC and detected using a coulometric porous carbon electrode or an amperometric BDD electrode versus a palladium reference. A specific potential was applied to the porous carbon working electrode relative to the reference electrode, and the resulting current is recorded at the working electrode. The oxidation current measured is proportional to the analyte concentration (Equation 1.1). This calculation is mediated by Faraday's law, which Q is the number of Coulombs, N is the number of moles, n is the number of electrons, and F is Faradays constant (9.65×10^4 C/eq).

$$Q = nFN \quad (1.1)$$

Lastly, HPLC with electrochemical detection can also be used to measure tissue levels of monoamine and purine molecules in the brain. In tissue content analysis,

brains are dissected into specific anatomic regions and neurotransmitter tissue content levels are evaluated. The primary difference between microdialysis and tissue content is that tissue content measures predominantly intracellular neurotransmitter levels, which can be upwards to 100-fold times higher than extracellular levels. Taken together, both intra- and extracellular tissue content levels can be measured using HPLC coupled to electrochemical detection.

1.2.3 Slice fast scan cyclic voltammetry

Fast scan cyclic voltammetry (FSCV) is an electrochemical technique that can be used *in vivo* or *in vitro* to investigate changes in release and uptake of specific neurotransmitters in the brain (53). In *in vitro* FSCV (which from this point on will be referred to as *slice* FSCV), DA is released from a coronal brain slice by electrical stimulation. Stimulation is one of the experimental parameters in FSCV that differs from microdialysis, where no stimulation is required to measure extracellular DA levels. Although stimulation is required for slice FSCV, it must be made clear that basal DA levels are not being measured, instead, stimulated DA release. DA detection is achieved by applying a voltage to a carbon fiber microelectrode. Specifically, a triangle waveform is applied to the carbon fiber microelectrode with an initial potential of -400 mV. The voltage is quickly ramped up linearly to +1200 mV, and then linearly decreased back down to -400 mV, versus a Ag/AgCl reference electrode at a scan rate of 400 V/s. It takes ~9.3 ms to complete the triangle waveform which is repeated every 100 ms. DA is oxidized to DA-*o*-quinone at a potential of ~ +600 mV (Figure 1.8), and DA-*o*-quinone is reduced to DA at ~ -200 mV during the reverse scan. The oxidation and reduction of

DA and DA-*o*-quinone occurring at the electrode surface generates a current, which is converted to concentration after electrode calibration.

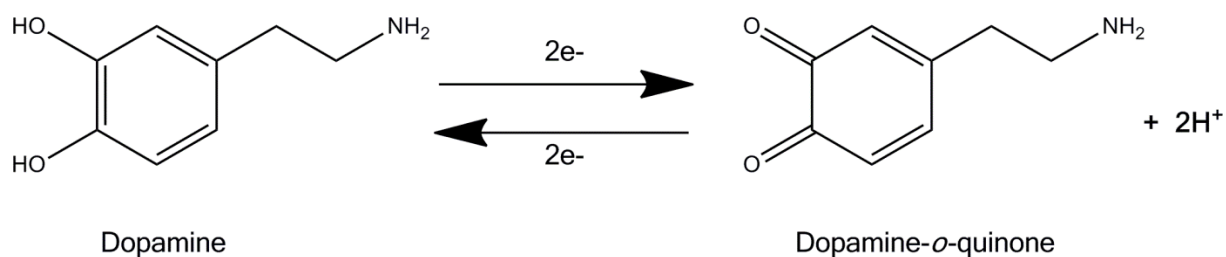


Figure 1.8 Oxidation of DA to DA-*o*-quinone.

FSCV is considered a complementary technique to microdialysis because it has excellent temporal resolution with the ability to measure DA release and uptake on a sub-second time scale. Moreover, the spatial resolution in FSCV is improved compared to microdialysis since the electrode is smaller with a diameter of 7 μm (versus a 240 μm diameter with a microdialysis probe) and a length of ~150–200 μm (versus a length of 1–2 mm with a microdialysis probe). As a result of the carbon fiber microelectrodes small size, the electrode can be inserted into discrete brain regions of interest (e.g. ability to discriminate between the NAc core and shell) in the brain causing minimal tissue damage. Typically an electrode without a separation component can measure one to two analytes at a time (54, 55). Despite the limited number of analytes that can be detected at the electrode surface, voltammetry provides good chemical selectivity as the location of the oxidation and reduction peaks on a voltammogram are unique for each analyte, providing a ‘fingerprint’ to identify the neurotransmitter of interest. An exception to this ‘fingerprint’ is with respect to DA and NE since they have similar structures, their oxidation and reduction peaks are very similar. However, NE is not the predominant neurotransmitter in brain regions with high DA innervation. An issue with making measurements in slices or *in vivo* with carbon fiber electrodes, is that the

electrode surface is always changing as molecules are being adsorbed to the surface, which can lead to fouling and an overall decrease in the sensitivity of the electrode. To circumvent the fouling problems associated with carbon fiber electrodes, BDD microelectrodes are often employed since they are more resistant to fouling and this is particularly true with molecules like 5-HT (56-59).

1.2.4 Locomotor activity

Thus far, the methods discussed in detail have focused on measuring the chemistry of the brain. However, in neuroscience, behavioral monitoring such as locomotor activity can also provide clues about the chemistry happening in the brain. Locomotor activity monitoring is a behavioral method where an animal's activities are measured in response to a pharmacological stimulation, toxicological insult, or genetic modification. Locomotor activity monitoring measures a multitude of behaviors and measurements such as ambulatory distance, stereotypy, and vertical counts. Locomotor activity places a mouse in a designated chamber or places the mouse's home cage in the activity chamber. The activity chamber placed around the animal's home cage or chamber has three sets of bars located outside the cage and are indicated as the x, y, and z plane (Figure 1.9), where the infrared (IR) beams transmit and receive signal. As the mouse moves in its home cage, the mouse breaks the IR beam connection from the transmitter to the receiver and a computer program records these beam breaks as the amount of movement made by the animal. Ambulatory distance measures the distance the animal moves in (cm), which is important since it indicates whether or not an animal is hyper- or hypo-locomotive. Animals that are hyperactive are often thought to have increased extracellular DA levels, while hypo-locomotive animals are believed to have

decreased extracellular DA levels (60). Hyperactivity may be a result of pharmacological stimulation (i.e. psychostimulants such as cocaine or METH) or a genetic alteration (e.g. DAT knockout mice). Stereotypic behavior measures repetitive movements an animal makes. Finally, vertical counts measure rearing events, which describe the rodent siting up on its hind legs. Rearing events are measured in the Z-plane, where the IR beams are set higher than the X- and Y-beams to properly measure when the animal rears.

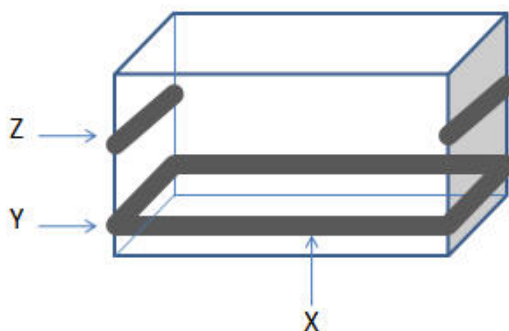


Figure 1.9 Diagram of a locomotor activity box.

1.3 Research objectives

1.3.1 Objective 1: *Characterization of the dopamine system in female BDNF^{+/-} mice*¹

The risk of specific neurological diseases and disorders such as Parkinson's disease and depression differ between men and women and sex steroid hormones may account for these differences. Additionally, there is increasing evidence that sex hormones may be responsible for the regulation of BDNF signaling since BDNF levels differ between the sexes (61-63). Besides diseases and disorders, sex differences have also been reported in drug abuse studies as well as the efficacy of therapeutic drugs.

¹This objective includes collaborative work from Madiha Khalid, Ph.D. who performed slice voltammetry work to further understand release and uptake of the female BDNF^{+/-} mice. These results complement the findings with microdialysis experiments, providing a better understanding of the changes that were seen between the genotypes. For more detailed roles, please see contribution section of this dissertation.

Previous studies done in the Mathews lab determined that male BDNF heterozygous (BDNF^{+/-}) mice that were approximately three months of age are hyperdopaminergic in nature (44). The purpose of this study was to determine if young female BDNF^{+/-} mice (~3 months of age) are also hyperdopaminergic like their male BDNF^{+/-} counterparts or if this is exclusive to male mice only.

1.3.2 Objective 2: Characterization of the dopamine system in aged BDNF^{+/-} mice²

The purpose of this study was to characterize the DA system in a heterozygous mouse model in which there was a lifelong reduction of endogenous BDNF protein and mRNA levels (25, 64). BDNF^{+/-} mice have no gross abnormalities compared to their wildtype littermates, but BDNF^{+/-} mice are heavier and slightly more aggressive as they age (65). Previous research in our laboratory has shown that male BDNF^{+/-} mice at ~3 months of age are hyperdopaminergic in nature (44). BDNF^{+/-} mice have increased extracellular DA levels using microdialysis with a concomitant decrease in release and uptake of DA as measured by FSCV.

Our hypothesis that this hyperdopaminergia seen in the young mice would persist throughout the animal's life, and that these elevated extracellular DA levels lead to even greater striatal impairments as the animal aged. We hypothesized that these striatal impairments would cause older mice to be more susceptible to increases in reactive oxygen species, which is a product of DA metabolism, and ultimately lead to greater harm to the aging DA neuronal system (66, 67). In this study, both *in vivo* microdialysis and slice FSCV were used in combination to characterize the DA system in 18 month old BDNF^{+/-} mice and their wildtype littermates. This study was the first to

²This objective includes collaborative work from Francis K. Maina, Ph.D. who performed slice voltammetry work to further understand release and uptake of the aged BDNF^{+/-} mice. For more detailed role, please see contribution section of this dissertation.

use slice FSCV in conjunction with *in vivo* microdialysis to obtain a comprehensive view of aging striatal DA dynamics with respect to basal DA concentrations, DA metabolism, and transporter functionality in aged BDNF^{+/-} mice.

1.3.3 Objective 3: *Method development for the simultaneous detection of purine and monoamine molecules using a boron-doped diamond electrode*

Ado and DA are important neurotransmitters in the brain and there is considerable evidence that they have reciprocal interactions through their receptors. Unfortunately, there is no reliable and robust electrochemical method available to detect baseline levels of Ado. Few papers have examined extracellular Ado levels in the brain because of the lack of reliable methods to quantify Ado. As a result only a few attempts have been made to measure extracellular or intracellular Ado levels in the rodent brain (9, 45, 54, 68-71). Those few reports that have measured Ado demonstrate the scant understanding of extracellular Ado levels in the rat striatum, since the reported extracellular Ado levels span a range from 50–240 nM (68, 70-72).

To date, the detection of Ado using carbon based electrode cells (glassy or porous carbon) with HPLC has not been achieved. This is primarily due to the high oxidation potential of Ado (~ +1500 mV versus a Ag/AgCl reference electrode) and the surface instability of these carbon-based electrodes. At potentials greater than +1000 mV, the surface of carbon begins to oxidize itself +1000 mV (49). Recently, BDD electrodes have become commercially available for electrochemical cells for HPLC analysis (50). BDD electrodes have numerous advantages over the carbon electrodes such as lower background potentials, wider potential ranges (up to +2000 mV), and reduced surface fouling (57, 73). These inherent advantages make the BDD electrode

ideally suited for the detection of Ado using electrochemistry in combination with HPLC. The goal of this study was to develop a method for the simultaneous detection of DA and Ado using HPLC with BDD electrochemical detection.

CHAPTER 2

Materials and Methods

(Portions of the text in this chapter were reprinted or adapted with permission from Birbeck, J. A., and Mathews, T. A. (2013) Simultaneous Detection of Monoamine and Purine Molecules Using High-Performance Liquid Chromatography with a Boron-Doped Diamond Electrode, *Anal Chem*. Copyright (2013) American Chemical Society, and submissions to *The Neurobiology of Aging*, and *ACS Chemical Neuroscience*.)

The objective of this chapter is to describe experimental details used throughout this dissertation. The experimental protocols were performed at Wayne State University and followed Wayne State Universities standards put forth by Occupational Safety and Health Administration (OSHA) and the Institutional Animal Care and Use Committee (IACUC).

2.1 Chemicals

Chemicals used for mobile phase, buffers, standards, genotyping, and anesthesia were of HPLC grade or higher purity, or medical grade, and were purchased from Sigma Aldrich (St. Louis, MO), Fisher Scientific (Pittsburgh, PA), and EMD (Gibbstown, NJ). Primers and dNTP's were obtained from Invitrogen (Carlsbad, CA).

2.2 Animals

Both wildtype (C57BL/6J) and a heterozygous (BDNF^{+/-}) mouse models were used in these studies. Complete knockout of the BDNF gene (BDNF^{-/-}) is lethal (25) and therefore, BDNF^{-/-} mice were not bred or used for this study. For breeding, female C57BL/6J and male BDNF^{+/-} mice were obtained from Jackson Laboratories (Bar

Harbor, ME, USA). Offspring from the breeding pairs were raised as a colony in-house (Wayne State University, Detroit, MI) and were housed 3–4 per cage. Animals had access to food and water *ad libitum* during their 12-h light/dark cycle. Experiments conducted on mice between the ages of 3 to 18 months included locomotor activity and 3–5 month old mice (young) or 18 month old mice (aged) for microdialysis and fast scan cyclic voltammetry (FSCV). All experiments and procedures were designed to minimize any pain and discomfort for the animals, and were in accordance with the National Institute of Health Animal guidelines and approved by the Wayne State University Institutional Animal Care and Use Committee.

2.3 Genotyping

The procedures for the breeding, weaning, and genotypic analysis were performed by Kelly E. Bosse, Ph.D. and Brooke Neman. Assistance with these procedures was provided by myself, Katie Logan, Parvejz Khan, Natasha Bohin, Andrej Czaja, Christopher Rogalla, Michelle Colombo, and Stephanie Godden.

Three weeks after birth, pups were ear punched for numerical identification, tails clipped (~3–5 mm), and separated from their parents based on sex into group-housed vivariums. Tail pieces were immediately placed in a -80 °C freezer until analysis. Each mouse's genotype was identified using polymerase chain reaction (PCR) analysis from the tail DNA collected. Tails were chopped into small pieces and lysed in 500 µL of lysis buffer (100 mM Tris-base, 1.5 mM NaCl, 5 mM EDTA, 0.2% sodium dodecyl sulfate; pH to 8.5) and 0.1mg/mL proteinase K. Tubes with tail pieces and lysis buffer were placed into a 55 °C water bath for 15–24 h to achieve complete protein digestion. After digestion was completed, the tubes were placed into the centrifuge and spun for 16 min

at a speed of 20 000 rcf. The tubes were uncapped to release pressure and then placed back into the centrifuge for another 16 min. After centrifugation was completed, 200 μ L of the supernatant was slowly withdrawn from the top layer of fluid and placed into newly labeled tubes with 500 μ L isopropyl alcohol. The tubes were capped and mixed by shaking until a white globular precipitate appeared. Tubes were centrifuged again for another 16 min at 20,000 rcf to spin down the pellet of DNA. This pellet was retained and washed by adding 500 μ L of a 75% ethanol solution and centrifuged again for another 5 min. The ethanol solution was withdrawn and 6 μ L of nanopure water was added to the DNA pellet in the tube. The tubes were then placed in a desiccator with the caps open for 15 min. After ethanol evaporated off, 85 μ L of tris-EDTA (TE) buffer was added to each vial of DNA and stored at 4 °C until further analysis was completed. To approximate how much DNA was present in the sample optical density was determined by using an ultraviolet spectrometer (UV-1800 Shimadzu, Columbia, MD) set at 260 nm. A mixture using 4 μ L of TE storage buffer and 400 μ L of nanopure water was placed into the cuvette for the blank reference. For the measurement of optical density of the DNA sample, a mixture of 4 μ L of DNA sample was mixed with 400 μ L water. This was repeated for all samples.

For PCR analysis, each DNA sample was split into two PCR tubes. One tube was labeled for the wildtype primer (5'-CCAGCAGAAAGAGTAGAGGAG-3') and the other with the BDNF mutant primer (5'-GGGAACTTCCTGACTAGGGG-3') each along with a common primer (5'-ATGAAGAAGTAAACGTCCAC-3'). The master PCR solutions were prepared for wildtype and BDNF mutant primers. These master mixes contained the following: 1.28 mM MgCl₂, 1.2 μ L PCR buffer A (10 mM Tris-HCl, 1.5 mM

MgCl₂, 50 mM KCl; pH 9.0), 0.096 mM of each deoxyribonucleotide triphosphates (dNTP's: dATP, dCTP, dGTP, and dTTP), 1 μM of one of the primers (wildtype or BDNF mutant), and 1 μM NEO primer. Each sample tube then contained 22.8 μL of master mix, 2 μL of tail DNA sample, and 0.2 μL of taq polymerase. Before tubes were placed into the thermocycler, a drop of mineral oil was placed into each PCR tube. The cycling conditions that were used are as followed: 94 °C for 5 min (melting), 58 °C for 1 min (annealing), 72 °C for 2 min (extension), followed by 35 cycles at 95°C for 1 min, 58 °C for 1 min, and 72 °C for 2 min. PCR products were then analyzed immediately or stored in the 4 °C for further analysis.

Analysis of the PCR product was imaged in a 2% agarose gel (6 μL per lane) in TBE buffer (89 mM Tris-base, 89 mM boric acid, 1mM EDTA, 1mM NaOH; pH 8.0). PCR products were separated between 125–135 V and visualized using ethidium bromide (60 μL added to 750 mL of TBE buffer). Wildtype mice were identified by a single band of genomic DNA in the first column (this column was always designated to identify the wildtype gene), while BDNF^{+/-} mice were identified from one band of genomic DNA (active BDNF, 275 base pairs (bp)) in the first column and a second band of genomic DNA (inactive BDNF, 340 bp) in the 'BDNF-mutation' column (Figure 2.1). The inactive BDNF gene was generated by inserting a neomycin (NEO) resistant cassette into the active BDNF gene. Addition of the NEO cassette increases the molecular weight of the BDNF gene, therefore slowing its travel through the gel electrophoresis (Figure 2.1).

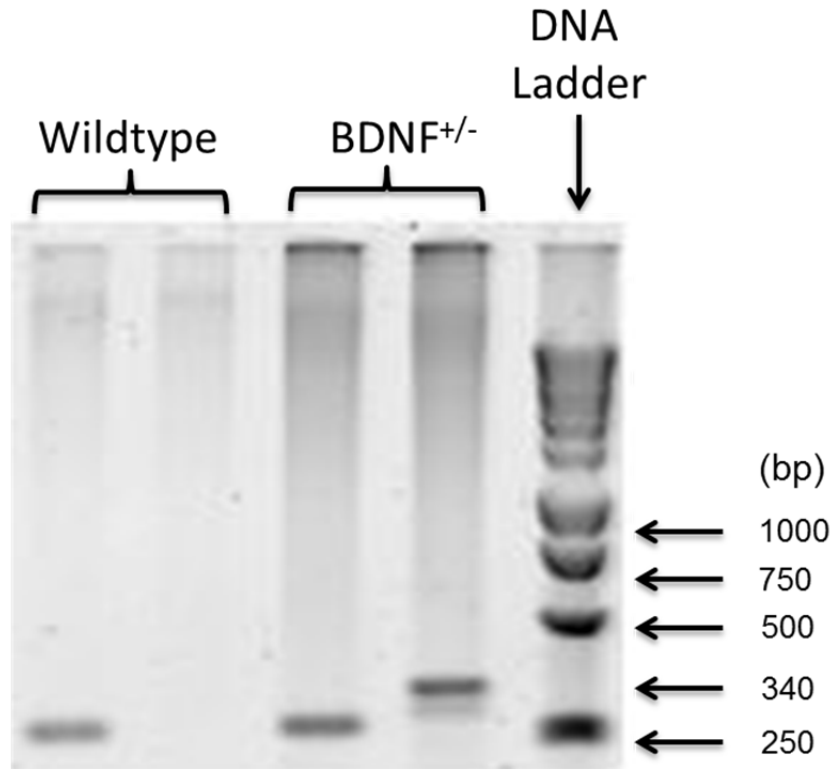


Figure 2.1 Gel electrophoresis image of genotypic identification for wildtype and BDNF^{+/-} mice. The first two lanes represent genotypic identification for a wildtype mouse. The second two lanes identify a BDNF^{+/-} genotype, and the final lane shows the DNA ladder. For wildtype identification, lane one shows a band at 275 bp, and the second lane is void of any bands. The third and fourth lanes identify the BDNF^{+/-} genotype in which the third lane shows the band at 275 bp representing the active BDNF gene, and the fourth lane has a band present at 340 bp representing the inactive BDNF gene. *Image courtesy of Stephanie Godden.*

2.4 *In vivo* microdialysis

2.4.1 Surgery

Both male and female mice were used for microdialysis experiments at 3–5 months and 18 months of age. Stereotaxic surgery was performed as follows. Mice were anesthetized using isoflurane (induction 2–4%; maintenance 0.5–3%). Once the mice were fully anesthetized, their eyes were protected with sterile ophthalmic ointment. The top of the mouse's head was shaved and sterilized using Betadine and alcohol three times. After confirming that the mouse was completely under surgical plane (which

is achieved by seeing no reaction from pinching the mouse's toes), an incision to the scalp was made and cleaned using a 10% peroxide until bregma was clearly visible on the skull. Next, the mouse was placed onto the stereotaxic frame, allowing for a burr hole to be drilled and a CMA/7 guide cannula to be inserted targeting the caudate-putamen (CPu). A second burr hole was drilled diagonally across from the cannula on the contra-lateral hemisphere for insertion of an anchoring screw. Coordinates were obtained from the mouse atlas to determine CPu placement, and further refined by experimental determination in mm from bregma: anterior: +1.0, lateral: -1.3, ventral: -2.5 for 18 month mice, and anterior: +0.8, lateral: -1.3, ventral: -2.5 for mice 3–5 months of age (74). The cannula and screw were anchored, and exposed skull sealed using fast drying dental cement (Teets, Diamond Springs, CA). After surgery, mice were allowed to recover for 3 h before the microdialysis probe (2 mm membrane length, 0.24 mm membrane diameter, Cuprophane, 6 kDa cut-off) was inserted through the guide cannula. Artificial cerebral spinal fluid (aCSF; composition in mM: 145 NaCl, 3.5 KCl, 2 Na₂HPO₄, 1.0 CaCl₂, 1.2 MgCl₂; pH 7.4) was perfused overnight at a flow rate of 0.40 μ L/min. Microdialysis experiments commenced the next day at 0700 h, where the first hour was to allow for equilibration as the flow rate was increased to 1.1 μ L/min. Dialysate samples were collected at 20 min intervals from the freely moving mice.

2.4.2 Microdialysis experiments

The microdialysis technique of zero-net flux was used to determine the basal extracellular DA levels in the mice (44, 75, 76). Four baseline samples were collected with aCSF, then using a CMA/402 programmable gradient infusion pump, perfusate containing 5, 10, and 20 nM DA was delivered through the microdialysis probe for 90

min each. The DA-containing aCSF solutions contained 200 μM ascorbic acid and the samples were stored in the $-80\text{ }^{\circ}\text{C}$ freezer until use (77). Determination of the DA concentration entering the probe (DA_{in}) was accomplished by *in vitro* calibration using DA-containing aCSF perfused through the dialysis system in absence of a mouse. DA-containing aCSF was prepared freshly on each day of analysis.

To determine pharmacological DA release with microdialysis, methamphetamine (METH) was used (Figure 2.2). Before all METH experiments, mice were weighed to administer the proper dose. Three baseline samples were collected, then mice were injected intraperitoneally (i.p.) with 1.0 mg/kg dose of METH and dialysate samples were collected every 20 min for 2 h after the METH injection.

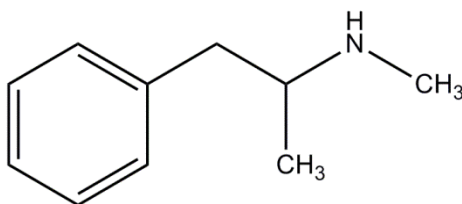


Figure 2.2 Chemical structure of methamphetamine (METH).

DA vesicular release by depolarization of the neuron was induced by perfusing high potassium aCSF at 60mM (in mM: 60 KCl, 90.5 NaCl, 2.0 Na_2HPO_4 , 1.2 MgCl_2 , 1.0 CaCl_2 ; pH 7.4) and 120 mM KCl aCSF (in mM: 120 KCl, 30.5 NaCl, 2.0 Na_2HPO_4 , 1.2 MgCl_2 , 1.0 CaCl_2 , pH 7.4) was used. In this method, three baseline samples were collected with regular aCSF, and following the third collected sample, high potassium aCSF (60 mM or 120 mM KCl) was perfused through the probe for 20 min. After the 20 min perfusion of the high potassium aCSF was completed, the perfusion media was switched to an infusion only of regular aCSF went through the brain for the last five subsequent dialysis fractions that were collected.

2.5 Slice fast scan cyclic voltammetry

All FSCV experiments were conducted by Francis K. Maina, Ph.D. (male and female mice 18 months of age), and Madiha Khalid, Ph.D. (female mice 3–5 months of age).

Mice were anesthetized using CO₂, sacrificed, and their brains rapidly removed. The brain was placed into pre-oxygenated (95% O₂/5% CO₂) cold high sucrose-aCSF buffer (composition in mM: 180 sucrose, 30 NaCl, 4.5 KCl, 1 MgCl₂, 26 NaHCO₃, 1.2 NaH₂PO₄, and 10 D-glucose; pH 7.4) for 10 min. A Vibratome[®] was used to section each brain into 400- μ m thick coronal slices containing the DA rich area of the CPu. Slices were then placed into oxygenated aCSF (composition in mM: 108 NaCl, 5 KCl, 2 CaCl₂, 8.2 MgCl₂, 4 NaHCO₃, 1 NaH₂PO₄, 11 D-glucose, 0.4 ascorbic acid; pH = 7.4) for 1 h before voltammetric analysis. After oxygenation, slices were then placed onto a custom-made submersion chamber that was kept at a temperature of 32 °C as oxygenated aCSF flowed over the brain slice at a rate of 1 mL/min.

Carbon fiber microelectrodes approximately 50–200 μ m in length were sealed in a glass capillary in-house for FSCV analysis of DA as previously described (7). The carbon fiber microelectrode was inserted in the CPu \sim 75 μ m below the surface of the slice, and the stimulating electrode was placed directly on the slice approximately 100–200 μ m away from the carbon fiber microelectrode. The parameters for detecting DA at the electrode surface were completed using a triangle waveform where the electrode potential was initially held at -0.4 V versus an Ag/AgCl reference electrode, ramped up to +1.2 V, and then returned to -0.4 V at 400 V/s at a frequency of 10 Hz (7, 44, 53). DA release was evoked every 5 min by a one pulse monophasic stimulation (350 μ A, 60 Hz

with 4 ms pulse width) from the stimulating electrode and stable baseline DA dynamics of release and uptake were measured for at least 30 min. All electrode and stimulation parameters were controlled by TH software.

Electrodes were post-calibrated with 3 μM DA and the peak oxidation current was converted to concentration. The current versus time plots were fit by non-linear regression using LabVIEW National Instrument software as described by John and Jones (53). Using a Michaelis-Menton base kinetic model, peak amplitude of release ($[\text{DA}]_p$), uptake kinetics (maximum velocity, V_{max}), and DA's 'apparent' transporter affinity (K_m) were determined by fitting DA concentration versus FSCV time traces (7).

To evaluate DA's affinity for DAT, slice FSCV was used with METH, a competitive inhibitor of the DAT. The competitive inhibition of DA reuptake is reflected by an increase in DA's affinity for the DAT, also known as the apparent K_m (53). Equation 2.1 below shows how apparent K_m is calculated, where K_m is the Michaelis-Menton constant and K_i is the inhibition constant. The K_i values are calculated from the slope of the linear regression line of METH concentration versus apparent K_m values (shown in equation 2.2). The chosen value of K_m was 0.16 μM , as previously reported in literature (53, 78-80).

$$\text{Apparent } K_m = K_m \times (1 + [i]/K_i) \quad (2.1)$$

$$\text{Slope} = \Delta y/\Delta x = K_m/K_i \quad (2.2)$$

After stable DA release was recorded, superfusion of METH began with increasing concentrations (0.01–10 μM) delivered to the slice every 30 min. Increasing concentrations of METH were applied to the brain slice since it was previously shown

that cumulative concentrations of perfused drugs over a slice do not affect DA release and uptake parameters (53).

2.6 Tissue Content

The majority of DA inside the neuron is sequestered in vesicles to prevent oxidation or metabolism of the neurotransmitter so it will be readily available upon receiving an action potential. Intracellular DA levels are approximately 1000-fold higher in concentration compared to extracellular levels, which are measured by microdialysis. Briefly, mice were sacrificed by cervical dislocation and their brains were rapidly removed. The brain regions of the frontal cortex, striatum, nucleus accumbens (NAc), hippocampus, and midbrain were dissected out, rapidly frozen in liquid nitrogen, and stored at -80 °C until analysis. On the day of analysis, the tissue was removed from freezer and allowed to thaw on ice. After being thawed for approximately 20 min, a 250 μ L of 0.1 M HClO₄ was added to each vial of tissue and was sonicated for 12 to 15 1-second pulses at 50% duty, and microtip setting at ~4. Vials were then centrifuged for 10 min at a rate of 12,000 rfc at 4°C. The supernatant was injected onto the HPLC at a volume of 20 μ L. Standard solutions were run to verify peak placement as well to quantify concentrations of each analyte. Monoamine and purine tissue levels were represented as ng monoamine or purine per mg of protein. Protein values were measured using Pierce BCA protein assay kit (Pierce Biotechnology, Rockford, IL).

2.7 HPLC and electrochemical detection

2.7.1 Detection of neurotransmitters using a porous carbon working electrode

Microdialysis or tissue content samples were separated and detected using a Shimadzu LC-20AD HPLC pump coupled with electrochemical detection, and were

separated using a reverse phase Phenomenex C₁₈ (2)-HST column (100 mm x 3 mm, 2.5 μm). The neurotransmitters DA and its metabolites, serotonin (5-HT) and its metabolite, and norepinephrine (NE) were detected using an ESA coulometric cell Model 5014B microdialysis cell (porous carbon working electrode set at potentials E₁ = -150 mV and E₂ = +220 mV versus a palladium reference electrode), with a guard cell (ESA 5020) set at +350 mV placed before the injection loop. Dialysate samples were eluted isocratically using a mobile phase (composition in mM: 75 NaH₂PO₄ monohydrate, 1.4–1.8 1-octanesulfonic acid, 0.125 EDTA, 10% acetonitrile, and 0.002% triethylamine; pH = 3.0 with phosphoric acid (85 wt %) with the flow rate of 0.400 mL/min. The retention times for NE, 3, 4-dihydroxyphenylacetic acid (DOPAC), DA, 5-hydroxyindoleacetic acid (5-HIAA), homovanillic acid (HVA), 3-methoxytyromine (3-MT), and 5-HT were ~3.6, 5.0, 6.5, 10.4, 12.5, 16.3, and 19.4 min, respectively. Analyte peak areas were determined against known standards by integration using LC Solutions Shimadzu Software.

2.7.2 Detection of neurotransmitters using a boron-doped diamond working electrode

Isocratic monoamine and purine separation were completed using a Shimadzu LC-20A HPLC coupled to an ESA Coulochem III detector. Detection was achieved using an ESA model 5041 analytical cell with a BDD disc electrode versus a palladium reference electrode. The column used was a Trinity™ P1, 100 x 3 mm and 3 μm particle size. Ammonium phosphate mobile phase was composed of the 45 mM ammonium phosphate, and 4% acetonitrile, pH = 3.00 using phosphoric acid (85 wt %). The mobile phase was subsequently purged with argon and sonicated. The flow rate was set at

0.65 mL/min. To determine the proper oxidation potential for the best analysis of DA and Ado simultaneously, a hydrodynamic voltammogram was constructed and then a potential was chosen that would sufficiently oxidize both of the analytes, which was set +840 mV. Approximate analysis time for both DA and Ado was less than 10 min. For NE, DA metabolites, 5-HT, and its metabolite, total analysis time was 30 min. Analyte peak areas for monoamine and purine molecules were determined against known standards and integrated using LC Solutions Shimadzu Software. The retention times for each molecule that was detected are as follows in min: AMP: 1.5, Ado: 3.1, NE: 4.1, DOPAC: 5.7, HVA: 6.7, DA: 8.7, 5-HIAA: 11.3, 3-MT: 13.6, and 5-HT: 28.

2.8 Locomotor activity

Mice were separated into singly housed cages 24 h prior to locomotor analysis. On the day of analysis, mice were transported from the animal facility to the testing facility, their food and water removed, and their home cage placed into the locomotor activity static chamber. Mice were allowed to habituate for 1 h to minimize the stress of transportation and the novel environment. Spontaneous locomotor activity was recorded using 3 sets of 16-beam infrared (IR) emitter-detector arrays (Med Associates, St. Albans, VT) (81). Interruptions of IR beams resulted in an analog signal being recorded by automated activity software (Open Field Activity Software [SOF-811], Med Associates, St. Albans, VT). The locomotor activity system quantified total beam breaks in both the vertical and horizontal planes, specifically encoding measures of distance traveled (cm; calculated from number of breaks of adjacent beams), ambulatory time (s), and number of rears. Baseline ambulatory distance was measured for a total of 2 h and binned into 10 min periods.

To determine locomotor stimulation following METH administration, baseline activity was determined for the first hour then mice were then injected i.p. with saline (1.0 mL) and locomotor activity was collected for a second hour. Mice were then injected with METH (1.0 mg/kg, i.p.) and locomotor activity was collected for an additional 2 h. Total analysis time was 4 h.

2.9 Statistical analysis

Neurochemical data analysis was performed using GraphPad Prism[®] software. Values were reported as mean \pm standard error of mean (SEM) with the criterion for statistical significance set to $P < 0.05$. For zero-net flux analysis linear regression analysis, the x -axis represents the concentration of DA being perfused into the probe determined by *in vitro* analysis (DA_{in}), and the y -axis represents the difference of DA_{out} , which is defined as the concentration of DA in the dialysate sample from DA_{in} (75). The point at which the regression line crosses the x -axis is known as DA_{ext} and indicates the basal extracellular concentration of DA. The slope of the regression line was used to determine the *in vivo* recovery of DA (E_d , dialysate extraction fraction) (82). Student's t -test was used to determine if a significant difference existed between the genotypes with respect to DA_{ext} , extracellular metabolite concentrations, metabolite/DA ratio, and tissue content. For analysis of high potassium and METH microdialysis studies, two-way analysis of variance (ANOVA) analysis was used.

Release and uptake, as determined by FSCV, were analyzed using the Michaelis-Menten kinetic based model which determines changes in $[DA]_p$, V_{max} , and apparent K_m (53, 79, 83). To determine differences in electrically stimulated DA uptake and release between genotypes a two-tailed Student's t -test was used.

Locomotor activity, baseline and METH-induced, were analyzed (IBM SPSS® Statistics for Windows) using a 2 x 3 x 12 three-way, repeated measures analysis of variance (ANOVA) with genotype (wildtype or BDNF^{+/-}) as the between-subjects factors, and month (12, 15, or 18) and the 12 time blocks as nested within-subjects factors.

CHAPTER 3

Potentiated striatal dopamine release leads to female BDNF^{+/-} mice hyperdopaminergia

(Portions of the text in this chapter were adapted from the submission to *ACS Chemical Neuroscience*)

3.1 Introduction

Risk of developing neurological diseases and disorders are different among men and women. An example of this is seen with regards to Parkinson's disease, a disease characterized by dopamine (DA) neuron degeneration in the striatum, which men are ~1.5 time more likely to develop the disease than women (35). In the case of depressive disorders, which include both the dopaminergic and serotonergic pathways, women are two times more prone to developing them than men (84). To better understand the gender differences in these neurological conditions, research has focused on the molecules implicated in these conditions, such as neurotransmitters DA and serotonin, as well as the neurotrophins that protect the neurons, such as brain-derived neurotrophic factor (BDNF) (37, 85, 86).

To better understand the sex-differences in disease risk and progression, gonadal hormones such as estrogen and testosterone have been investigated in addition to other associated molecules such as DA and BDNF. In ovariectomized rats, a physiological dose of estrogen increased striatal extracellular DA concentrations and tyrosine hydroxylase activity (38). Furthermore, estrogen was shown to act upon and stimulate similar downstream second messengers, ERK1 and ERK2, in a similar manner as BDNF in cortical explant cultures (87). Additionally, female rats showed an

increase in depression vulnerability in comparison to males rats when their BDNF levels were at their lowest, which was shown to correlate to when estrogen levels are at their highest (36, 88, 89).

Sex differences are also observed in neurological disorders, such as addiction, in which females and males respond differently to drugs of abuse. For example, women are more likely to start using illicit drugs sooner than men, and consume greater quantities of these drugs (90, 91), while men are more likely to die from an overdose versus women (92). Taken together, these observations in animal and clinical studies, have led researchers to hypothesize that females may be protected from the neurotoxic effects of drugs because of their naturally higher levels of estrogen (93-95).

Numerous studies have elucidated the importance of BDNF in maintaining the function and survival of DA neurons in the striatum (26, 28-30). To better understand BDNF's endogenous role throughout the brain and body, genetically modified heterozygous (BDNF^{+/-}) mice developed by Ernfors and colleagues were used (25). With respect to DA neurochemistry, male BDNF^{+/-} mice have increased extracellular and intracellular DA levels, (29, 44, 96), which were not associated with alterations in the DA transporter. The objective of this study was to determine if these striatal DA alterations are present in female BDNF^{+/-} mice. Using the complementary techniques of *in vivo* microdialysis and slice fast scan cyclic voltammetry (FSCV), DA dynamics were investigated in female wildtype and BDNF^{+/-} mice.

3.2 Results and Discussion

3.2.1 Elevated basal striatal DA levels in female BDNF^{+/-} mice

Female BDNF^{+/-} mice, 3–5 months of age, were used to determine the effect of reduced BDNF protein and mRNA on the striatal dopaminergic system compared to

female wildtype littermates. Using the technique of microdialysis, the uncorrected extracellular DA levels (averages of 3–4 baseline samples per mouse) in the caudate putamen (CPu) of wildtype and BDNF^{+/-} mice showed no difference between genotypes (Figure 1 inset; wildtype mice: 3.5 ± 0.5 nM, $n = 7$ and BDNF^{+/-} mice: 3.8 ± 0.5 nM, $n = 10$, $P = 0.62$). When extracellular DA levels were evaluated in-depth using the *in vivo* microdialysis method of zero-net flux, basal extracellular DA ($[DA]_{\text{ext}}$) levels and extraction fraction (E_d) were determined for each genotype (Figure 3.1). An ~2-fold increase in $[DA]_{\text{ext}}$ was observed in the female BDNF^{+/-} compared to their wildtype littermates (Figure 3.1, wildtype mice: 8.2 ± 1.6 nM, $n = 7$ and BDNF^{+/-} mice: 15.0 ± 1.8 nM, $n = 10$, $P < 0.05$). The basal DA levels in female BDNF^{+/-} mice are similar to male BDNF^{+/-} mice of the same age such that both sexes have an ~2-fold increase in striatal DA levels compared to their wildtype littermates (44). To determine if this difference in basal DA levels is due to alterations in the DA transporter (DAT), E_d (slope of the line) was calculated. E_d is a measure of DAT mediated uptake (82), and was not different between female BDNF^{+/-} (0.30 ± 0.02 , $n = 10$) and female wildtype (0.31 ± 0.04 , $n = 7$, $P = 0.47$) mice (Figure 3.1, inset). This is in agreement with other's that show striatal DAT density and activity is unchanged in BDNF^{+/-} mice (29, 64). Although female BDNF^{+/-} mice have elevated extracellular DA levels, our zero-net flux results suggest this is not a result of striatal DAT alterations.

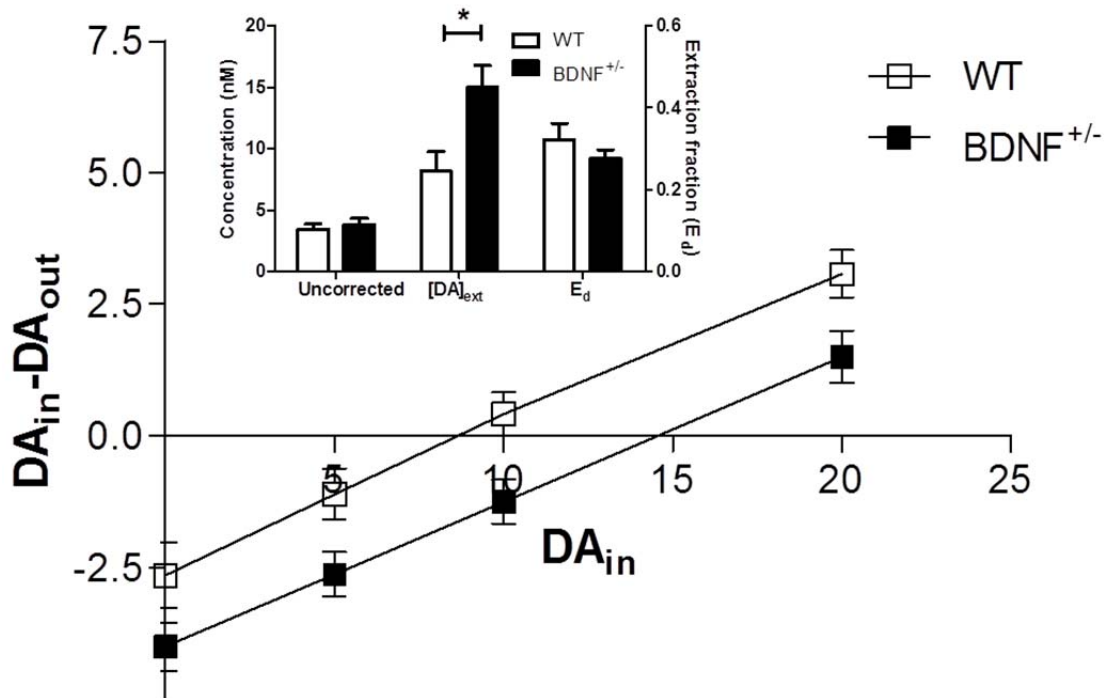


Figure 3.1 Extracellular DA concentration as measured by zero-net flux. Inset shows uncorrected DA extracellular levels, $[DA]_{ext}$, and the extraction fraction, E_d . Significance was seen between the wildtype (WT) and BDNF^{+/-} mice with regards to $[DA]_{ext}$ (WT: 8.2 ± 1.6 nM and BDNF^{+/-}: 15.0 ± 1.8 nM, * $P < 0.05$). No difference was observed in the uncorrected DA levels or E_d . N values are 7–10 mice per genotype.

3.2.2 DA metabolites are not different across genotypes

Inactivation of extracellular DA is regulated through the enzymatic breakdown of DA by the enzymes monoamine oxidase (MAO) to form 3,4-dihydroxyphenylacetic acid (DOPAC) and catechol-o-methyl transferase (COMT) to form the metabolite 3-methoxytyramine (3-MT). The DA metabolite 3-MT is transient in the brain and is not found in sufficiently high concentrations for detection, and therefore only DOPAC and HVA were measured. For both DOPAC and HVA, 3–4 microdialysis samples were collected and analyzed. Both the female wildtype and BDNF^{+/-} mice showed similarities in their extracellular metabolite concentrations of DOPAC (wildtype mice: 378 ± 69 nM,

n = 8, and BDNF^{+/-} mice: 421 ± 110 nM, n = 7, *P* = 0.73, Figure 3.2) and HVA (wildtype mice: 610 ± 52 nM, n = 7, and BDNF^{+/-} mice: 672 ± 120 nM, n = 5, *P* = 0.61, Figure 3.2). Metabolite levels are not different between the genotypes suggesting that the increase in extracellular DA is not caused by alterations in DA metabolism. Our DA metabolite data is consistent with what has been previously observed using male wildtype and BDNF^{+/-} mice (44).

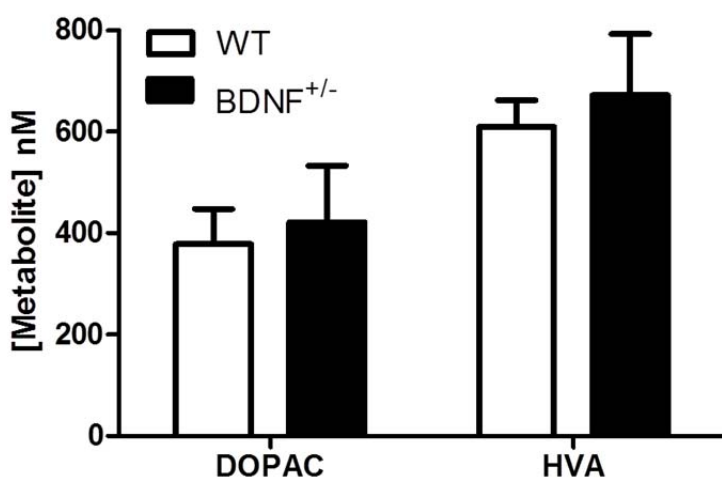


Figure 3.2 Extracellular DA metabolite levels as measured by microdialysis. No difference is observed between the genotypes for metabolites DOPAC or HVA. Data represented as mean ± SEM, and n values are 5–9 mice per genotype.

3.2.3 Slice FSCV: DA release is elevated in the female BDNF^{+/-} mice

All slice voltammetry experiments and analysis was conducted by Madiha Khalid, Ph.D.

Presynaptic DA release ($[DA]_p$) and DA reuptake (V_{max}) were examined to determine if these parameters were altered in female BDNF^{+/-} mice, which may contribute to the elevation of extracellular striatal DA levels. Using 400 μ m thick brain slices that contain the CPU of the mouse, a bi-polar stimulating electrode was used to evoke electrically stimulated DA release, which was subsequently measured using a carbon-fiber microelectrode. The female BDNF^{+/-} mice revealed increased DA release

per pulse ($[DA]_p = 1.4 \pm 0.2 \mu\text{M}$, $n = 8$) compared to their wildtype counterparts ($[DA]_p = 0.70 \pm 0.6 \mu\text{M}$, $n = 6$, $P < 0.05$, Figure 3.3A), but there was no difference between the genotypes with respect to the rate of DA uptake (V_{max} values wildtype: $3.2 \pm 0.2 \mu\text{M/s}$, $n = 6$, and $\text{BDNF}^{+/-}$: $3.4 \pm 0.3 \mu\text{M/s}$, $n = 8$, $P = 0.54$; Figure 3.3B).

The increase in stimulated DA release corroborates with our zero-net flux findings, where higher basal DA levels in the striatum of the female $\text{BDNF}^{+/-}$ mice were observed compared to the wildtype female mice. Interestingly, when the slice FSCV results from the sexes are compared, the evoked DA release from the female $\text{BDNF}^{+/-}$ mice is potentiated compared to male $\text{BDNF}^{+/-}$ mice (44). Unlike the female $\text{BDNF}^{+/-}$ mice, male $\text{BDNF}^{+/-}$ mice have a decrease in both DA release and uptake in comparison to their wildtype littermates (44). Thus low endogenous BDNF levels appear to have a greater impact on influencing stimulated DA release in the female $\text{BDNF}^{+/-}$ mice compared to their male counterparts.

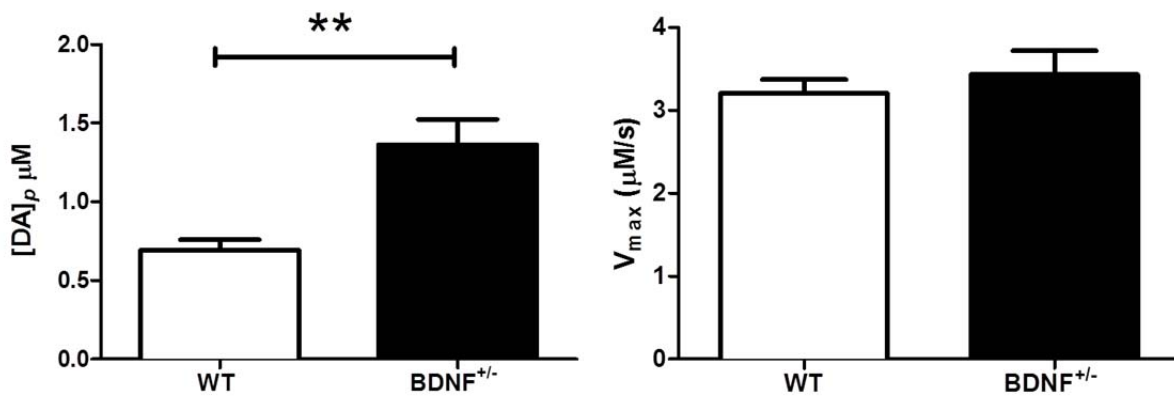


Figure 3.3 DA release and uptake in the CPU of female mice as measured by slice fast scan cyclic voltammetry. A) Average DA release per pulse $[DA]_p$ in μM , and B) average DA uptake rates, V_{max} , in $\mu\text{M/s}$. Data represented as mean \pm SEM.'s and n values are 6–8 per genotype, $**P < 0.01$.

3.2.4 Microdialysis stimulated DA release is potentiated in female BDNF^{+/-} mice

To determine vesicular DA release, *in vivo* microdialysis was used to infuse a high concentration of potassium (K⁺) to induce stimulation at the striatal neuronal terminals. In these experiments, three baseline samples were collected after which high K⁺ (60 mM KCl) containing artificial cerebral spinal fluid (aCSF) was perfused through the microdialysis probe for one 20 minute sample, followed by aCSF for the remainder of the experiment (Figure 3.4). The 60 mM K⁺ aCSF elevated extracellular DA levels by at least 5-fold in both genotypes. There appears to be a trend towards higher DA levels in the female BDNF^{+/-} mice versus their wildtype littermates, but striatal extracellular DA levels were not significant by a two-way ANOVA. Post-hoc analysis revealed a significant potentiation in DA levels in female BDNF^{+/-} mice 20 min after high K⁺ perfusion versus wildtype mice (Bonferroni posttest, $P < 0.01$).

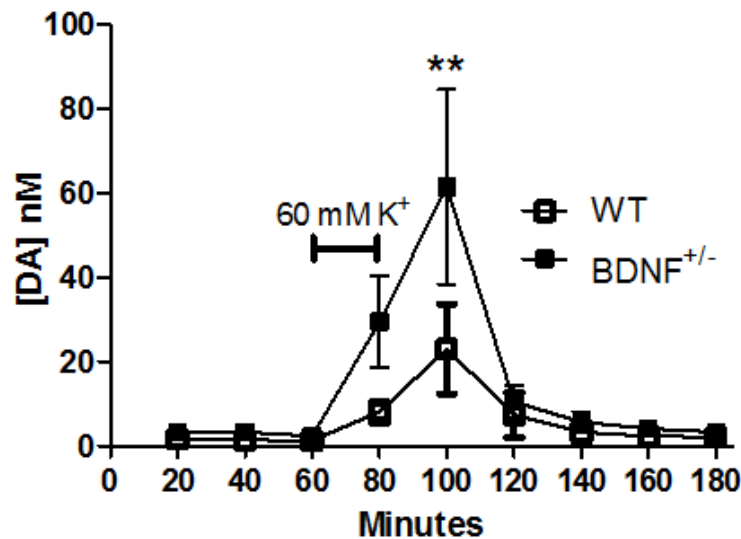


Figure 3.4 High potassium (K⁺) stimulated DA release from the CPu. Three 20 minute baseline samples were collected after which one 20-min perfusion of 60 mM K⁺ aCSF was administered through the dialysis probe directly into the CPu. Data are mean \pm SEM. 's show change in extracellular DA concentration upon K⁺ infusion. N values are 6 mice per genotype, ** $P < 0.01$ (Bonferroni posttest).

Overall, both *in vivo* microdialysis and slice FSCV demonstrate that stimulated DA release in the CPu of female BDNF^{+/-} mice was potentiated compared to female wildtype mice. When comparing the BDNF^{+/-} female mice to their male counterparts, a divergence in their response to high K⁺ stimulation with 60 mM KCl aCSF was observed, where there was a decrease or no effect on DA release in the male BDNF^{+/-} mice compared to their wildtype littermates (44, 64). This potentiation in stimulated DA release in females could be supported by the presence of estrogen, since estrogen pretreatment on the striatum significantly enhances DA extracellular levels, while testosterone treatment has no effect (97-99). However, to clearly delineate the roles of these sex hormones on striatal DA release dynamics, it is imperative that future studies evaluate these interactions to assist our understanding of this estrogen and its complex effects on neurotransmitter systems. Overall, both microdialysis and slice FSCV data suggests that female BDNF^{+/-} mice release more DA when the system is stimulated either via high K⁺ or electrical stimulation. If the striatal DA system is hyper-responsive then these results could possibly explain why the female BDNF^{+/-} mice have elevated extracellular DA levels without a difference in DAT activity.

3.2.5 Methamphetamine-stimulated DA release via microdialysis is potentiated in the female BDNF^{+/-} mice

Methamphetamine (METH), a substrate for the DAT, causes a conformational change to the DAT in which DA is primarily released from its transporter instead of being re-uptaken. Furthermore, METH disrupts the vesicular monoamine transporter (VMAT)-proton pump causing DA to be displaced from the vesicle. In clinical and animal models, high doses of METH or repeated doses in a single day of METH are neurotoxic

to the DA system by perturbing the central DA signaling (100-103). METH induced elevations in non-sequestered intracellular DA levels is thought to lead to an environment in where there is a greater probability of DA oxidation leading to the eventual formation of reactive oxygen species (ROS) in the cytosol, and ultimately nerve terminal damage (104, 105). However, low doses of METH, as used in this study, can be locomotor activating, and research has shown that increases in locomotor activity can be indicative of increases in extracellular DA levels (106).

METH was used to investigate BDNF's role with respect to gender upon pharmacological manipulation of the DAT. Female wildtype and BDNF^{+/-} mice were injected with a low dose of METH (1 mg/kg, intraperitoneally (i.p.)) which is known to activate locomotor activity (107, 108). Microdialysis samples were collected in 20 minute fractions for 3 hours after injection (Figure 3.5). Two-way ANOVA analysis revealed a main effect of genotype ($F_{1, 178} = 17.7, P < 0.001$), treatment ($F_{11, 178} = 20.7, P < 0.001$), and a significant interaction effect ($F_{11, 178} = 1.91, P < 0.05$) demonstrating that METH induced genotype-dependent elevations in extracellular DA levels. The maximal METH-induced response for both genotypes was 40 min after injection. A *post-hoc* test indicated that stimulated DA release was significantly potentiated at 100 and at 120 min ($P < 0.01$, and $P < 0.05$, respectively) in female BDNF^{+/-} mice compared to their wildtype controls (Figure 3.5).

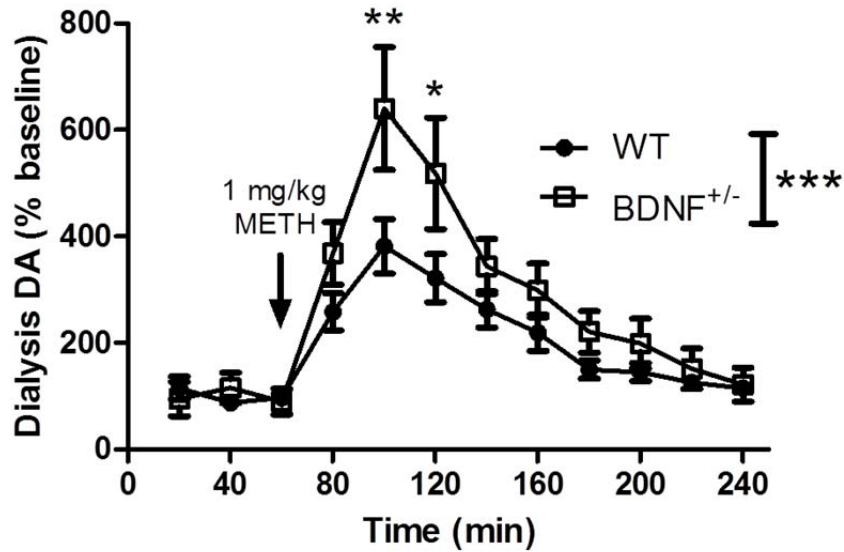


Figure 3.5 Methamphetamine (METH) stimulated striatal DA release. METH (1 mg/kg, i.p.) was administered at the end of the third baseline sample and DA levels were measured for the next 180 min. Data are represented as percent baseline of extracellular DA. N values are 7–10 per genotype. Two-way ANOVA indicates main effect of time and genotype, *** $P < 0.001$. * $P < 0.05$ and ** $P < 0.01$, Bonferroni posttest.

The balance between gonadal sex hormones, neurotransmitters and other neuromodulators like BDNF influence the susceptibility of sex differences in different neurological diseases/disorders. For example with drugs of abuse, often individuals experiment with drugs of abuse to self-medicate stress, anxiety, and depression (109). Women are more susceptible to experiencing depression and anxiety disorders, and a leading hypothesis is the BDNF plays a critical role in regulating mood (36, 110). These results disagree with previous work done by Dluzen, in which he suggested that the reduction in BDNF in the heterozygous mice might protect the heterozygous mice from the deleterious effects of METH because of reduced re-uptake of DA (93). However, this appears not the case with our finding since the female BDNF^{+/-} mice do not have a reduction in DA uptake from the DAT when compared to their wildtype counterparts.

Therefore, our results suggest that BDNF is important for regulation of DA dynamics in the striatum, and there is a considerable difference on how low BDNF levels influence striatal DA dynamics depending on the sex. These results further suggest that neuromodulators like BDNF and sex hormones combined have a powerful impact on striatal DA dynamics, where female BDNF^{+/-} mice appear to be altered only with respect to DA release while male BDNF^{+/-} mice have both release and uptake altered. These sex differences may be of particular interest when it comes to the administration of pharmacological agents that are meant to relieve anxiety or depression.

3.5 Conclusions

The increase in extracellular DA as measured by the microdialysis method of zero-net flux suggests that female BDNF^{+/-} mice are hyperdopaminergic like their male counterparts. This hyperdopaminergia is not a result of alterations in DAT functionality or DA metabolism, as they were consistent between the genotypes. However, there appears to be a difference in how the sexes reach a hyperdopaminergic state. Female BDNF^{+/-} mice have potentiated DA release as measured in three-independent experiments: slice FSCV, high K⁺ microdialysis, and microdialysis following a low-dose of the psychostimulant METH. Overall, these DA release findings suggest that there is a complex relationship between BDNF, the sex hormones, and how they influence striatal DA release together. The potentiation in extracellular DA levels in female BDNF^{+/-} mice appears to be due to an increase in DA release, while the elevated extracellular DA levels in male BDNF^{+/-} mice is hypothesized to be a result of compensatory mechanism between their release and uptake. Estrogen may be responsible for these DA changes, since it has been hypothesized that estrogen acts directly on the DA terminals

increasing DA release by down-regulating DA D₂ receptors (111). Taken together, when comparing these current findings with regards to differences in DA dynamics with female BDNF^{+/-} mice with respect to their male counterparts (44), it appears that there is a more intricate relationship at work between BDNF and sex hormones.

3.4 Materials and Methods

3.4.1 Mice

Female C57/Bl6J (wildtype) and BDNF^{+/-} (heterozygote) mice between 3–5 months of age were used in this study. Mice were bred in house from breeder pairs of female wildtype and male BDNF^{+/-} mice obtained from Jackson Laboratories (Bar Harbor, ME, USA). Mice were weaned 21 days after birth, tail clipped, and ear punched for identification purposes. Genotyping was done by PCR reaction using DNA from the tail clippings in order to identify the wildtype mice from the heterozygotes as there are no phenotypic differences observed in these mice (44). Mice were group housed as 3–6 animals per cage. All procedures and experiments were designed to minimize any pain and/or discomfort to the animals and were in accordance with the National Institute of Health Animal guidelines and approved by the Wayne State University Institutional Animal Care and Use Committee.

3.4.2 Microdialysis: Surgery and Experimentation

Female mice were used for all experiments and were not examined for their estrous cycle phase when microdialysis and voltammetry experiments were conducted. The estrous cycle was not taken into account for any experimental conditions because as Walker and Yu showed DA release and uptake is independent of estrous state and does not change in C57BL6/J mice (112-114). Mice were anesthetized using isoflurane

and a burr hole was drilled from coordinates relative to the bregma (anterior: +0.8, lateral: -1.3, ventral: -2.5) (44, 74). A CMA/7 guide cannula was inserted into the burr hole that was drilled into the skull targeting the CPU. The guide cannula was affixed to the skull using dental cement and the mice were allowed to recover for 3–4 hours after surgery before a microdialysis probe (2 mm membrane length, 0.24 mm membrane diameter, Cuprophane, 6 kDa cut-off) was inserted through the guide cannula. Next, aCSF (composition in mM: 145 NaCl, 3.5 KCl, 2 Na₂HPO₄, 1.0 CaCl₂, 1.2 MgCl₂; pH 7.4) was perfused at a flow rate of 0.4 μ L/min overnight. The next morning, flow rate was increased to 1.1 μ L/min and equilibrated for one hour before experimentation began. Dialysate samples were collected in 20 min fractions for a total sample volume of 22 μ L from the freely moving mice.

To determine basal extracellular levels of DA, the method of zero-net flux was employed as previously described (44, 75, 76). Four 20 min baseline samples were collected, and aCSF perfusate containing 5, 10, and 20 nM DA was perfused into the striatum using a CMA/402 programmable gradient infusion pump. Collected dialysate samples were stored in a -80 °C freezer until analysis (77).

For the zero-net flux experiments, the plotted x-axis represents the DA concentration perfused into the probe, DA_{in} (determined by *in vitro* analysis), and the y-axis is plotted as the difference in concentration perfused in from the concentration of DA collected from the probe (DA_{out}). The point at which this linear regression line crosses the x-axis is known as the DA_{ext}, which corresponds to the basal extracellular DA concentration DA_{in} (75). The slope of the regression line, E_d, was used to determine the *in vivo* recovery of DA (82).

DA vesicular release by depolarization of the neuron, a method which requires perfusion of high K^+ aCSF at 60 mM (in mM: 60 KCl, 90.5 NaCl, 2.0 Na_2HPO_4 , 1.2 $MgCl_2$, 1.0 $CaCl_2$; pH 7.4) was used. In this method, three baseline samples were collected with standard aCSF, and following the third collected sample, high K^+ aCSF was perfused through the probe for 20 min. After the 20 min perfusion of the high K^+ aCSF was completed, the pump was switched so that only standard aCSF was perfused for the last five subsequent dialysis fractions that were collected.

Pharmacological release of extracellular DA was achieved by using METH. Mice were weighed before analysis in order to calculate proper doses for intraperitoneal (i.p) injection. Three baseline samples were collected before mice were injected with a 1 mg/kg dose of METH, and samples were collected every 20 min for another 3 h after injection.

3.4.3 Slice fast scan cyclic voltammetry

All slice voltammetry experiments and analysis was conducted by Madiha Khalid, Ph.D.

Slice fast scan cyclic voltammetry experiments are the same as previously described (44, 115). Briefly, female mice were asphyxiated using CO_2 and immediately sacrificed, after which their brains were removed and placed into pre-oxygenated (95% O_2 /5% CO_2) cold high sucrose aCSF buffer (in mM: 180 sucrose, 30 NaCl, 4.5 KCl, 1 $MgCl_2$, 26 $NaHCO_3$, 1.2 NaH_2PO_4 , and 10 D-glucose; pH 7.4) for 10 min. The brain was sectioned into 400 μm thick coronal slices, and the slices containing the CPU were placed into an oxygenating aCSF (in mM: 108 NaCl, 5 KCl, 2 $CaCl_2$, 8.2 $MgCl_2$, 4 $NaHCO_3$, 1 NaH_2PO_4 , 11 D-glucose, 0.4 ascorbic acid; pH = 7.4) chamber at room temperature. After a 1 h equilibration period, the slices were placed onto a custom-

made submersion chamber kept at a temperature of 32 °C and the oxygenated aCSF was perfused over the brain slices at 1 mL/min for the remainder of the experiment.

Carbon fiber microelectrodes (50–200 μm in length) were made in-house for FSCV analysis of DA as previously described (115, 116). The microelectrode were placed in the CPU $\sim 75 \mu\text{m}$ into the tissue of the slice. The stimulating electrode was placed $\sim 100\text{--}200 \mu\text{m}$ away from the carbon microelectrode. A triangle waveform was used to detect DA from the surface of the electrode by applying a potential starting at -0.4 V versus a Ag/AgCl reference electrode, ramping it up to +1.2 V, then bringing it back down to -0.4 V at a frequency of 10 Hz and scan rate of 400 V/s (44, 115, 116). Stimulation was applied every 5 min and subsequent DA release and uptake were recorded until three stable baseline readings were achieved. All of the electrode and stimulation parameters were controlled by TH software. Post-calibration of electrodes were completed after each experiment using a 3 μM DA solution so that peak oxidation could be converted to concentration. Current versus time plots were fitted by non-linear regression as described by John and Jones, using LabVIEW National Instrument software (53). DA release, $[\text{DA}]_p$, and uptake, V_{max} , were determined using Michaelis-Menten based kinetics by fitting DA concentration versus time traces (7, 116).

3.4.4 Statistical Analysis

All analysis for microdialysis experiments were performed using GraphPad Prism® software. Values are reported as mean \pm standard error of the mean (SEM) with statistical significance set at $P < 0.05$. Student's *t*-test was used to determine significance between genotypes with respect to uncorrected DA, DA_{ext} , and metabolites

while genotypic analysis for high K^+ and METH were compared using two-way ANOVA analysis.

FSCV results of DA release and uptake were analyzed using Michaelis-Menten kinetic model, which measures the change in $[DA]_p$ and V_{max} (53, 79, 83). Student's *t*-tests were used to determine change in electrically stimulated DA release and uptake rates between the genotypes.

CHAPTER 4

Normalized striatal dopamine dynamics in aged BDNF deficient mice

(Portions of the text in this chapter were adapted from the submission to *The Neurobiology of Aging*)

4.1 Introduction

Aging is a natural process that all living organisms experience. Though the rate of aging is different across species, changes in the biological processes during aging are similar. One of the main hallmarks of aging is the slowing of motor movements and coordination typically associated with striatal dopamine function (117). Over a lifetime, degradation of nigral-striatal neurons occurs at a rate up to ~35% and correlates with an ~60% decrease in dopamine (DA) levels in humans (5, 118, 119). Specifically, aging causes substantial changes to the striatal DA system in these ways: 1) decreases in DA levels (5, 120), 2) decreases in D₂ receptors and the DA transporter (DAT) (121, 122), 3) decreases in tyrosine hydroxylase (TH) concentrations and neurons (123, 124), and 4) increases in free radicals by monoamine oxidase (MAO) during DA metabolism (66, 125). Severe striatal DA deficits contribute to specific neurological diseases or disorders associated with age such as Parkinson's and Huntington's disease (3, 119, 126). However, it is naïve to suggest that a single neurotransmitter or neuromodulator system is involved with these age-related neurological diseases. Recent evidence indicates there is also an associated decrease in levels of brain-derived neurotrophic factor (BDNF) along with DA deficits (3, 127, 128).

BDNF is a neurotrophic factor responsible for neuronal maintenance, survival, and growth. BDNF is synthesized in the substantia nigra (SN) and the cortical pyramidal

neurons and is anterogradely transported to the medium spiny neurons (MSNs) (31, 129, 130). Upon synaptic stimulation, BDNF binds to its receptor tyrosine kinase receptor B (TrkB) expressed on striatal MSNs (24). When BDNF is applied exogenously to mouse striatal slices or rat striatal neuronal cultures, BDNF increases DA release and survival of DA neurons, respectively (28, 44). During the normal aging process, protein levels of BDNF in the striatum have been shown to decrease in both rats and mice (131), as well as a concomitant decreases in TrkB and TH messenger ribonucleic acid (mRNA) levels in the striatum (64, 123). Furthermore, in animal models mimicking Parkinson's disease, dopaminergic neuronal cultures treated with BDNF before the application of 1-methyl-4-phenyl-1, 2, 3, 6-tetrahydropyridine (MPTP) were protected from the neurotoxic effects of its metabolite 1-methyl-4-phenylpyridinium (MPP⁺) (28). Additionally, results from various studies to date suggest that there is a reciprocal relationship between DA and BDNF.

With the relationship between DA and BDNF becoming ever more apparent, the purpose of this study was to characterize the DA system in a heterozygous mouse model in which there was a lifelong reduction of endogenous BDNF protein and mRNA levels (25, 64). BDNF^{+/-} mice have no gross abnormalities compared to their wildtype littermates, but are heavier and slightly more aggressive as they age (65). Previous research in our laboratory has shown that BDNF^{+/-} mice at ~3 months of age are hyperdopaminergic by nature (44). Our hypothesis was that this hyperdopaminergia would persist throughout the animal's life, and that these elevated extracellular DA levels would lead to even greater striatal impairments. These striatal impairments are thought to be caused by older mice being more susceptible to increases in reactive

oxygen species (ROS), a product of DA metabolism and harmful to an aging neuronal system (66, 67). In this study, both *in vivo* microdialysis and slice fast scan cyclic voltammetry (FSCV) were used in combination to characterize the DA system in 18 month old BDNF^{+/-} mice and their wildtype littermates. This study was the first to use slice FSCV in conjunction with *in vivo* microdialysis to obtain a comprehensive view of aging striatal DA dynamics with respect to basal DA concentrations, DA metabolism, and transporter functionality in aged BDNF^{+/-} mice.

4.2 Methods

4.2.1 Animals

A heterozygous (BDNF^{+/-}) mouse model was used in this present study because a complete knockout of BDNF (BDNF^{-/-}) in mice is lethal (25). Female C57BL/6J and male BDNF^{+/-} mice were obtained from Jackson Laboratories (Bar Harbor, ME, USA). Offspring from these mice were raised as a colony in-house (Wayne State University, Detroit, MI) and were housed 3–4 per cage. Animals had access to food and water *ad libitum* during their 12-h light/dark cycle. Each mouse's genotype was identified using PCR analysis of tail DNA and performed as previously described (132). Experiments conducted on mice between the ages of 12 to 18 months included locomotor activity and microdialysis at 18 months, and voltammetry on 3–5 month old mice (young) or 18 month old mice (aged). All experiments and procedures were designed to minimize any pain and discomfort for the animals, and were in accordance with the National Institute of Health Animal guidelines and approved by the Wayne State University Institutional Animal Care and Use Committee.

4.2.2 Microdialysis

Both aged male and female mice were used for microdialysis experiments. Stereotaxic surgery was performed as previously described (44) except that mice at 18 months were anesthetized using isoflurane (induction 2-4%; maintenance 0.5-3%). A burr hole was drilled and a CMA/7 guide cannula was inserted targeting the caudate-putamen (CPu). Coordinates were obtained from the mouse atlas and experimental determination (in mm from Bregma: Anterior: +1.0, Lateral: -1.3, Ventral: -2.5) (74). After surgery, mice were allowed to recover for 3 h before the microdialysis probe (2 mm membrane length, 0.24 mm membrane diameter, Cuprophane, 6 kDa cut-off) was inserted through the guide cannula. Artificial cerebral spinal fluid (aCSF; composition in mM: 145 NaCl, 3.5 KCl, 2 Na₂HPO₄, 1.0 CaCl₂, 1.2 MgCl₂; pH 7.4) was perfused overnight at a flow rate of 0.40 μ L/min. Microdialysis experiments were started the next day at 0800 h and at least 1 h before the flow rate was increased to 1.1 μ L/min to allow for equilibration. Dialysate samples were collected at 20 min intervals from the freely moving mice.

The microdialysis technique of zero-net flux was used to determine the basal extracellular DA levels in the 18 month old mice as previously described (44, 75, 76). Four baseline samples were collected with aCSF, then using a CMA/402 programmable gradient infusion pump, perfusate containing 5, 10, and 20 nM DA was delivered through the microdialysis probe for 90 min each. The DA-containing aCSF solutions contained 200 μ M ascorbic acid and the samples were stored at -80 °C until use (77). Determination of the DA concentration entering the probe (DA_{in}) was accomplished by *in vitro* calibration using DA-containing aCSF perfused through the

dialysis system in absence of a mouse. DA-containing aCSF was prepared freshly on each day of analysis. To determine pharmacological DA release using microdialysis, methamphetamine (METH) was used. Before all METH experiments, mice were weighed to achieve proper dosing. At least three baseline samples were collected, then mice were injected intraperitoneally (i.p.) with 1.0 mg/kg dose of METH and dialysate samples were collected for 2 h after the METH injection.

Samples were separated and detected using a Shimadzu LC-20AD HPLC pump coupled with electrochemical detection, and were separated using a reverse phase Phenomenex C₁₈ (2)-HST column (100 mm x 3 mm, 2.5 μ m). DA was detected using an ESA coulometric cell Model 5014B microdialysis cell (potential E₁ = -150 mV and E₂ = +220 mV versus a palladium reference electrode), with a guard cell (ESA 5020), set at +350 mV, placed before the injection loop. Dialysate samples were eluted isocratically using a mobile phase (composition in mM: 75 NaH₂PO₄ monohydrate, 1.4–1.8 1-octanesulfonic acid, 0.125 EDTA, 10% acetonitrile, and 0.002% triethylamine; pH = 3.0, adjusted with 85% phosphoric acid) with the flow rate of 0.400 mL/min. The retention times for 3, 4-dihydroxyphenylacetic acid (DOPAC), DA, and homovanillic acid (HVA) were ~5, 6.5, and 12.5 min, respectively. Analyte peak areas were determined against known standards by integration using LC Solutions Shimadzu Software. After dialysis experiments were completed, mice were sacrificed, and brains were sectioned for histological confirmation of probe placement.

4.2.3 Slice voltammetry

Slice voltammetry experiments and analysis was conducted by Francis K. Maina, Ph.D.

Slice voltammetry experiments were similar to those described in Bosse *et al.*, (44). Briefly, mice were anesthetized with CO₂ and their brains were rapidly removed, and were placed into pre-oxygenated (95% O₂/5% CO₂) cold high sucrose-aCSF buffer (composition in mM: 180 sucrose, 30 NaCl, 4.5 KCl, 1 MgCl₂, 26 NaHCO₃, 1.2 NaH₂PO₄, and 10 D-glucose; pH 7.4) for 10 min. A Vibratome[®] was used to section each brain into 400 μm thick coronal slices containing DA rich areas of the CPu and nucleus accumbens (NAc). Slices were then placed into oxygenated aCSF (composition in mM: 108 NaCl, 5 KCl, 2 CaCl₂, 8.2 MgCl₂, 4 NaHCO₃, 1 NaH₂PO₄, 11 D-glucose, 0.4 ascorbic acid; pH = 7.4) for 1 h before being placed onto a custom-made submersion chamber for voltammetric analysis. The submersion chamber was kept at a temperature of 32 °C as oxygenated aCSF flowed at a rate of 1 mL/min.

Carbon fiber microelectrodes approximately 50–200 μm in length were sealed in a glass capillary in-house for FSCV analysis of DA as previously described (7). The carbon fiber microelectrode was placed in the CPu ~75 μm below the surface of the slice in the CPu, and the stimulating electrode was placed directly on the slice approximately 100 - 200 μm away from the carbon fiber microelectrode. The parameters for detecting DA at the electrode surface were completed using a triangle waveform where the electrode potential was initially held at –0.4 V versus an Ag/AgCl reference electrode, ramped up to +1.2 V, and then returned to –0.4 V at 400 V/s at a frequency of 10 Hz (7, 44, 53). DA release was evoked every 5 min by a one pulse monophasic stimulation (350 μA, 60 Hz with 4 ms pulse width) from the stimulating electrode. All electrode and stimulation parameters were controlled by TH software. Stable baseline DA dynamics (release and re-uptake) were measured for at least 30 min.

After stable DA release was recorded, superfusion of METH began with increasing concentrations (0.01–10 μM) delivered to the slice every 30 min. To evaluate DA's affinity for DAT, slice FSCV was used with METH. METH, a competitive inhibitor for the DAT, decreases the amount of DA taken back up into the neuron. The competitive inhibition of DA reuptake is reflected as an increase in the apparent K_m (DA's affinity for the DAT) (53). Equation 4.1 below shows how apparent K_m is calculated, where K_m is the Michaelis-Menton constant and K_i is the inhibition constant. The K_i values are calculated from the slope of the linear regression of METH concentration versus apparent K_m values (shown in equation 4.2). The value of K_m chosen was 0.16 μM , as previously reported in literature (53, 78-80).

$$\text{Apparent } K_m = K_m \times (1 + [i]/K_i) \quad (4.1)$$

$$\text{Slope} = \Delta y/\Delta x = K_m/K_i \quad (4.2)$$

Increasing concentrations of METH were applied to the brain slice since it was previously shown that cumulative concentrations of perfused drugs over a slice do not affect DA release and uptake parameters (53).

Electrodes were post-calibrated with 3 μM DA and the peak oxidation current was converted to concentration. The current versus time plots were fit by non-linear regression using LabVIEW National Instrument software as described by John and Jones (53). Using a Michaelis-Menton base kinetic model (7) peak amplitude of release ($[\text{DA}]_p$), DA uptake kinetics (maximum velocity, V_{max}), and DA's 'apparent' affinity for the transporter (K_m) were determined by fitting DA concentration versus FSCV time traces.

4.2.4 Locomotor activity

Mice were separated into singly housed cages 24 h prior to locomotor analysis. On the day of analysis, mice were transported from the animal facility to the testing facility, their food and water removed, and their home cage was placed into the locomotor activity static chamber. Mice were allowed to habituate for 1 h to minimize the stress of transportation and the novel environment. Spontaneous locomotor activity was recorded using 3 sets of 16-beam infrared (IR) emitter-detector arrays (Med Associates, St. Albans, VT) (81). Interruptions of IR beams resulted in an analog signal being recorded by automated activity software (Open Field Activity Software [SOF-811], Med Associates, St. Albans, VT). This system quantified total beam breaks in both the vertical and horizontal planes, specifically encoding measures of distance traveled (cm; calculated from number of breaks of adjacent beams), ambulatory time (s), and number of rears. Baseline ambulatory distance was measured for a total of 2 h and binned into 10 min periods. To determine locomotor stimulation following METH administration, baseline activity was determined for the first hour then mice were then injected with saline (1.0 mL) i.p. and locomotor activity was collected for a second hour. Mice were then injected with METH (1.0 mg/kg) and locomotor activity was collected for an additional 2 h.

4.2.5 Statistical analysis

Neurochemical data analysis was performed using GraphPad Prism[®] software. Values were reported as mean \pm standard error of mean (SEM) with the criterion for statistical significance set to $P < 0.05$.

For zero-net flux analysis linear regression analysis, the x -axis represents the concentration of DA being perfused into the probe determined by *in vitro* analysis (DA_{in}), and the y -axis represents the difference of DA_{out} , which is defined as the concentration of DA in the dialysate sample from DA_{in} (75). The point at which the regression line crosses the x -axis is known as DA_{ext} and indicates the basal extracellular concentration of DA. The slope of the regression line was used to determine the *in vivo* recovery of DA (E_d , dialysate extraction fraction) (82). Student's t -tests were used to determine if a significant difference existed between the genotypes with respect to DA_{ext} , extracellular metabolite concentrations, and metabolite/DA ratio.

Release and uptake, as determined by FSCV, were analyzed using the Michaelis-Menten kinetic based model which determines changes in $[DA]_p$, V_{max} , and apparent K_m (53, 79, 83). To determine differences in electrically stimulated DA uptake and release between genotypes, two-tailed Student t -tests were used.

Locomotor activity, baseline and METH-induced, were analyzed (IBM SPSS[®] Statistics for Windows) using a 2 x 3 x 12 three-way, repeated measures analysis of variance (ANOVA) with Genotype (WT or BDNF^{+/-}) as the between-subjects factors, and month (12, 15, or 18) and the 12 time blocks as nested within-subjects factors.

4.3 Results

Slice voltammetry experiments and analysis was conducted by Francis K. Maina, Ph.D.

One of the main phenotypic differences reported between wildtype and BDNF^{+/-} mice is that BDNF^{+/-} mice are often heavier than their wildtype counterparts, though the point at which the divergence in weight starts is controversial (64, 65, 123). In the present study, mice were weighed monthly starting at 3 months of age through 18

months to determine when the $BDNF^{+/-}$ mice showed the typical weight gain compared to the age matched wildtype mice. $BDNF^{+/-}$ mice were significantly heavier than their wildtype counterparts as demonstrated by the main effect of genotype (Figure 4.1, $F_{1, 277} = 87.78$, $P < 0.001$). As shown in Figure 4.1, a two-way ANOVA indicates no difference with respect to the main effect of time ($P = 0.19$) or an interaction ($P = 0.95$). To determine if weight was a factor in total locomotor activity, wildtype and $BDNF^{+/-}$ mice weights were analyzed and compared to distance traveled. No difference was observed between heavier mice (40–50 g) and the lean mice (22–30 g) in the amount of distance traveled in cm during a 2 h period, regardless of the genotype (data not shown).

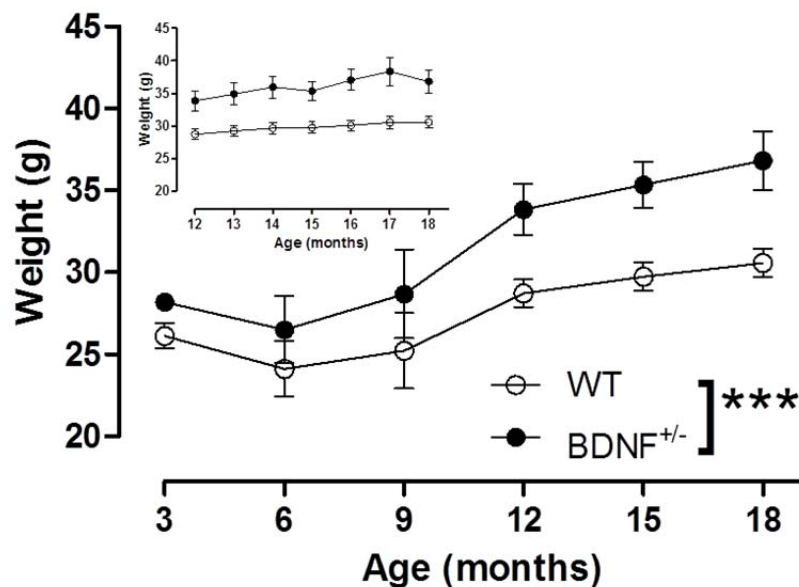


Figure 4.1 Monthly weight in grams of wildtype (WT) and $BDNF^{+/-}$ mice from 3 to 18 months of age. $BDNF^{+/-}$ mice were significantly heavier compared to their wildtype littermates. Inset shows monthly weights from 12–18 months of age. Each point represents the mean \pm SEM for each genotype ($n = 21\text{--}24/\text{genotype}$). Two-way ANOVA showed main effect of genotype ($***P < 0.001$).

Locomotor activity can be an indirect way to measure increases in extracellular DA levels. Locomotor activity testing was conducted at 12, 15, and 18 months of age for both wildtype and $BDNF^{+/-}$ mice to determine if basal activity was different. If differences in locomotor activity were observed it could possibly be indicative of dopaminergic alterations. Using a three-way repeated measures ANOVA analysis, no significance was observed for genotype ($P = 0.96$) or interaction (Figure 4.2; $P = 0.37$), though a significant main effect of time was observed ($F_{11, 374} = 3.81$, $P < 0.001$), and shown in Figure 4.2A–C. Total ambulatory distance for each genotype at 12, 15, and 18 months decreased as the session progressed. No other significant interactions were observed.

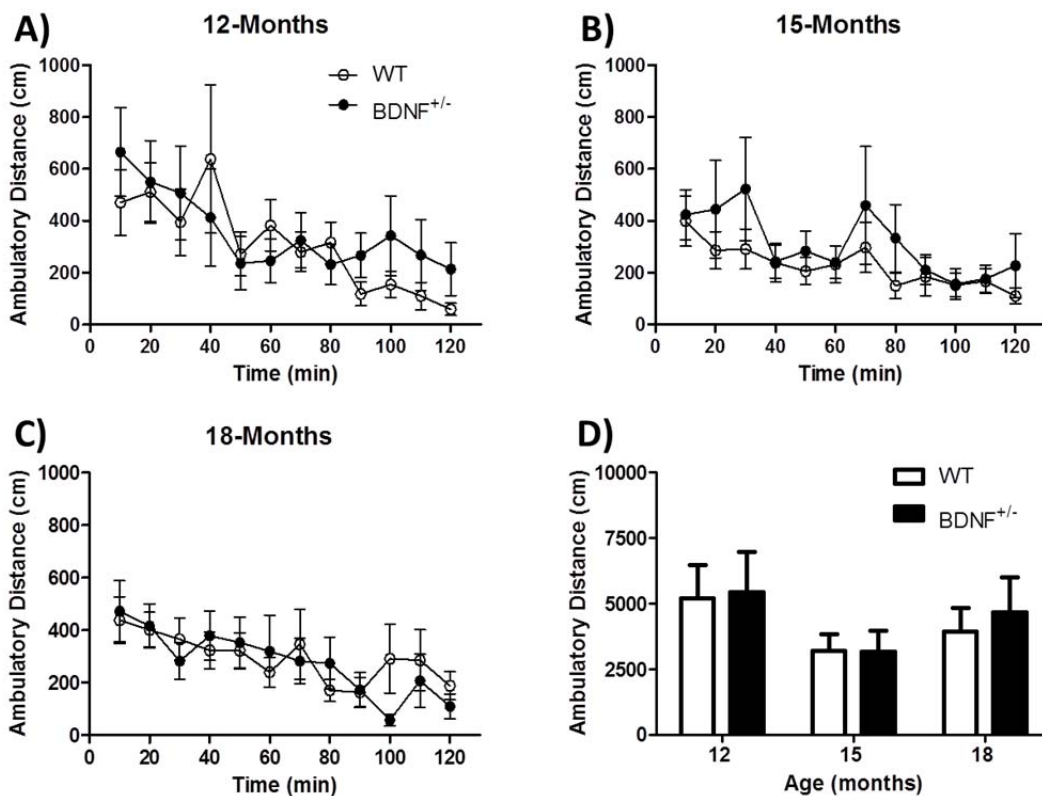


Figure 4.2 Homecage locomotor activity for wildtype (WT) and $BDNF^{+/-}$ mice as they age from 12 to 18 months. A) Ambulatory distance (in cm) for 12 month old mice. B) Ambulatory distance (in cm) for 15 month old mice. C) Ambulatory distance (in cm) for 18 month old mice. D) Cumulative distance traveled during the 2 h at 12, 15, and 18 months of age.

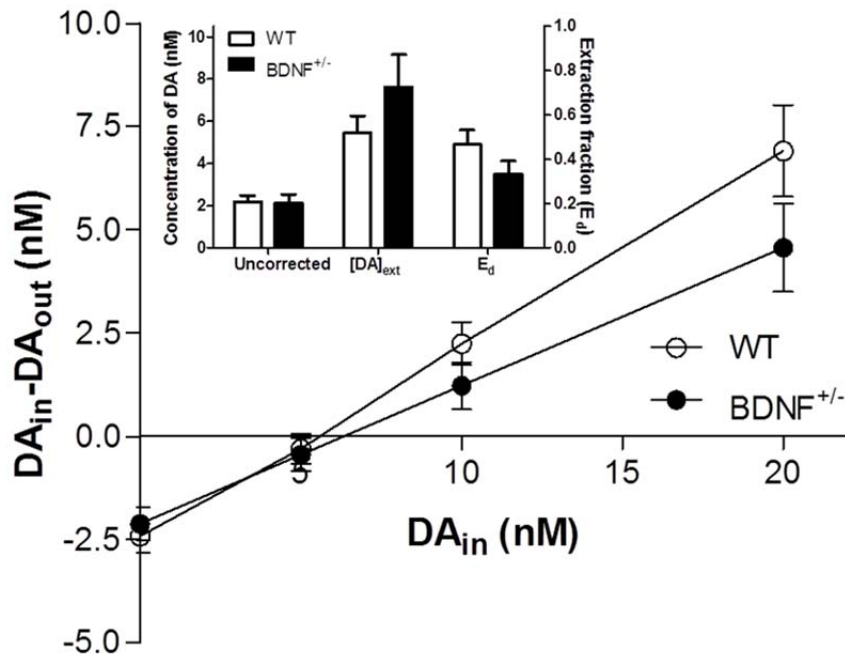


Figure 4.3 DA zero-net flux in the CPU of wildtype and $BDNF^{+/-}$ mice. Linear regression analysis of DA levels from wildtype (WT) and $BDNF^{+/-}$ mice. Apparent extracellular DA levels (DA_{ext}) are represented by the x-intercept. Inset shows mean \pm SEM of the uncorrected DA concentration (extraction fraction; E_d), apparent $[DA_{ext}]$, and slope for both WT and $BDNF^{+/-}$ mice ($n = 11-12$ /group).

Microdialysis experiments were used to determine the influence of a lifelong reduction of BDNF has on the DA system. The uncorrected extracellular DA levels were averaged from three to four baseline fractions, and no difference was observed between the wildtype (2.2 ± 0.3 nM) and $BDNF^{+/-}$ (2.5 ± 0.5 nM) mice (Figure 4.3 inset; $P = 0.86$). Using the *in vivo* microdialysis method of zero-net flux (75), corrected extracellular DA levels (DA_{ext}), and the slope of the regression line (extraction fraction, E_d) for both wildtype and $BDNF^{+/-}$ mice were evaluated in the CPU. DA_{ext} determined from the linear regression line of the zero-net flux experiment (Figure 4.3, x-intercept), for both wildtype and $BDNF^{+/-}$ mice, showed extracellular DA levels at 5.5 ± 0.8 nM and 7.6 ± 1.5 nM, respectively (Figure 4.3 inset; $P = 0.21$). At 18 months of age, both genotypes had corrected extracellular DA (DA_{ext}) concentrations in the CPU consistent with literature

(44, 133, 134). The E_d did not differ between the wildtype (0.47 ± 0.65) and $BDNF^{+/-}$ (0.33 ± 0.58) mice (Figure 4.3 inset; $P = 0.15$).

DA's metabolites, DOPAC and HVA, were also evaluated using *in vivo* microdialysis in both genotypes (Figure 4.4A). Aged $BDNF^{+/-}$ mice had significantly higher DOPAC (710 ± 140 nM, $n = 10$) and HVA levels (710 ± 110 nM, $n = 9$) compared to their aged wildtype littermates (DOPAC 400 ± 145 nM, $n = 14$, and HVA 470 ± 53 nM, $n = 15$; $P < 0.05$). Extracellular DA turnover ratios were determined by dividing the extracellular metabolite concentration by the corresponding uncorrected DA concentrations (Figure 4.4B). Aged $BDNF^{+/-}$ mice had 3-fold increase in their [metabolite]/[DA] ratio for both the [DOPAC]/[DA] and [HVA]/[DA] (600 ± 160 , $n = 10$; and 630 ± 150 , $n = 10$, respectively) compared to their aged wildtype counterparts ([DOPAC]/[DA] 190 ± 33 , $n = 14$; and [HVA]/[DA] 230 ± 34 , $n = 14$; $P < 0.01$).

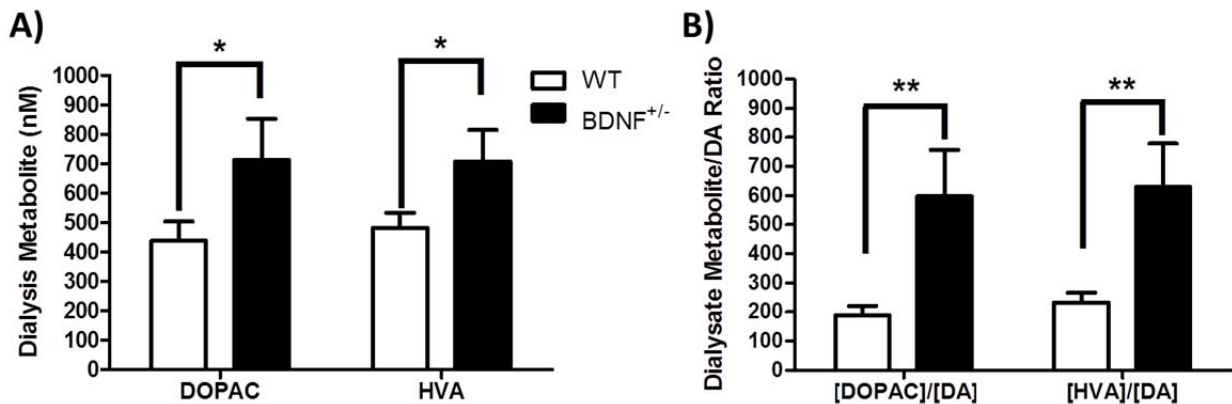


Figure 4.4 Extracellular levels of the DA metabolites DOPAC and HVA and their turnover ratios. A) Extracellular concentration of DOPAC and HVA levels measured by microdialysis from the CPu. B) Extracellular [DOPAC]/[DA] and [HVA]/[DA] ratios. Data are mean \pm SEM ($n = 10-14$). * $P < 0.05$ as compared to wildtype (WT) mice (Student's *t*-test). B) ** $P < 0.01$ as compared to WT mice (Student's *t*-test).

Slice FSCV examined electrically evoked DA release and DA uptake by a single pulse in the CPu of both aged wildtype and $BDNF^{+/-}$ mice. Figure 4.5A shows

representative concentration versus time plot for both genotypes with their corresponding cyclic voltammogram (Figure 4.5A inset). Electrically-evoked DA release ($[DA]_p$) did not differ between genotypes at 18 months of age (wildtype mice: $[DA]_p = 1.8 \pm 0.1 \mu\text{M}$, $n = 19$; $\text{BDNF}^{+/-}$ mice: $[DA]_p = 2.1 \pm 0.2 \mu\text{M}$, $n = 11$; Figure 4.5B). Similarly DA uptake, V_{max} , was not different between genotypes at this age (Figure 4.5C, wildtype mice: $V_{\text{max}} = 4.1 \pm 0.3 \mu\text{M/s}$, $n = 18$; $\text{BDNF}^{+/-}$ mice: $V_{\text{max}} = 4.0 \pm 0.2 \mu\text{M/s}$, $n = 12$).

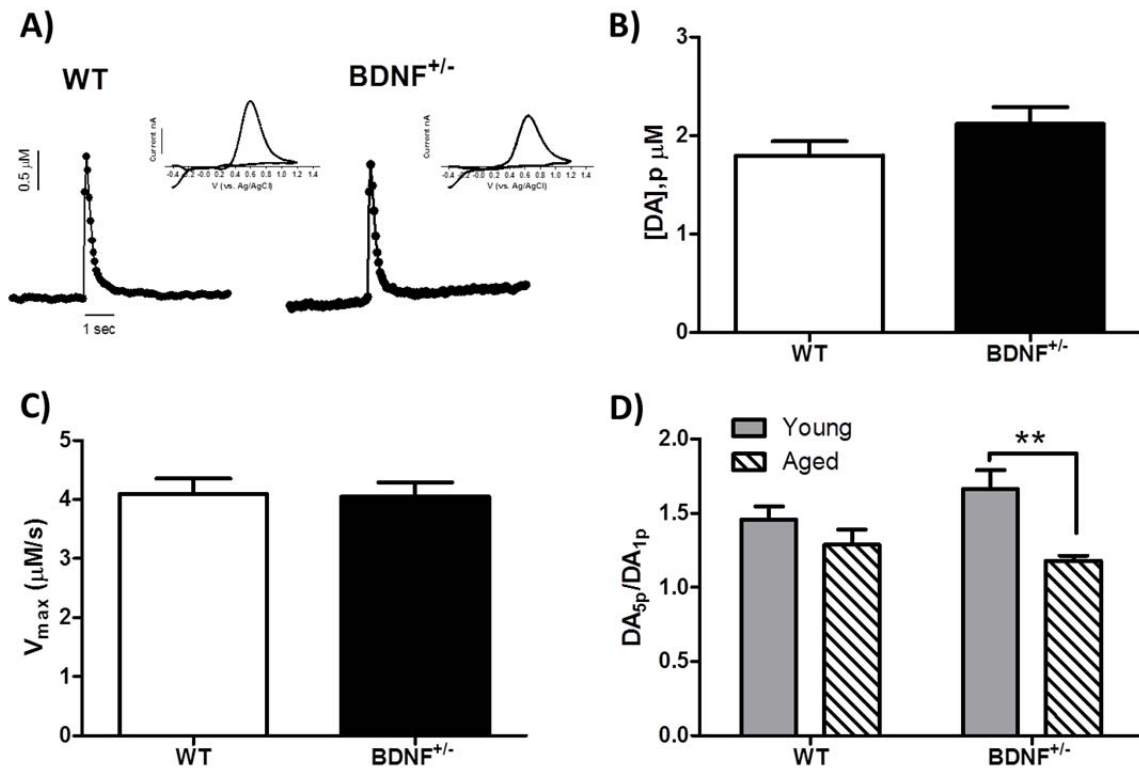


Figure 4.5 Slice FSCV of presynaptic striatal DA dynamics. A) Representative current versus time electrically-evoked DA release and uptake in the CPu from wildtype (WT) and $\text{BDNF}^{+/-}$ mice with corresponding cyclic voltammogram indicating DA detection. B) Average electrically evoked DA release ($[DA]_p$) from the CPu of aged mice. C) Average striatal DA uptake rates (V_{max}). D) The average ratio of phasic-to-tonic for young adult (3-5 months) and aged (18 month) mice in the CPu. Data is represented as mean \pm SEM ($n = 11-17$, $**P < 0.01$).

As the adult $\text{BDNF}^{+/-}$ mice age, electrically evoked striatal DA release changes with respect to time. Where young $\text{BDNF}^{+/-}$ mice had decreased electrically evoked

striatal DA release, the aged BDNF^{+/-} mice electrically evoked DA release did not change with respect to their wildtype littermates (44). As a result of this difference in evoked DA release in the BDNF^{+/-} mice as they age, tonic and phasic DA transmission in both young adult (4 months) and aged (18 months) wildtype and BDNF^{+/-} mice were observed by varying the stimulation pulses (p) from 1p (tonic) to a 5p (phasic) train. Two-way ANOVA revealed a main effect of age in BDNF^{+/-} mice with respect to phasic-to-tonic (5p/1p) DA signaling (Figure 4.5D, $F_{1, 49} = 10.23$, $P < 0.01$). There was no main effect of genotype or genotype X age interaction ($F_{1, 49} = 0.22$, $P = 0.64$ and $F_{1, 49} = 2.36$, $P = 0.13$, respectively).

Similar to evoked DA release, DAT functionality increases in the aged BDNF^{+/-} mice to the DAT uptake rates observed in the aged wildtype mice. Therefore, another experiment using microdialysis was done to better understand DAT dynamics in aged mice using METH. METH was used to probe the transporter functionality with microdialysis, FSCV, and locomotor activity. METH is known to disrupt the vesicular monoamine transporters ability to sequester DA in vesicles resulting in a greater efflux of DA into the extracellular space (135). In our microdialysis experiment, 60 min of baseline samples were collected, at which time the mouse was administered 1.0 mg/kg, i.p. injection of METH (Figure 4.6A), and samples were collected for an additional 120 min. Extracellular DA levels are reported as a percent of DA baseline. METH induced a maximal response 40 min after an injection in both genotypes (wildtype: 561% and BDNF^{+/-}: 724%). Using a two-way repeated measure ANOVA main effect time ($F_{8, 208} = 30.47$, $P < 0.001$) was observed but not genotype ($F_{1, 208} = 1.52$, $P = 0.23$).

Locomotor activity was assessed in the aged mice after an acute injection of METH (Figure 4.6B). Using two-way ANOVA, there was a significant main effect of time ($F_{29, 1106} = 2.0$, $P < 0.01$), but no difference was observed between genotypes or an interaction ($F_{1, 1106} = 0.35$, $P = 0.55$, and $F_{29, 1106} = 0.51$, $P = 0.99$, respectively). At the 190 min time point, a sharp increase in locomotor activity is seen for both genotypes which continued for 30 min before descending back towards baseline locomotor activity levels. The effect of a single METH concentration was measured for 30 min. Figure 4.6C shows non-linear fitting (Figure 4.6D is the linear portion of 4.6C) of a dose-dependent increase in apparent K_m with increasing METH concentrations. This increase in apparent K_m represents a decrease in affinity of DA for its transporter. Both aged genotypes had a dose dependent increase in the apparent K_m values. Two-way ANOVA for the analysis of non-linear fitting showed a significant main effect of METH treatment ($F_{6, 316} = 96.50$, $P < 0.001$), but no significant difference in apparent K_m was observed between the aged mice at either genotype ($P = 0.89$). There was no interaction between genotype X treatment ($P = 0.99$), thus, the potency of METH is the same across the aged genotypes. To quantify K_i , DA uptake inhibition, values for METH, the slopes of the lines from Figure 4.6D were calculated, and slopes are similar for both genotypes (wildtype mice: 0.026 ± 0.002 , $n = 14$, and BDNF^{+/-} mice: 0.021 ± 0.002 , $n = 12$).

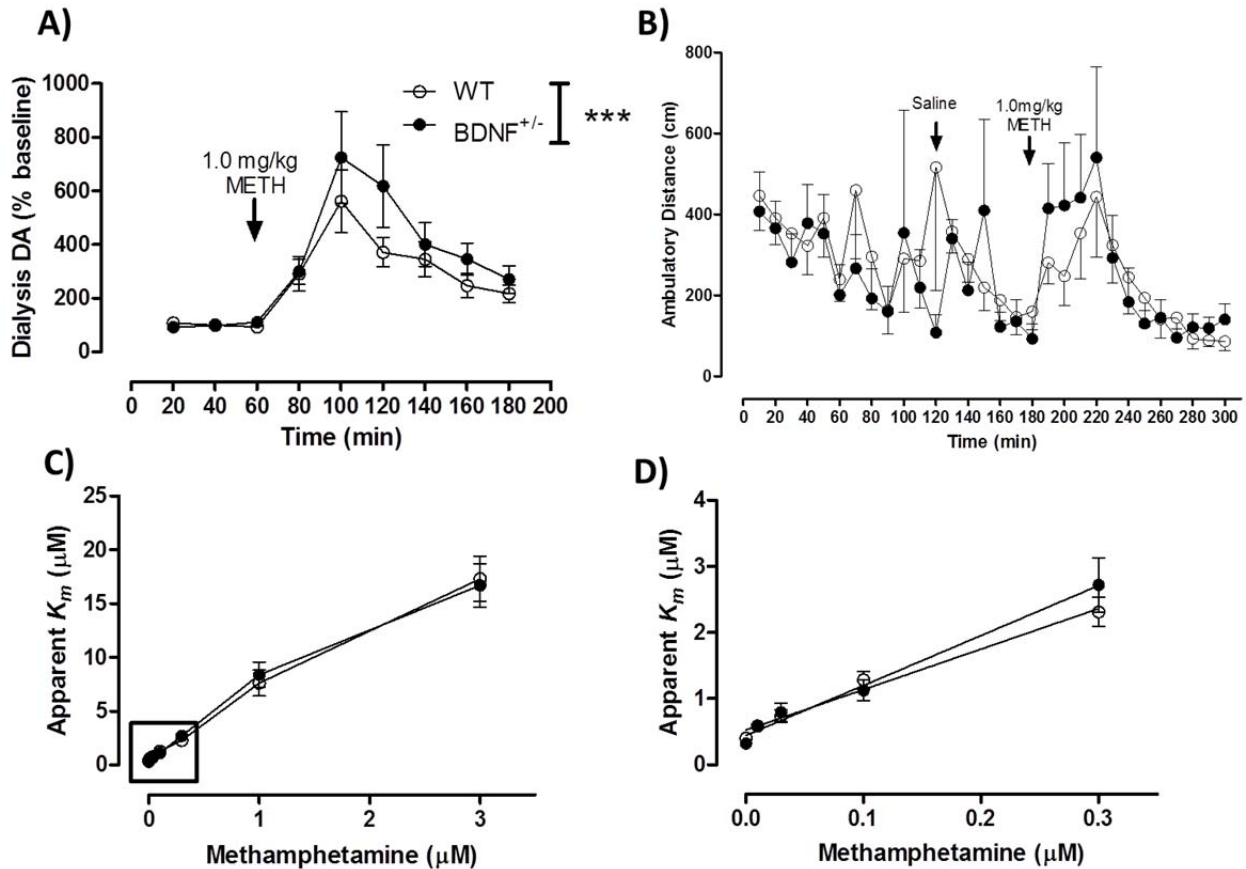


Figure 4.6 Influence of methamphetamine (METH) on striatal DA dynamics and locomotor behavior. A) Microdialysis measurement of METH induced dopamine release, reported as percent baseline. B) Ambulatory distance traveled of wildtype (WT) and BDNF^{+/-} mice. Baseline was collected for the first 2 h then saline was injected (arrow) and the ambulatory distance was measured. At the 180 min mark, an i.p. injection of METH (1 mg/kg) was administered and ambulatory distance was measured. (n = 17–25/per group). C) Non-linear fitting of dose-dependent increase in apparent K_m values with increasing METH concentrations using FSCV. D) Linear regression plots of the apparent K_m values using FSCV with increasing concentrations of METH.

4.4 Discussion

A lifelong reduction in BDNF results in a striatal dopaminergic system which changes with respect to age. Instead of the aged BDNF^{+/-} mice having a hyperdopaminergic striatal system as seen in the young BDNF^{+/-} mice, the aged BDNF^{+/-} mice dopaminergic system appears to ‘normalize’ to a level comparable to the young adult and aged wildtype mice with respect to extracellular DA levels, DA release,

and DAT uptake rates. Extracellular DA levels in the aged BDNF^{+/-} mice are attenuated from 12.0 nM in young, to 7.6 nM in aged BDNF^{+/-} mice (see Table 4.1) (44). Interestingly, extracellular DA levels in aged BDNF^{+/-} mice decrease to levels similar to the aged wildtype mice. Our steady state striatal DA concentrations are in agreement with our basal uncorrected DA levels (see Figure 4.3 inset) where no differences between the genotypes were observed. However, a previous microdialysis study in aged BDNF^{+/-} mice reported a decrease in uncorrected extracellular DA levels compared to their wildtype counterparts in both young adult (3 months) and middle aged mice (12 months) (64). Strain and age differences, as well as method parameters like microdialysis probe size (1 vs. 2 mm probe) and slight medial-lateral variation in probe placement in the CPU may account for these divergences in extracellular DA levels between our aged results and those reported by Boger (64). No changes in extracellular DA levels further suggest that there is no significant degeneration of striatal DA neurons in these aged animals (136, 137). Supporting the hypothesis of the absence of neuronal degeneration, is cell morphology of nigral-striatal DA neurons and MSNs in the dorsal striatum were no different in aged BDNF^{+/-} mice (18 to 24 months old) (23, 123, 138).

	Young WT [#]	Young BDNF ^{+/-} [#]	Aged WT	Aged BDNF ^{+/-}
DA _{ext} (nM)	5.0 ± 0.2	12.0 ± 0.4 ^{###}	5.5 ± 0.8	7.6 ± 1.5*
DOPAC (nM)	410 ± 70	330 ± 90	400 ± 145	710 ± 140*
HVA (nM)	465 ± 65	560 ± 120	467 ± 53	710 ± 110
Release ([DA] _p) (μM)	1.8 ± 0.1	1.2 ± 0.1 ^{###}	1.8 ± 0.1	2.1 ± 0.2***
Uptake (V _{max}) (μM/s)	4.1 ± 0.1	2.7 ± 0.1 ^{###}	4.1 ± 0.3	4.0 ± 0.2***

Table 4.1 Young mice (3–5 months) versus aged mice (18 months). Student-*t* test showed significance between young wildtype (WT) and BDNF^{+/-} (###*P* < 0.001), and between young BDNF^{+/-} and aged BDNF^{+/-} (**P* < 0.05, ****P* < 0.0001). #Data from (44).

Although no alterations were observed in extracellular DA levels between aged wildtype and BDNF^{+/-} mice, there was an increase in DA metabolism as measured by microdialysis. An increase in both extracellular DOPAC and HVA levels in the aged BDNF^{+/-} mice could contribute to the reduced extracellular DA levels in the aged BDNF^{+/-} mice to that of the aged wildtype mice. Monoamine metabolic abnormalities have been observed in BDNF-deficient mice with respect to the serotonin system (65). Similarly, young (Table 4.1, (44)) and aged neurochemical measurements parallel the dysregulation of serotonin in aged BDNF^{+/-} mice by Lyons (65). Together, the dysregulation of the aging DA and serotonin systems in BDNF^{+/-} mice strongly supports the hypothesis that normal BDNF levels are required for proper monoamine functioning. Young adult BDNF^{+/-} mice showed no metabolism or synthesis differences (44). Thus, it appears as the BDNF^{+/-} mice age, activity or function of metabolic enzymes such as MAO is enhanced, and age-related changes in MAO isoforms are not uncommon. For example, levels of the MAO isoforms diverge as C57BL/6J mice age, where MAO-A levels were steady as the animals aged to 25 months, while MAO-B levels gradually increased (129). Furthermore, a MAO-B transgenic mouse with 2.5 times the expression of MAO-B shows a 60% reduction in striatal DA levels measured by tissue content at 2–6 months of age, with a concomitant 50% reduction in dopaminergic substantia nigra (SN) neurons by 14 months of age (67) suggesting a pivotal role for MAO in regulating the DA system during the aging process. Elevated MAO-B levels could be detrimental to the surrounding systems because increased DA metabolism could lead to an elevated production of ROS. In the aged BDNF^{+/-} and wildtype mice, there are no differences in striatal DA levels are observed, which contradicts previous

literature findings with respect to elevated MAO-B expression (67, 129). To further support the hypothesis that MAO is upregulated or has increased functionality in aged BDNF^{+/-} mice, the extracellular turnover ratio between [DOPAC]/[DA] and [HVA]/[DA] are significantly elevated in BDNF^{+/-} mice compared to their age matched wildtype mice. The increase in the [DOPAC]/[DA] ratio in aged BDNF^{+/-} mice suggests an elevation in MAO activity or function throughout the lifespan of the BDNF^{+/-} mice. To better understand these monoaminergic changes in aging mice, future studies should focus on the expression and activity of the MAO isoforms in the striatum of aged BDNF^{+/-} mice to fully assess these alterations in metabolism. Increases in MAO activity may provide crucial evidence affirming the metabolic alterations observed in the aged BDNF^{+/-} mice.

Extracellular DA levels are not strictly regulated by metabolism. The dominant mechanism for regulating extracellular DA is uptake via the DAT. As the BDNF^{+/-} mice aged from 3 to 18 months, DA uptake rates increased in the aged BDNF^{+/-} mice to rates similar to their aged matched wildtype mice. Thus, young adult BDNF^{+/-} mice have a slower DAT function that is likely to cause their elevated striatal extracellular DA levels (44). As the BDNF^{+/-} mice age, DAT function appears to increase approximately to the uptake rate of the aged wildtype mice. Presumably, this faster rate of DA clearance leads to decreasing extracellular DA levels in aged BDNF^{+/-} mice. Autoradiography studies support this hypothesis since DAT expression is not different between the genotypes (64). Together, these findings support the proposition that DAT function increases with age in the BDNF^{+/-} mice.

When a 100 ng/mL infusion of BDNF was applied to young adult BDNF^{+/-} mouse striatal slices, it increased stimulated DA release by 20%, while BDNF infusion resulted

in no difference in stimulated DA levels in the wildtype mice (44). Taken together, these results from the young mice suggest that BDNF's primary role is to regulate DA release. Based upon the findings by Bosse *et al.*, and our current findings that suggest DA dynamics in BDNF^{+/-} mice normalize with age, the next step was to evaluate the role of endogenous BDNF on tonic and phasic DA release between young and aged mice (44). The frequency of DA release in the dorsal and ventral striatum can be regulated either endogenously or exogenously by other factors (139). Young adult BDNF^{+/-} mice showed a 40% reduction in evoked DA release during a 1 pulse (1 p) stimulation in the CPu and correlated with a stronger facilitation of DA release during a 5 p 'phasic-like' stimulation. Furthermore, young and aged wildtype mice had a relatively greater evoked DA release by a 1 p stimulation in the CPu when compared to the younger BDNF^{+/-} mice, and upon a phasic-like stimulation the relative DA response was similar between young and aged wildtype mice. Interestingly, the aged BDNF^{+/-} mice parallel their wildtype counterparts with restored 1 p release in which no difference was observed in the aged BDNF^{+/-} mice phasic-like release. The tonic and phasic results in the CPu of young wildtype and BDNF^{+/-} mice parallels the tonic versus phasic results between the dorsal and ventral striatum (139) further suggesting that endogenous BDNF levels are a strong contributor to the regulation of DA release in the CPu, particularly in young animals. Measurements of BDNF protein levels in BDNF^{+/-} mice by others show significantly lower levels at three distinct time points versus their wildtype littermates (64). Although Boger *et al.* reported no difference on striatal BDNF levels due to age, there appears to be a trend toward decreased BDNF levels with age across the two genotypes (64). In both genotypes, the difference in BDNF levels in 21 month old mice are less than at 3 months of age, further

suggesting that BDNF dynamics are more similar between the two genotypes at advanced ages versus a younger age (64). Our striatal DA results are in agreement with the notion that there is a greater difference in striatal BDNF levels when mice are young. As the mice age, the difference in BDNF levels is minimized resulting in the two aged genotypes appearing more similar with respect to their DA dynamics.

With these significant alterations in the aging striatal DA system of BDNF^{+/-} mice, we further evaluated the effect of an acute dose of METH. Numerous studies have examined the effect of psychostimulants, specifically amphetamine related compounds in BDNF^{+/-} mice. Administration of psychostimulants to BDNF^{+/-} mice blunts their monoamine response compared to their wildtype littermates (30, 65, 140). For instance, Saylor and McGinty observed no difference in the TH synthesis after an acute injection of amphetamine in 3 month old BDNF^{+/-} mice, suggesting an abnormality in DA release and not DA synthesis (140). An acute injection of amphetamine elevated mRNA expression of TrkB, BDNF, and TH in the CPu of wildtype mice, but no differences in these expression levels were observed in the BDNF^{+/-} mice, suggesting that amphetamine is responsible for changes in gene expression of not only TH, but also BDNF and its receptor TrkB (140). Furthermore, Dluzen and colleagues proposed that young BDNF^{+/-} mice are protected from the neurotoxic effects of amphetamines due to this reduced DA uptake and release (96). Many of these amphetamine studies have been done in younger mice, and to better understand psychostimulant effects on a DA system with a lifelong reduction of BDNF, an acute injection of METH was administered to the aged BDNF^{+/-} mice. Similar to the results throughout this paper, METH-induced DA release via *in vivo* microdialysis and locomotor activity was not different between the

two genotypes. No alterations in DA dynamics of aged BDNF^{+/-} mice may be a result of the DAT having an increase in functionality in comparison to the young BDNF^{+/-} mice. When probing the functionality of the DAT with METH, the K_m values were not significantly different between the aged genotypes, suggesting the potency of METH's effects on DAT is similar across genotypes. These results contradict our predicted hypothesis, that METH-induced stimulation would potentiate the release of extracellular DA in aged BDNF^{+/-} mice, which was based on the initial belief that BDNF^{+/-} mice have a slower rate of DAT uptake or decrease in function versus aged wildtype mice. The alterations that were observed in DAT function suggests that the BDNF^{+/-} mice are not protected from METH's effects as proposed by Dluzen (93). Our results would suggest that the aged BDNF^{+/-} mice are equally susceptible to METH-induced DA release, via the reversal of DAT, to being no longer different from their aged wildtype mice (93).

One caveat in using knockout animals, even animals with only a 50% reduction of BDNF, is that the gene mutation has been present since conception and numerous neuroadaptations are possible. Thus, it is possible that other neurotrophic systems have taken on a more prominent role, leading to these age-dependent DA alterations occurring in the BDNF^{+/-} mice. One possible candidate is neurotrophin 4 (NT-4), which also binds and acts on the TrkB receptor. For example, Hill *et al.*, demonstrated that striatal TrkB levels in 3 month old BDNF^{+/-} mice are not different from wildtype mice, while striatal NT-4 levels are increased in BDNF^{+/-} mice compared to their wildtype littermates (61). These results suggest that the NT-4 system may be upregulated and compensating for the decrease in BDNF levels. To further validate this hypothesis, experiments using double knockout mice lacking both BDNF and NT-4 showed that

these mice had a 25% decrease in TH cells in a visceral sensory population of the nodose–petrosal ganglion complex compared to only BDNF^{+/-} mice (141). If NT-4 increases with respect to age, then future experiments need to evaluate at what age NT-4 begins to take on a more compensatory role in the striatum of BDNF^{+/-} mice.

Overall, our results on the striatal dopaminergic system in the aged BDNF^{+/-} mice demonstrate that this system dynamically adjusts to lifelong reductions in BDNF. In particular, aged BDNF^{+/-} mice are not more susceptible to the aging process and the detrimental effects associated with aging. Instead, it appears that the DA system adjusts accordingly as these mice age. Aged BDNF^{+/-} mice show a decrease in extracellular DA levels, and potentiated DA release, and uptake compared to their younger counterparts (44). This normalization of the dopaminergic system in BDNF^{+/-} mice appears to be persistent as the mice age, and is also apparent with respect to locomotor activity, in which no difference is observed between the BDNF^{+/-} mice and their wildtype counterparts between 12 to 18 months of age. The results from the aged BDNF^{+/-} mice highlight the dynamic role that BDNF plays throughout the life of an organism; specifically, with respect to the striatal DA system. However, the ability of the DA system to normalize with respect to age begs for a deeper understanding of the mechanism that causes these changes in BDNF^{+/-} mice. Ultimately, these results will assist our understanding on how life-long reductions of BDNF influence striatal DA dynamics and may provide further insight on how lower BDNF levels increases ones susceptibility to the detrimental diseases of the brain that can occur during aging process.

CHAPTER 5

Simultaneous Detection of Monoamine and Purine Molecules using High-Performance Liquid Chromatography with a Boron-Doped Diamond Electrode

(Portions from the text in this chapter were reprinted or adapted with permission from Birbeck, J. A., and Mathews, T. A. (2013) Simultaneous Detection of Monoamine and Purine Molecules Using High-Performance Liquid Chromatography with a Boron-Doped Diamond Electrode, *Anal Chem*. Copyright (2013) American Chemical Society.)

5.1 Introduction

The detection of neurotransmitters in an *in vivo* or *in vitro* environment typically employs a separation operation such as high performance liquid chromatography (HPLC) or capillary electrophoresis with corresponding detection methods such as electrochemical (monoamines), UV absorbance (amino acids), fluorescence (amino acids), or mass spectrometry (peptides) (44-47). A notable bioanalytical challenge is the simultaneous detection of multiple neurotransmitter families together using a single analytical tool. Mass spectrometry has successfully been used to simultaneously detect monoamines, purines, and amino acids through a derivatization step with benzyl chloride (142). Although mass spectrometry is frequently the method of choice for detecting multiple analytes across various families, limitations of using this technique in neurochemistry include the cost and expertise needed to analyze the samples. Instead, most neuroscientists use HPLC with electrochemical, UV, and fluorescence detection, to separate, detect, and quantify neurotransmitters. Electrochemical detection has been used to identify monoamines and amino acids, although typically not simultaneously

(143, 144). Often, electrochemical detection, in conjunction with HPLC, utilizes a glassy carbon amperometric cell or a porous carbon coulometric cell and is limited to the detection of molecules which are electrochemically active, such as the monoamines dopamine (DA), serotonin (5-HT), and their metabolites (44, 45, 76). Amino acids such as glutamate, glutamine, and γ -aminobutyric acid (GABA) also are detected electrochemically, but are derivatized, for example, using *o*-phthalaldehyde (OPA) or naphthalene-2,3-dicarboxaldehyde (NDA) (143, 145-147). However, derivatization using OPA has disadvantages such as instability, chromatographic contamination, and incompatibility with biological matrixes such as dialysate and tissue content samples (145, 148, 149).

Within the last few decades, alternative carbon-based electrode materials have been discovered and developed, with one of particular interest being the boron-doped diamond (BDD) electrode. BDD electrodes began as home-built microelectrodes (51, 56, 150). The original laboratories pioneered the development and biochemical application of the BDD electrode in many areas throughout neuroscience and also in gastrointestinal tract and cancerous tumor (59, 150-153). In comparison with the carbon electrode, the BDD electrode has a higher potential working range, decreased background noise, electrochemical stability due to diamond surface coordination, insensitivity to dissolved oxygen, and less susceptibility to electrode fouling (51, 52). These advantages, along with the advent of a new commercially available BDD disk electrode for use with HPLC, make the BDD electrode an attractive detection method for molecules with higher oxidation potentials and those that are easily oxidizable.

The objective of this work was to develop a method based on the commercially available BDD electrode for the simultaneous detection of adenosine (Ado) and DA. Little is known about the *in vivo* function of Ado, but there is considerable data linking DA and Ado through their respective receptors, the DA D₂ receptors and the Ado A_{2A} receptors (2, 154, 155). Furthermore, DA and Ado were chosen because of their intertwining relationship in the brain and in diseases and disorders like Parkinson's disease and schizophrenia (2, 11, 156, 157). Multiple detection methods are available for the analyzing DA and Ado such as HPLC coupled with electrochemical and UV detection, capillary LC with electrochemical detection, mass spectrometry, or fast scan cyclic voltammetry (9, 45, 54, 55, 158). However, drawbacks of some of these methods are long analysis time from a two-component system, poor detection limits, and the ability to measure only one or two of the analytes at a time (45, 54). To date, the detection of Ado using carbon-based electrode cells (glassy or porous) with HPLC has not been achieved. This limitation relates to the fact that oxidation of Ado at a bulk electrode is not feasible because of the high potential required to oxidize Ado (approximately +1500 mV); potentials greater than +1000 mV cause surface oxidation, instability, and high background noise with carbon-based electrodes (49). The developed HPLC-BDD method described in this article shows the separation and detection of nine molecules including DA and Ado and other members of the monoamines and purine families in 28 min. The advent of developing a method that determines multiple classes of neurotransmitters in a single run is valuable because smaller sample size can be utilized, analysis costs will be lower, and fewer animals will be sacrificed.

5.2 Materials and Methods

5.2.1 Chemicals

Chemicals used for mobile phase, buffers, and standards were of HPLC grade or higher purity and were purchased from Sigma-Aldrich (St. Louis, MO), Fisher Scientific (Pittsburgh, PA), and EMD (Gibbstown, NJ). For DA, standards were made up in 1 mM stock solutions by adding 0.1 M HClO₄, 10% methanol, and 10 μg/mL ascorbic acid, and stored at -80 °C until analysis. 3,4-Dihydroxyphenylacetic acid (DOPAC), homovanillic acid (HVA), 3-methoxytyramine (3-MT), norepinephrine (NE), 5-HT, and 5-hydroxyindoleacetic acid (5-HIAA) were made up in 0.1 M HClO₄ and stored in at -4 °C until analysis. Ado and adenosine monophosphate (AMP) were made up in 0.1 M HClO₄ and at -80 °C stored until further use.

5.2.2 Analytical parameters

Isocratic monoamine and purine separation were completed using a Shimadzu LC-20A HPLC instrument coupled to a Thermo Scientific ESA Coulochem III detector. The electrochemical cell used for detection was a Thermo Scientific ESA model 5041 analytical cell with a BDD disk electrode (Figure 5.1A). The column used was a Thermo Scientific Acclaim Trinity P1 column (100 x 3 mm, 3 μm particle size). Mobile phase was composed of 45 mM (NH₄)₃PO₄, 1.1 mM Na₄P₂O₇, 4% acetonitrile, and was adjusted to pH 3.00 using phosphoric acid (85 wt %). The mobile phase was subsequently purged with argon and then sonicated. The flow rate was set at 0.65 mL/min. The potential for simultaneous detection of DA and Ado was determined by a hydrodynamic voltammogram, and the optimal potential to detect both analytes was +840 mV versus a palladium reference electrode. The approximate analysis time for both DA and Ado was

less than 10 min. For a more comprehensive analysis of monoamines such as DOPAC, HVA, 3-MT, NE, 5-HT, and 5-HIAA, and the purine AMP, the total analysis time was 28 min. Analyte peak areas for monoamine and purine molecules were determined against known standards and integrated using LC Solutions Shimadzu Software.

For isocratic carbon-based electrochemical cell analysis, a Thermo Scientific ESA coulometric cell model 5014B microdialysis cell with potentials for the working electrodes 1 and 2 (E_1 and E_2) set at -150 and +220 mV, respectively, versus a palladium reference electrode. The mobile phase used for separation of monoamines at the carbon electrode consisted of (in mM concentrations) 75 NaH_2PO_4 monohydrate, 1.4–1.8 1-octanesulfonic acid, 0.125 ethylenediaminetetraacetic acid (EDTA), 10% acetonitrile, 0.002% triethylamine; adjusted to pH 3.00 with phosphoric acid (85 wt %). The mobile phase was then purged with argon before being placed onto the system, and the flow rate was set to 0.35 mL/min. The column used for analysis was a Phenomenex Luna 2.5 μm C_{18} (2)-HST (100 x 3 mm, 2.5 μm particle size). The analyte peak areas for monoamines were analyzed against known standards and integrated using LC Solution Shimadzu Software.

5.2.3 Tissue content

The animals used in the tissue-content experiments were female C57BL6/J mice that were bred in-house. Breeder mice were obtained from Jackson Laboratories (Bar Harbor, ME). Mice were sacrificed by cervical dislocation, and their brains were rapidly removed. The brain regions of the frontal cortex and striatum were dissected out, rapidly frozen in liquid nitrogen, and stored at -80 °C until analysis. On the day of analysis, tissue was removed from the freezer and allowed to thaw on ice for approximately 30

min. A volume of 250 μL of 0.1 M HClO_4 was added to each vial of tissue and the tissue was homogenized. Vials were centrifuged for 10 min at a rate of 12000 rpm at 4 °C. A 20 μL volume of supernatant was injected onto the HPLC instrument. Tissue concentrations of monoamines and purines were determined using a linear regression analysis from peak areas that were integrated and quantified against a set of standards using LC Solutions Shimadzu Software. Monoamine and purine tissue levels are represented as nanograms monoamine or purine per milligram of protein. Protein values were measured using Pierce bicinchoninic acid (BCA) protein assay kit. All experiments and procedures were in accordance with the National Institute of Health Animal guidelines, were approved by Wayne State University Institutional Animal Care and Use Committee, and were designed to minimize discomfort in the animals.

5.3 Results and Discussion

5.3.1 Electrode Characterization

Figure 5.1B shows a scanning electron microscopy (SEM) image of the relatively uniform surface of a BDD disk electrode (length along the straight edge: 1.20 cm, radius of arch = 1.50 cm) used for experimentation herein, which was manufactured and is distributed by Thermo Scientific ESA (50). The design of the Thermo Scientific ESA 5041 analytical cell is versatile in that it accommodates the BDD electrode as well as other various electrode materials such as glassy carbon, platinum, silver, and gold. Furthermore, no pretreatment of the BDD electrode is required after it has been placed into the 5041 Analytical Cell.

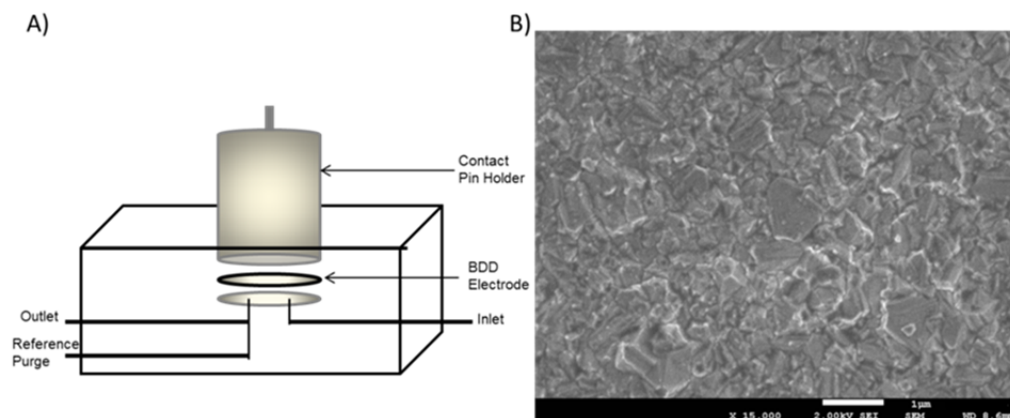


Figure 5.1 A) Schematic amperometric cell design for the commercially available boron-doped diamond electrode manufactured by Thermo Scientific ESA Inc.TM B) SEM image of the bare electrode surface taken at 15,000 x 2.0 V.

5.3.2 Mobile Phase Parameters

Initial experiments focused on determining the proper mobile-phase configuration for the simultaneous detection of DA and Ado using the BDD electrode. Numerous mobile phases were examined with the BDD electrode, including the sodium phosphate mobile phase that is described for use with the porous carbon electrode in Materials and Methods and a sodium acetate mobile phase. However, there were limitations with these mobile phases, including that the sodium phosphate mobile phase was able to detect only DA and not Ado and generated too many unknown peaks and the presence of EDTA in the mobile phase at potentials greater than +500 mV lead to an increase in the background noise. Even though the sodium acetate mobile phase was able to detect both DA and Ado, after three days of analysis, the mobile phase was completely unusable because of increasing background noise due to the oxidation of the acetate. Methanol was also evaluated in place of acetonitrile, but it also increased the background noise in a manner similar to that of EDTA with the BDD electrode. Therefore, acetonitrile was used. The final mobile phase that was developed consisted of ammonium phosphate, sodium pyrophosphate, and acetonitrile, and lead to reliable

separation and detection of DA and Ado. After further refinement of the current mobile phase, NE, DOPAC, HVA, 3-MT, 5-HT, 5-HIAA, and AMP were clearly separated.

5.3.3 Hydrodynamic Voltammogram

A hydrodynamic voltammogram was constructed for DA and Ado to determine the optimal working potential sufficient for the simultaneous detection of both of these molecules using the BDD electrode. The initial potential for the hydrodynamic voltammogram was set to 0 mV, and the potential was subsequently increased by +20 and +100 mV until a final potential of +1200 mV was obtained. The responses of DA and Ado were measured in triplicates using a 300 nM standard, and the averages are plotted as the percentages of the normalized response in Figure 5.2. The optimum oxidation potential for detecting DA and Ado at the BDD electrode were found to be +740 mV and +1200 mV, respectively. The DA oxidation potential reported here is slightly negative compared to previous reports using BDD electrode (150, 159). This shift in DA oxidation is due to the fact that the reference electrode is palladium and not the standard Ag/AgCl reference electrode, where the palladium electrode detection is ~300 mV lower than the Ag/AgCl reference electrode. When this potential difference is taken into account, the equivalent applied potential at a BDD electrode using a Ag/AgCl reference electrode would be approximately +1040 mV, which is in agreement with literature for DA detection (150, 159). The large oxidation potential difference observed between DA and Ado at the BDD electrode is similar to results obtained using a carbon-fiber microelectrode with a Ag/AgCl reference, where the peak oxidation separation was ~900 mV (55). For the BDD electrode method, a working potential of +840 mV was chosen because it provided optimal detection for both DA and Ado (Figure 5.2, dashed

line). Although +840 mV is not strictly the average of the two potentials, this oxidation potential was specifically chosen because it is more sensitive for DA than for Ado. This criterion was set because extra- and intracellular DA levels in the brain are reported to be between 6- and 100-fold lower in concentration compared to Ado (44, 142, 144, 160, 161). Therefore, it is imperative that the sensitivity for DA be greater than that for Ado.

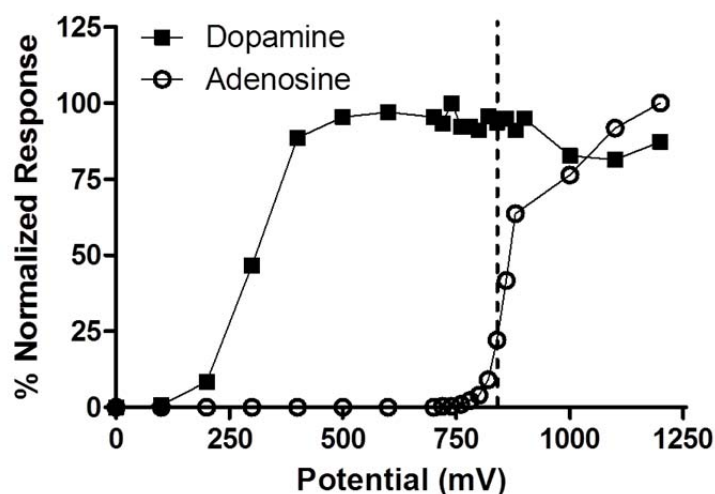


Figure 5.2 Hydrodynamic voltammogram to determine the optimal potential for the oxidation of adenosine (○) and dopamine (■). Dashed line from the x-axis represents the optimal potential selected for measuring adenosine and dopamine.

5.3.4 Linearity

To determine whether these analytes respond in a concentration-dependent manner, linear calibration curves were created for both DA and Ado at different gains. DA and Ado stock standards were diluted in water, injected onto the HPLC instrument, and plotted as the area under the curve versus concentration. After the plots had been constructed, linear regression analysis was used to determine the slope of the line (sensitivity: Table 5.1), y-axis intercept, and correlation values (R^2) for each analyte. At a potential of +840 mV and gain of 5 nA (representing the lowest detection window), the linear concentration ranges for DA and Ado were 1–100 nM and 1–400 nM, respectively

(Figure 5.3). Both analytes had linear correlation values of at least 0.998. The sensitivity for DA was 8.4×10^4 , which was approximately twice the sensitivity of Ado (2.9×10^4) (Table 5.1). We hypothesize that the difference in sensitivity is a result of the oxidation potential chosen of +840 mV for this method, for which the hydrodynamic voltammogram (Figure 5.2) shows a 100% response of DA oxidation, whereas only ~20% of Ado is oxidized at this potential. Again, the method was intentionally biased to favor DA oxidation, because extracellular striatal DA levels (extracellular: 5–10 nM) are significantly lower compared to Ado levels (extracellular: 40–210 nM) (14, 133, 134). The total linear range detected for DA and Ado were 0.001–5 μM and 0.001–200 μM , respectively (data not shown). The lowest detectable concentration observed for both DA and Ado was at 1 nM, with a reporting limit of 0.5 nM. These lower limits are well within the range of concentration monoamines and purines in biological systems.

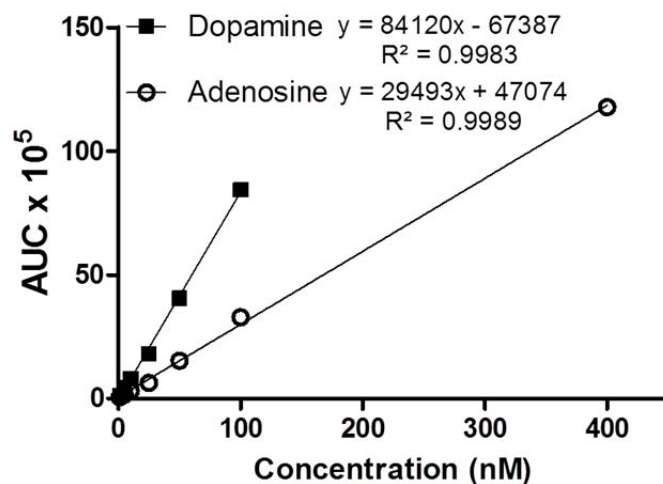


Figure 5.3 Linear calibration curve for the oxidation of adenosine (○) and dopamine (■) at a potential of +840 mV. Linear range for dopamine was 1–100 nM, and for adenosine, 1–400 nM.

Comparisons between porous carbon and the BDD electrode can only be made with respect to DA, as Ado is not detectable at the carbon surface. At a potential of

+220 mV and gain of 2 nA, the linear concentration range for DA was from 0.5 to 15 nM. DA calibration curves at the porous carbon routinely had linear correlation values of at least 0.998. The average sensitivity for DA was 7.0×10^5 , which was approximately 10 times higher than the sensitivity of DA at the BDD electrode. However, it must be noted that our method for DA detection at the porous carbon electrode was optimized for routine microdialysis measurements, which includes a $2.5\text{-}\mu\text{m}$ particle-size column versus $3\text{-}\mu\text{m}$ particle-size column used with the BDD electrode. The lowest detectable concentration for DA at the porous carbon electrode is 0.5 nM (data not shown). Thus, the lowest detectable concentrations for DA were approximately the same for these two electrode surfaces. Taken together, these results indicate that the BDD electrode can compete very favorably to the porous carbon electrode with respect to DA, but the advantage of the BDD electrode is its ability to detect purine molecules such as Ado. We anticipate that, with future experimental refinements such as using a column with smaller particles, the BDD electrode will be able to achieve the sensitivity and lowest detectable concentration of DA that is seen with the porous carbon electrode as well as improve upon these parameters with Ado.

5.3.5 Limit of Detection and Quantification

The limits of detection and quantification were determined using averages of 10 nM standards of DA and Ado fit to the calibration curve from Figure 5.3. Using equations

$$\text{Limit of Detection} = \frac{3.3\sigma}{m} \quad (5.1)$$

$$\text{Limit of Quantification} = \frac{10\sigma}{m} \quad (5.2)$$

where σ is the standard deviation and m is the mean (Table 5.1), the limit of detection and quantification were determined for both DA and Ado. The limit of detection for DA and Ado, calculated using eq 5.1, were determined to be 0.021 nM, and 1.2 nM, respectively. The limits of quantification (eq 5.2) were determined to be 0.063 nM and 3.7 nM for DA and Ado, respectively.

5.3.6 Precision and Accuracy

To determine the accuracy and precision of the method, standard concentrations of DA and Ado were assessed using the average relative percentage deviation (DEV, %) and the relative standard deviation (RSD, %), which were calculated as

$$\text{DEV (\%)} = \frac{m}{\text{nominal concentration}} \quad (5.3)$$

$$\text{RSD (\%)} = \frac{\sigma}{m} \quad (5.4)$$

where m is the average calculated concentration and σ is the standard deviation.

The accuracy of the method was determined by measuring 10 nM standard of DA and Ado in replicates and calculating their means and standard deviations. The calculated accuracy of the method for DA and Ado (eq 3) demonstrated that the standard values were within acceptable range for both analytes: 99% and 101%, respectively. Furthermore, the precision of the method was quantitated (eq 4) with both analytes being less than 10%, specifically, with DA at 7% and Ado at 3% (Table 5.1).

Table 5.1 Figures of merit for the simultaneous detection of dopamine and adenosine using HPLC with BDD electrode.

	Dopamine	Adenosine
Limit of Detection (nM)	0.021	1.2
Limit of Quantification (nM)	0.063	3.7
RSD (%)	7	3
DEV (%)	99	101
Sensitivity	8.4×10^4	2.9×10^4

5.3.7 Analysis of monoamine and purine neurotransmitters

Once the electrochemical parameters for DA and Ado were validated, the detection of other monoamines and purines was assessed. All monoamine and purine standards were analyzed at +840 mV, gain of 20 nA, and standard concentrations of 300 nM were evaluated except for 5-HIAA, which was measured at 100 nM (Figure 5.4A). AMP cannot be observed in this representative chromatogram (Figure 5.4A) because concentrations >300 nM are required for its detection at +840 mV. This HPLC electrochemical method provides ample separation between analytes from both the monoamine and purine families with an analysis run time of ~28 min (Figure 5.4A), whereas a run time of less than 8.5 min was needed for DA and Ado. Taken together, our results demonstrate the feasibility of using the BDD electrode not only to detect easily oxidized species such as monoamines but also purine molecules, to provide a more comprehensive analysis of neurotransmitters and even neurotransmission.

The validity of the method was determined using brain tissue samples from the striatum and frontal cortex of female C57BL6/J mice, as both regions are known to contain DA and Ado. Tissue-content analysis of monoamine and purine molecules was performed using the same mobile phase as the standard chromatogram with the BDD electrode. Eight molecules (six monoamines and two purines) were detected simultaneously in approximately 28 min (Figure 5.4B). The DA metabolite HVA was separated clearly in the standard chromatogram, but was not visibly defined in the tissue-content sample chromatogram because of an overlap by an unknown peak. Therefore, HVA levels could not be accurately determined (Figure 5.4B).

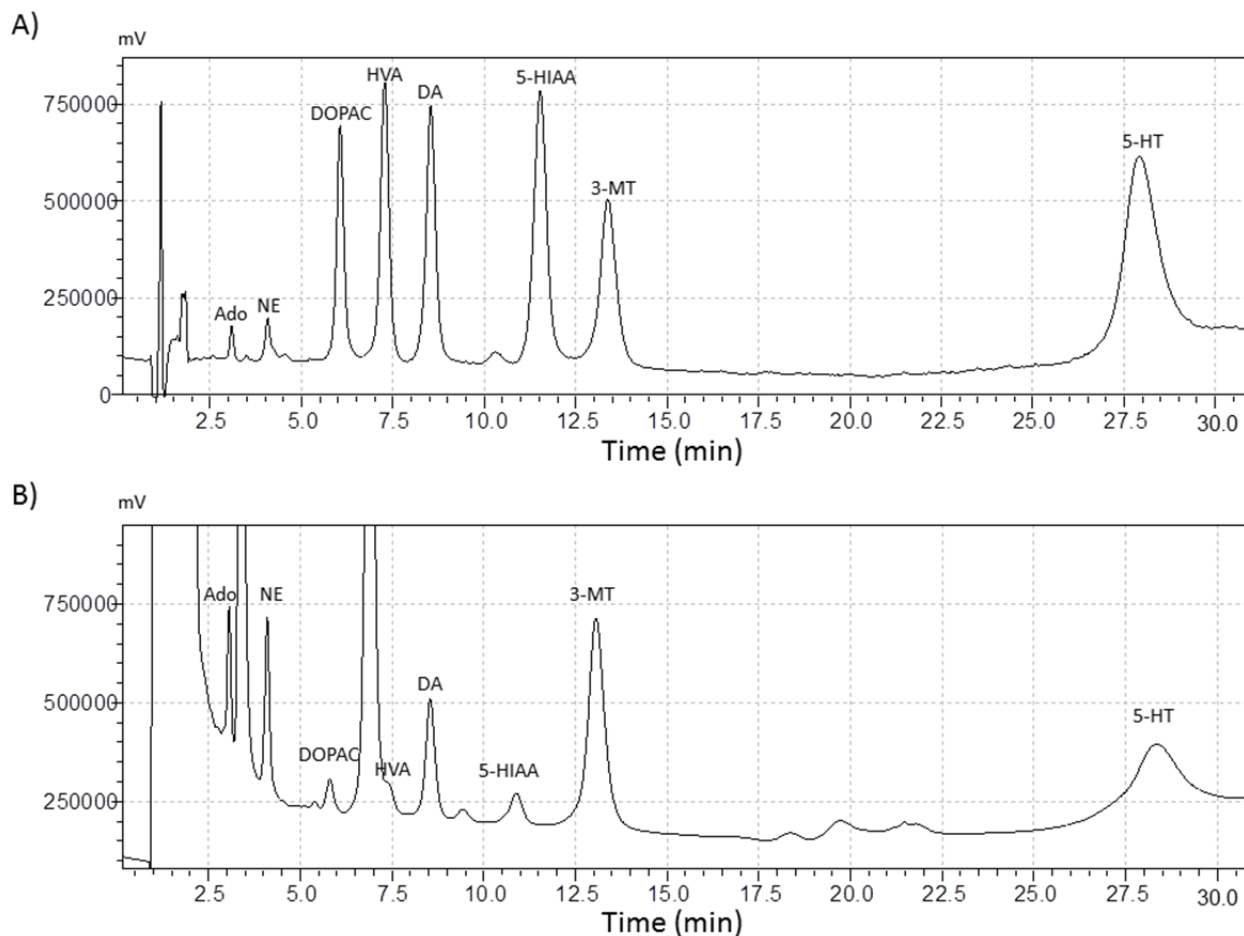


Figure 5.4 A) Representative 300 nM standard chromatogram of adenosine (Ado), 3,4-dihydroxyphenylacetic acid (DOPAC), homovanillic acid (HVA), dopamine (DA), 3-methoxytyrosine (3-MT), serotonin (5-HT), and 100 nM 5-hydroxyindoleacetic acid (5-HIAA) at an applied potential of +840 mV. B) Representative striatal tissue content chromatogram with the appropriate neurotransmitters labeled.

To fully assess this method's ability to accurately and quantitatively measure monoamines and purines in biological samples, a side-by-side comparison was made with the standard method used to detect monoamines using a porous carbon electrochemical cell (model 5014B, Thermo Scientific ESA). Although this cell is not the same cross-flow cell design as used for the BDD electrode, comparison between these two different cell types were made since the majority of tissue-content analysis in the literature uses a porous carbon electrode (45, 162, 163). Tissue-content samples

from the frontal cortex and striatum of mice were both run on two separate HPLC's, one with a porous carbon electrode and the other with the BDD electrode. The porous carbon electrode detected all seven monoamine molecules, but was unable to detect the purine molecules Ado and AMP, whereas the BDD electrode was able to detect all six monoamines and two purines (Table 5.2). Furthermore, the BDD method accurately detected six monoamines in the striatum and frontal cortex. Within the striatum, only 5-HIAA levels were significantly different compared to those from the carbon electrode (Student's *t*-test, 5-HIAA detected at BDD at 35 ± 8 ng/mg protein and by carbon at 94 ± 20 ng/mg protein, $P < 0.05$). In the frontal cortex, 3-MT levels were significantly different between the two electrode surfaces, where the BDD electrode measured a higher concentration compared to the porous carbon electrode (Student's *t*-test, 3-MT detected by BDD at 16 ± 1 ng/mg protein and by carbon at 5.3 ± 0.3 ng/mg protein, $P < 0.001$). One possible reason for these discrepancies in concentrations lies in the fact that the BDD method was optimized for the simultaneous detection of DA and Ado and not for the other monoamine or purine molecules, each of which has its own optimal oxidation potential. To improve on the discrepancy in concentrations, the mobile-phase configuration and working potential chosen for the BDD electrode should both be taken into consideration. Although the primary focus was on separation and detection of DA and Ado, we were still able to accurately quantify the monoamine and purine molecules using the BDD electrode with good correlation with the porous carbon.

Table 5.2 Comparison of BDD electrode and carbon electrode for the detection of monoamine and purine molecules.

Monoamines and Purines	Striatum BDD	Striatum Carbon	Frontal Cortex BDD	Frontal Cortex Carbon
DA (ng/mg)	1190 ± 100	1310 ± 120	38 ± 10	22 ± 4
Ado (ng/mg)	1.40 x10 ⁵ ± 1.7 x10 ⁴	ND	1.28 x 10 ⁵ ± 5.8 x 10 ⁴	ND
DOPAC (ng/mg)	210 ± 20	230 ± 50	35 ± 10	22 ± 5
3-MT (ng/mg)	63 ± 5	82 ± 10	16 ± 1	5.3 ± 0.3***
5-HIAA (ng/mg)	35 ± 8*	94 ± 20	31 ± 4	70 ± 20
5-HT (ng/mg)	160 ± 40	110 ± 20	60 ± 8	82 ± 20
NE (ng/mg)	130 ± 20	91 ± 20	115 ± 30	100 ± 8
AMP (ng/mg)	1.19 x 10 ⁶ ± 2.3 x 10 ⁵	ND	1.57 x 10 ⁶ ± 2.9 x 10 ⁵	ND

Monoamine and purine tissue content levels measured as ng/mg protein.

ND = not detected. *P* values: **P* < 0.05, ****P* < 0.001, n values are 3–8 per set.

To further expand on our results with tissue-content, other studies were examined with respect to tissue-content concentration. One caveat when comparing tissue contents is the wide range of concentrations reported in the literature (Table 5.3), emphasizing that tissue content measures relative differences and not absolute neurotransmitter concentrations. There are numerous reasons for these discrepancies in tissue-content neurotransmitter levels such as dissection techniques (free hand versus punch), use of anesthesia prior to sacrifice, and time required to dissect the tissue, as well as conditions used to store the tissue, buffer solutions used, and the type of analysis for the tissue itself (164). In this study, tissue was normalized by using the BCA protein method, while others have used wet weight, or a different protein assay such as Lowry (45, 69, 86, 96, 160, 162, 165-169). Thus, despite these methodological

differences for normalizing tissue, our tissue content neurotransmitter levels are well within this wide range of values reported in the literature (Table 5.3).

Although our reported neurotransmitter levels are well within the documented range, they do tend to be on the higher side. We believe this is a result of using female C57BL6/J mice, because this was a proof-of-concept study and female mice were used instead of male mice. Interestingly, the majority of tissue-content experiments performed often examined only male mice or rats for their neurotransmitter levels. Although few studies have examined female intracellular neurotransmitter levels, one study showed that female mice have approximately twice as much striatal intracellular DA as males with respect to tissue content (168). When the sex of the animal is taken into consideration as well as differences in methodological conditions, these differences could account for why our intracellular neurotransmitter values are on the higher end compared to other values from the literature. With all these parameters considered, our HPLC-BDD electrode method can measure monoamine and purine neurotransmitters quickly and accurately.

Table 5.3 Comparison of tissue content from the literature.

Brain Region	Sex, Strain, Species	DA	Ado	Method of Quantification	Method of Detection
Cerebral cortex (158)	Male Wistar rats	N/A	265.6 ± 2.0 pmol/mg wet tissue	Wet tissue weight	HPLC-UV photodiode-array
Frontal Cortex (163)	Albino mice	N/A	3075 ± 251 mmol/kg protein	Lowry protein	HPLC-UV
Frontal Cortex (164)	Male C57BL/6J mice	~ 0.7 µg/g wet tissue	N/A	Wet tissue weight	HPLC-electrochemical
Prefrontal Cortex (165)	Male C57BL/6N mice	~ 4 nM	N/A	No correction for tissue dissected	HPLC-electrochemical
Striatum (158)	Male Wistar rats	N/A	618.93 ± 2.0 pmol/mg wet tissue	Wet tissue weight	HPLC-UV photodiode-array
Striatum (47)	Male Wistar rats	8.09 ± 2.1 µg/g wet tissue	171.28 ± 57.78 µg/g ww	Wet tissue weight	HPLC-UV and electrochemical
Striatum (88)	Male C57BL/6J mice	11,286.92 ± 478.42 pg/mg ww	N/A	Wet weight	HPLC-electrochemical
Striatum (164)	Male C57BL/6J mice	~ 14 µg/g wet tissue	N/A	Wet tissue weight	HPLC-electrochemical
Striatum (160)	129 x C57B/6	~ 550 ng/mg protein	N/A	BCA protein	HPLC-electrochemical
Striatum (166)	LRRK2 mice	246 ± 9 ng/mg protein	N/A	BCA protein	HPLC
Corpus Striatum (96)	Balb/c 129 strain	20437 ± 1395 pg/mg wet tissue	N/A	Wet tissue weight	HPLC-electrochemical
Corpus Striatum (93)	Male CD-1 mice	~ 6000 pg/mg wet tissue	N/A	Wet tissue weight	HPLC-electrochemical
Corpus Striatum (93)	Female CD-1 mice	~ 15000 pg/mg wet tissue	N/A	Wet tissue weight	HPLC-electrochemical

5.4 Conclusion

The advent of a commercially available BDD electrode has opened doors for researchers to detect biological molecules with oxidation potentials greater than +1000 mV. In this work, we reported the first BDD electrode method to simultaneously detect DA and Ado using HPLC with electrochemical detection. This BDD electrode method measures DA and Ado in a single chromatogram in less than 8.5 min with excellent accuracy and precision. Furthermore, the BDD method developed here can easily separate and detect six other monoamines and two purine molecules with a run time of ~28 min. When this BDD method was compared to a similar method using a porous carbon electrode, there was no difference between the quantified concentrations of monoamine molecules from tissue-content samples. An advantage of the BDD working electrode is that it can detect both Ado and AMP, which is not possible using the porous carbon working electrode. This BDD method is effective for *in vitro* studies, and further work is being done to develop it into a more sensitive method for *in vivo* microdialysis samples. Taken together, our results demonstrate that the BDD electrode method is easy to implement, detects analytes from the monoamine and purine family in a single chromatogram, and accurately represents the tissue-content levels when compared to the more traditional carbon electrode.

CHAPTER 6

Conclusions and Future Directions

Brain-derived neurotrophic factor (BDNF) is an important neurotrophin in the brain, and many studies have alluded to its importance for maintaining the structural function and survival of dopamine (DA) neurons in the striatum (26, 28-30). Additionally, irregularities within the DA system as well as BDNF expression have been identified in neurological diseases and disorders such as Parkinson's disease, Huntington's disease, schizophrenia, attention deficit hyperactivity disorder (ADHD), addiction, and depression (1, 2, 27, 35, 110, 170-172). Furthermore, studies have indicated that there is an increased risk for males developing neurological disorders such as Parkinson's disease as well as an earlier onset of the disease in comparison to woman (35, 173). To better understand how lifelong low endogenous BDNF effects striatal DA dynamics, two of the studies throughout this dissertation examined BDNF modulation of the striatal DA system in both young (~3 months of age) female BDNF^{+/-} mice and aged (~18 months of age) BDNF^{+/-} mice, Chapter 3 and Chapter 4, respectively. The overarching findings from this dissertation demonstrate that a lifelong reduction in BDNF causes sex- and age-dependent alterations in striatal DA dynamics in the striatum.

Therapeutic treatment for many of neurological diseases/disorders typically focuses on the altered neurotransmitter system implicated in a given disease. For example, Parkinson's disease corresponds to a dysregulation of nigrostriatal DA, and most treatment options focus on treating deficiencies in nigrostriatal DA for symptomatic relief. L-3,4-Dihydroxyphenylalanine (L-DOPA), which is a precursor to DA synthesis, enzymatic inhibitors that prevent the breakdown of DA such monoamine oxidase (MAO)

inhibitors, and catechol-*o*-methyltransferase (COMT) inhibitors are used to treat motor dysfunction associated with Parkinson's disease (19). Although these treatments decrease the adverse motor effects associated with Parkinson's disease, they are also associated with numerous side effects such as dyskinesia, hallucinations, and eventually stop working completely. Thus, there is interest in finding new treatments options. The adenosine (Ado) receptor A_{2A} has received considerable attention because A_{2A} antagonists alleviate motor symptoms of Parkinson's disease without causing the side effects of the current treatment (20). Ado A_{2A} receptors are highly expressed in DA rich brain regions and have also been shown to co-localize with the DA D_2 receptors (174, 175). However, the *in vivo* function of Ado is not fully understood, which is in part because there are few robust and sensitive analytical techniques to determine extracellular Ado concentrations in the brain. Therefore, the third study in this dissertation (Chapter 5) was to develop a method for the simultaneous detection of DA and Ado. To date, this is the first method developed which utilizes high-performance liquid chromatography (HPLC) with electrochemistry (a boron-doped diamond (BDD) electrode) to detect DA and Ado, along with key members from their respective neurotransmitter families.

6.1 Characterization of striatal dopamine dynamics in female $BDNF^{+/-}$ mice

Previous work conducted in the Mathews' laboratory characterized the striatal DA system in male $BDNF^{+/-}$ mice and their wildtype counterparts at 3–5 months of age, and determined that the $BDNF^{+/-}$ mice were hyperdopaminergic in nature due to decreases in their DA release and uptake (44). Our objective in this study was to determine if female $BDNF^{+/-}$ mice are hyperdopaminergic as well or if BDNF modulates the DA

system differently with respect to the female BDNF^{+/-} mice. The goal was to determine if the female BDNF^{+/-} mice are hyperdopaminergic, and if so, what is the mechanism that causes the hyperdopaminergia state, and is it the same as the male BDNF^{+/-} mice?

Female BDNF^{+/-} mice exhibited increased striatal extracellular DA levels in comparison to their wildtype counterparts as measured by *in vivo* microdialysis experiment of zero-net flux. This increase in extracellular DA levels was associated with an increase in DA release as confirmed by three different experiments: electrically stimulated DA release by fast scan cyclic voltammetry (FSCV), vesicular mediated release by high potassium (K⁺) infusion with microdialysis, and pharmacological mediated DA release with an injection of methamphetamine (METH). This hyperdopaminergic state in the female BDNF^{+/-} mice was not mediated by DA metabolism, since no differences were observed between the genotypes, or via DA uptake as measured by FSCV. We propose that the mechanism that causes the female BDNF^{+/-} mice to be hyperdopaminergic results from an overall potentiation in DA release. Interestingly, young male BDNF^{+/-} mice of the same age are hyperdopaminergic but it is believed to be a result of a compensatory mechanism, as young male BDNF^{+/-} mice have *both* decreased DA uptake and release compared to their wildtype controls (44). In male BDNF^{+/-} mice, the DA striatal alterations have been suggested as a result of a functional change in DAT, which decreases the rate of DA uptake, leading to the elevation in extracellular DA levels.

Women are more likely to be afflicted by depression, stress, and anxiety compared to men (36), and BDNF appears to be a central molecule in all of these disorders. Therefore, the research conducted here was done to understand if female

BDNF^{+/-} mice exhibit different striatal DA dynamics compared to their male counterparts that may make them more susceptible to depression, stress, and anxiety. Although mice were not controlled for their estrous cycle, it does appear there is a significant difference between male and female BDNF^{+/-} mice regulating striatal DA, in particular DA release. To better understand these complex interactions that may be a result of the differences between the male and female BDNF^{+/-} mice, estrogen application should be investigated with respect to BDNF and DA. Previous work in our lab has examined the effect of BDNF infusions on brain slices, where exogenous application of BDNF increases stimulated DA release in the male BDNF^{+/-} mice (44). Similarly future experiments could evaluate independently the effect of estrogen and BDNF, alone and in combination, which will provide valuable insight to how these neuromodulators regulate striatal DA, specifically the mechanisms behind the increase in release in females. Numerous studies have shown that both BDNF and estrogen modulate DA release (44, 168, 176). However, it is imperative to understand their interactions in the female BDNF^{+/-} mice.

6.2 Characterization of a lifelong reduction of brain-derived neurotrophic factor effects on the dopaminergic system in aged BDNF^{+/-} mice

Parkinson's disease is a debilitating disease, which manifest as a loss in motor coordination corresponding to a loss of ~80% substantia nigra dopaminergic neurons. Postmortem studies of Parkinson's disease patient's brains not only have decreases in DA levels, but also in BDNF protein levels in the substantia nigra (SN) (5, 27). The goal of this study was to determine if a lifelong reduction in BDNF levels negatively impacts the striatal DA system. A previous study done in our lab using young (~3 month old)

male BDNF^{+/-} mice determined that they were hyperdopaminergic in nature (44). We hypothesized that this hyperdopaminergia could be harmful as the animal progresses in age because elevated extracellular DA levels in the striatum could lead to increases in reactive oxygen species (ROS), leading to dopaminergic toxicity over the lifespan. A combination of increased extracellular and intracellular DA levels produces ROS which are hypothesized to induce irreversible damage to DA neurons (66, 125).

The results from our study indicate that aged (18 month old) BDNF^{+/-} mice striatal dopaminergic system appears to adjust to a lifelong reduction in BDNF. The hyperdopaminergia that was observed in young BDNF^{+/-} mice (Chapter 3 and (44)) is no longer evident in the aged BDNF^{+/-} mice. Extracellular DA levels in these aged heterozygous mice are normalized to that of the wildtype mice, which is opposite of what we hypothesized. *In vivo* microdialysis evaluation of basal extracellular DA levels was determined to be not different among the aged BDNF^{+/-} and wildtype mice. When observing the basal DA levels between the young and aged BDNF^{+/-} mice, aged BDNF^{+/-} mice basal DA levels have decreased to the levels shown in the young and aged wildtype counterparts. Upon further analysis, this “normalization” of basal DA levels in the aged BDNF^{+/-} mice could be result of either (1) increased DA metabolism, and/or (2) increased release and uptake of DA when compared to young BDNF^{+/-} mice (44). The results from this thesis showed that aged BDNF^{+/-} mice have significantly increased DA metabolism, which was demonstrated by an increase in basal levels of 3,4-dihydroxyphenylacetic acid (DOPAC) and homovanillic acid (HVA) in comparison to their aged wildtype mice. Stimulated DA release and uptake of DA were not different between the aged genotypes, while these parameters were different in the young

BDNF^{+/-} mice. Young BDNF^{+/-} mice had reduced DA release and DA uptake function (44). Pharmacological stimulation of DA release using METH in the aged mice also indicated that release was not different between genotypes. Although this study proved our original hypothesis wrong that increases in extracellular DA in the young BDNF^{+/-} mice would be detrimental overtime (44). In fact, it appears that the DA system in the BDNF^{+/-} mice compensated for the increase in extracellular DA levels overtime, by regulating striatal release and uptake as well as increasing DA metabolism.

In the future, more research should focus on fully understanding why the DA system in the aged BDNF^{+/-} mice eventually normalizes itself. BDNF protein levels in aged BDNF^{+/-} mice do not change over the lifespan of the animal (64). Therefore one may speculate that other neurotrophic factors may be responsible and possibly compensate for a system partially devoid of BDNF. A prime neurotrophic factor candidate that may be responsible for possible compensatory actions may be neurotrophin 4 (NT-4). To determine if this NT-4 hypothesis is correct further evaluation of NT-4 levels and activity need to be determined in the aged BDNF^{+/-} mice. Although there are numerous neurotrophic factors that could be altered in BDNF^{+/-} mice, NT-4 was chosen because it belongs to the same family of neurotrophic factors as BDNF and it binds to the same receptor as BDNF, tyrosine kinase B (TrkB). In young BDNF^{+/-} mice, striatal NT-4 protein tissue levels are elevated in comparison to their wildtype littermates, but striatal TrkB levels are unchanged (61), which suggests NT-4 levels are altered and may be compensating for a 50% reduction of BDNF.

One of the most pressing issues to better understand is to determine the mechanism behind the increase in DA metabolism of the aged BDNF^{+/-} mice. Young

BDNF^{+/-} mice do not show an increase in metabolism, so over time DA metabolism increases in BDNF^{+/-} mice. Two enzymes that are responsible for the metabolism of DA are MAO and COMT. From the microdialysis results that we garnered, it appears that MAO activity or function is enhanced in the aged BDNF^{+/-} mice since DOPAC levels are increased, and therefore, future work should evaluate their function and expression

6.3 Simultaneous detection of dopamine and adenosine using HPLC with electrochemical detection using a boron-doped diamond electrode

The objective of this work was to develop a method which could detect DA and Ado simultaneously using HPLC with a BDD electrode. Typically, monoamine molecules are detected using electrochemical detection because they are easily oxidized. Purine molecules such as Ado are also electrochemically active, but oxidize at potentials greater than +1000 mV at a carbon surface with respect to a Ag/AgCl reference electrode. However, potentials greater than +1000 mV are often not possible with carbon electrodes because of the structural damage to the carbon surface (49). To circumvent this problem, a newly commercially available BDD electrode has been developed to be used with HPLC instrumentation. The BDD electrode is advantageous because it has a large potential working range (up to +2000 mV), lower background noise, and is less susceptible to electrode fouling (51, 73). In this project, the BDD electrode was utilized in conjunction with an HPLC instrument to develop a method for the simultaneous detection of DA and Ado. This BDD method was able to accurately separate and detect six monoamine and two purine molecules in about 28 min with good separation. When a proof-of-concept study evaluated and compared the neurotransmitter levels from tissue-content samples from the striatum and frontal cortex

of mice with a porous carbon electrode or BDD electrode coupled to an HPLC instrument, the BDD electrode method detected and quantify monoamine levels that corresponded to the levels detected with the carbon electrode. However, the advantage of the BDD electrode was its ability to also detect Ado and adenosine monophosphate (AMP), which were not detected at the carbon electrode.

The *in vivo* function of Ado is not well understood, and that is mainly because of a lack of reliable methods to routinely detect low levels of Ado. Current methods show extracellular levels of Ado to be between 40–240 nM in the striatum, a range that is far too large (14, 68, 160, 161). Furthermore, there is increasing evidence of DA and Ado interacting in the striatum. To truly understand these interactions with respect to DA and Ado levels, future work will take this method and refine and apply it to detect extracellular DA and Ado levels, which are about a 100-fold less than tissue content samples. If this BDD method proves successful at measuring baseline DA and Ado levels via microdialysis, it will provide a much more user-friendly method to measure extracellular Ado levels. Currently, our BDD method is good enough for the detection of Ado *in vivo*, but not for DA. We believe to achieve DA detection, the column must be similar to the one that we currently use for routine dialysis experiments; one with a smaller particle size or a shorter column length, since decreasing these parameters will increase peak height and sensitivity. The length of the column dictates the flow of analyte and sample capacity while the size of the particles in the column control column efficiency and increase peak height due to its direct correlation to mass transfer of the analyte through the column. By decreasing the particle size or the column length may lead to further modifications/refinements of the mobile phase. However, we believe

these adjustments will not require a complete revamp of the current mobile phase and that *in vivo* detection of Ado and DA at a BDD electrode surface is just around the corner.

REFERENCES

1. Wise, R. A., and Rompre, P. P. (1989) Brain dopamine and reward, *Annu Rev Psychol* 40, 191-225.
2. Nestler E. J., H., S.E., and Malenka, R.C. (2009) *Molecular Neuropharmacology: A foundation for clinical neuroscience*, 2nd Edition ed., McGraw Hill Medical, New York.
3. Zuccato, C., Marullo, M., Conforti, P., MacDonald, M. E., Tartari, M., and Cattaneo, E. (2008) Systematic assessment of BDNF and its receptor levels in human cortices affected by Huntington's disease, *Brain Pathol* 18, 225-238.
4. Ferre, S. (1997) Adenosine-dopamine interactions in the ventral striatum. Implications for the treatment of schizophrenia, *Psychopharmacology (Berl)* 133, 107-120.
5. Kish, S. J., Shannak, K., Rajput, A., Deck, J. H., and Hornykiewicz, O. (1992) Aging produces a specific pattern of striatal dopamine loss: implications for the etiology of idiopathic Parkinson's disease, *J Neurochem* 58, 642-648.
6. Pierce, R. C., and Kumaresan, V. (2006) The mesolimbic dopamine system: the final common pathway for the reinforcing effect of drugs of abuse?, *Neurosci Biobehav Rev* 30, 215-238.
7. Maina, F. K., and Mathews, T. A. (2010) A functional fast scan cyclic voltammetry assay to characterize dopamine D2 and D3 autoreceptors in the mouse striatum, *ACS Chem Neurosci* 1, 450-462.

8. Phillips, P. E., Hancock, P. J., and Stamford, J. A. (2002) Time window of autoreceptor-mediated inhibition of limbic and striatal dopamine release, *Synapse* 44, 15-22.
9. Deng, Q., Kauri, L. M., Qian, W. J., Dahlgren, G. M., and Kennedy, R. T. (2003) Microscale determination of purines in tissue samples by capillary liquid chromatography with electrochemical detection, *Analyst* 128, 1013-1018.
10. Bours, M. J., Swennen, E. L., Di Virgilio, F., Cronstein, B. N., and Dagnelie, P. C. (2006) Adenosine 5'-triphosphate and adenosine as endogenous signaling molecules in immunity and inflammation, *Pharmacol Ther* 112, 358-404.
11. Fuxe, K., Marcellino, D., Borroto-Escuela, D. O., Guescini, M., Fernandez-Duenas, V., Tanganelli, S., Rivera, A., Ciruela, F., and Agnati, L. F. (2010) Adenosine-dopamine interactions in the pathophysiology and treatment of CNS disorders, *CNS Neurosci Ther* 16, e18-42.
12. Kumar, V., Chapple, C. R., Rosario, D., Tophill, P. R., and Chess-Williams, R. (2010) In vitro release of adenosine triphosphate from the urothelium of human bladders with detrusor overactivity, both neurogenic and idiopathic, *Eur Urol* 57, 1087-1092.
13. Sawada, K., Echigo, N., Juge, N., Miyaji, T., Otsuka, M., Omote, H., Yamamoto, A., and Moriyama, Y. (2008) Identification of a vesicular nucleotide transporter, *Proc Natl Acad Sci U S A* 105, 5683-5686.
14. Latini, S., and Pedata, F. (2001) Adenosine in the central nervous system: release mechanisms and extracellular concentrations, *J Neurochem* 79, 463-484.

15. Kloor, D., and Osswald, H. (2004) S-Adenosylhomocysteine hydrolase as a target for intracellular adenosine action, *Trends Pharmacol Sci* 25, 294-297.
16. Latini, S., Pazzagli, M., Pepeu, G., and Pedata, F. (1996) A2 adenosine receptors: their presence and neuromodulatory role in the central nervous system, *Gen Pharmacol* 27, 925-933.
17. Lloyd, H. G., Lindstrom, K., and Fredholm, B. B. (1993) Intracellular formation and release of adenosine from rat hippocampal slices evoked by electrical stimulation or energy depletion, *Neurochem Int* 23, 173-185.
18. Schiffmann, S. N., and Vanderhaeghen, J. J. (1993) Adenosine A2 receptors regulate the gene expression of striatopallidal and striatonigral neurons, *J Neurosci* 13, 1080-1087.
19. Olanow, C. W. (2004) The scientific basis for the current treatment of Parkinson's disease, *Annu Rev Med* 55, 41-60.
20. Xu, K., Bastia, E., and Schwarzschild, M. (2005) Therapeutic potential of adenosine A(2A) receptor antagonists in Parkinson's disease, *Pharmacol Ther* 105, 267-310.
21. Binder, D. K., and Scharfman, H. E. (2004) Brain-derived neurotrophic factor, *Growth Factors* 22, 123-131.
22. Liebl, D. J., Tessarollo, L., Palko, M. E., and Parada, L. F. (1997) Absence of sensory neurons before target innervation in brain-derived neurotrophic factor-, neurotrophin 3-, and TrkC-deficient embryonic mice, *J Neurosci* 17, 9113-9121.
23. Luellen, B. A., Bianco, L. E., Schneider, L. M., and Andrews, A. M. (2007) Reduced brain-derived neurotrophic factor is associated with a loss of

- serotonergic innervation in the hippocampus of aging mice, *Genes Brain Behav* 6, 482-490.
24. Numan, S., and Seroogy, K. B. (1999) Expression of trkB and trkC mRNAs by adult midbrain dopamine neurons: a double-label in situ hybridization study, *J Comp Neurol* 403, 295-308.
 25. Ernfors, P., Lee, K. F., and Jaenisch, R. (1994) Mice lacking brain-derived neurotrophic factor develop with sensory deficits, *Nature* 368, 147-150.
 26. Howells, D. W., Porritt, M. J., Wong, J. Y., Batchelor, P. E., Kalnins, R., Hughes, A. J., and Donnan, G. A. (2000) Reduced BDNF mRNA expression in the Parkinson's disease substantia nigra, *Exp Neurol* 166, 127-135.
 27. Mogi, M., Togari, A., Kondo, T., Mizuno, Y., Komure, O., Kuno, S., Ichinose, H., and Nagatsu, T. (1999) Brain-derived growth factor and nerve growth factor concentrations are decreased in the substantia nigra in Parkinson's disease, *Neurosci Lett* 270, 45-48.
 28. Hyman, C., Hofer, M., Barde, Y. A., Juhasz, M., Yancopoulos, G. D., Squinto, S. P., and Lindsay, R. M. (1991) BDNF is a neurotrophic factor for dopaminergic neurons of the substantia nigra, *Nature* 350, 230-232.
 29. Joyce, J. N., Renish, L., Osredkar, T., Walro, J. M., Kucera, J., and Dluzen, D. E. (2004) Methamphetamine-induced loss of striatal dopamine innervation in BDNF heterozygote mice does not further reduce D3 receptor concentrations, *Synapse* 52, 11-19.

30. Dluzen, D. E., Anderson, L. I., McDermott, J. L., Kucera, J., and Walro, J. M. (2002) Striatal dopamine output is compromised within +/- BDNF mice, *Synapse* 43, 112-117.
31. Altar, C. A., Cai, N., Bliven, T., Juhasz, M., Conner, J. M., Acheson, A. L., Lindsay, R. M., and Wiegand, S. J. (1997) Anterograde transport of brain-derived neurotrophic factor and its role in the brain, *Nature* 389, 856-860.
32. Goggi, J., Pullar, I. A., Carney, S. L., and Bradford, H. F. (2002) Modulation of neurotransmitter release induced by brain-derived neurotrophic factor in rat brain striatal slices in vitro, *Brain Res* 941, 34-42.
33. Guillin, O., Diaz, J., Carroll, P., Griffon, N., Schwartz, J. C., and Sokoloff, P. (2001) BDNF controls dopamine D3 receptor expression and triggers behavioural sensitization, *Nature* 411, 86-89.
34. Ryoo, H. L., Pierrotti, D., and Joyce, J. N. (1998) Dopamine D3 receptor is decreased and D2 receptor is elevated in the striatum of Parkinson's disease, *Mov Disord* 13, 788-797.
35. Taylor, K. S., Cook, J. A., and Counsell, C. E. (2007) Heterogeneity in male to female risk for Parkinson's disease, *J Neurol Neurosurg Psychiatry* 78, 905-906.
36. Sun, M. K., and Alkon, D. L. (2006) Differential gender-related vulnerability to depression induction and converging antidepressant responses in rats, *J Pharmacol Exp Ther* 316, 926-932.
37. MacQueen, G. M., Ramakrishnan, K., Croll, S. D., Siuciak, J. A., Yu, G., Young, L. T., and Fahnstock, M. (2001) Performance of heterozygous brain-derived

- neurotrophic factor knockout mice on behavioral analogues of anxiety, nociception, and depression, *Behav Neurosci* 115, 1145-1153.
38. Pasqualini, C., Olivier, V., Guibert, B., Frain, O., and Leviel, V. (1995) Acute stimulatory effect of estradiol on striatal dopamine synthesis, *J Neurochem* 65, 1651-1657.
 39. Davies, M. I., Cooper, J. D., Desmond, S. S., Lunte, C. E., and Lunte, S. M. (2000) Analytical considerations for microdialysis sampling, *Adv Drug Deliv Rev* 45, 169-188.
 40. Chaurasia, C. S. (1999) In vivo microdialysis sampling: theory and applications, *Biomed Chromatogr* 13, 317-332.
 41. Olson, R. J., and Justice, J. B., Jr. (1993) Quantitative microdialysis under transient conditions, *Anal Chem* 65, 1017-1022.
 42. Schultz, K. N., and Kennedy, R. T. (2008) Time-resolved microdialysis for in vivo neurochemical measurements and other applications, *Annu Rev Anal Chem (Palo Alto Calif)* 1, 627-661.
 43. Lee, W. H., Slaney, T. R., Hower, R. W., and Kennedy, R. T. (2013) Microfabricated sampling probes for in vivo monitoring of neurotransmitters, *Anal Chem* 85, 3828-3831.
 44. Bosse, K. E., Maina, F. K., Birbeck, J. A., France, M. M., Roberts, J. J., Colombo, M. L., and Mathews, T. A. (2012) Aberrant striatal dopamine transmitter dynamics in brain-derived neurotrophic factor-deficient mice, *J Neurochem* 120, 385-395.

45. Betto, P., Popoli, P., Ricciarello, G., Caporali, M. G., and Antonini, R. (1994) Simultaneous high-performance liquid chromatographic determination of adenosine and dopamine in rat striatal tissue with combined ultraviolet absorbance and electrochemical detection, *J Chromatogr B Biomed Appl* 662, 21-25.
46. Devall, A. J., Blake, R., Langman, N., Smith, C. G. S., Richards, D. A., and Whitehead, K. J. (2007) Monolithic column-based reversed-phase liquid chromatography separation for amino acid assay in microdialysates and cerebral spinal fluid, *J Chromatogr B* 848, 323-328.
47. Mabrouk, O. S., Li, Q., Song, P., and Kennedy, R. T. (2011) Microdialysis and mass spectrometric monitoring of dopamine and enkephalins in the globus pallidus reveal reciprocal interactions that regulate movement, *J Neurochem* 118, 24-33.
48. Birbeck, J. A., and Mathews, T. A. (2013) Simultaneous Detection of Monoamine and Purine Molecules using High-Performance Liquid Chromatography with a Boron-Doped Diamond Electrode, *Anal Chem*.
49. McCreery, R. L., and Cline, K. K. (1996) Carbon Electrodes, in *Laboratory Techniques in Electroanalytical Chemistry* (Kissinger, P. T., and Heineman, W. R., Eds.) 2nd ed., pp 293-332, Marcel Dekker, Inc., New York.
50. Acworth, I., Gamache, P., and Granger, M. (2007) DETECTION METHODS AND DEVICES, in *U.S. Patent Application Publication*, United States.
51. Swain, G. M. (1994) The Use of Cvd Diamond Thin-Films in Electrochemical Systems, *Adv Mater* 6, 388-392.

52. Xu, J. Z., and Swain, G. M. (1998) Oxidation of azide anion at boron-doped diamond thin-film electrodes, *Anal Chem* 70, 1502-1510.
53. John, C. E., and Jones, S. R. (2007) Fast Scan Cyclic Voltammetry of Dopamine and Serotonin in Mouse Brain Slices, in *Electrochemical Methods for Neuroscience* (Michael, A. C., and Borland, L. M., Eds.), Boca Raton (FL).
54. Swamy, B. E., and Venton, B. J. (2007) Subsecond detection of physiological adenosine concentrations using fast-scan cyclic voltammetry, *Anal Chem* 79, 744-750.
55. Cechova, S., and Venton, B. J. (2008) Transient adenosine efflux in the rat caudate-putamen, *J Neurochem* 105, 1253-1263.
56. Martin, H. B., Argoitia, A., Landau, U., Anderson, A. B., and Angus, J. C. (1996) Hydrogen and oxygen evolution on boron-doped diamond electrodes, *J Electrochem Soc* 143, L133-L136.
57. Swain, G. M., and Ramesham, R. (1993) The Electrochemical Activity of Boron-Doped Polycrystalline Diamond Thin-Film Electrodes, *Anal Chem* 65, 345-351.
58. Robinson, D. L., Venton, B. J., Heien, M. L., and Wightman, R. M. (2003) Detecting subsecond dopamine release with fast-scan cyclic voltammetry in vivo, *Clin Chem* 49, 1763-1773.
59. Zhao, H., Bian, X., Galligan, J. J., and Swain, G. M. (2010) Electrochemical measurements of serotonin (5-HT) release from the guinea pig mucosa using continuous amperometry with a boron-doped diamond microelectrode, *Diam Relat Mater* 19, 182-185.

60. Hurd, Y. L., and Herkenham, M. (1992) Influence of a single injection of cocaine, amphetamine or GBR 12909 on mRNA expression of striatal neuropeptides, *Brain Res Mol Brain Res* 16, 97-104.
61. Hill, R. A., and van den Buuse, M. (2011) Sex-dependent and region-specific changes in TrkB signaling in BDNF heterozygous mice, *Brain Res* 1384, 51-60.
62. Miranda, R. C., Sohrabji, F., and Toran-Allerand, C. D. (1993) Neuronal colocalization of mRNAs for neurotrophins and their receptors in the developing central nervous system suggests a potential for autocrine interactions, *Proc Natl Acad Sci U S A* 90, 6439-6443.
63. Sohrabji, F., Miranda, R. C., and Toran-Allerand, C. D. (1995) Identification of a putative estrogen response element in the gene encoding brain-derived neurotrophic factor, *Proc Natl Acad Sci U S A* 92, 11110-11114.
64. Boger, H. A., Mannangatti, P., Samuvel, D. J., Saylor, A. J., Bender, T. S., McGinty, J. F., Fortress, A. M., Zaman, V., Huang, P., Middaugh, L. D., Randall, P. K., Jayanthi, L. D., Rohrer, B., Helke, K. L., Granholm, A. C., and Ramamoorthy, S. (2011) Effects of brain-derived neurotrophic factor on dopaminergic function and motor behavior during aging, *Genes Brain Behav* 10, 186-198.
65. Lyons, W. E., Mamounas, L. A., Ricaurte, G. A., Coppola, V., Reid, S. W., Bora, S. H., Wihler, C., Koliatsos, V. E., and Tessarollo, L. (1999) Brain-derived neurotrophic factor-deficient mice develop aggressiveness and hyperphagia in conjunction with brain serotonergic abnormalities, *Proc Natl Acad Sci U S A* 96, 15239-15244.

66. Cantuti-Castelvetri, I., Shukitt-Hale, B., and Joseph, J. A. (2003) Dopamine neurotoxicity: age-dependent behavioral and histological effects, *Neurobiol Aging* 24, 697-706.
67. Mallajosyula, J. K., Kaur, D., Chinta, S. J., Rajagopalan, S., Rane, A., Nicholls, D. G., Di Monte, D. A., Macarthur, H., and Andersen, J. K. (2008) MAO-B elevation in mouse brain astrocytes results in Parkinson's pathology, *PLoS One* 3, e1616.
68. Ballarin, M., Fredholm, B. B., Ambrosio, S., and Mahy, N. (1991) Extracellular levels of adenosine and its metabolites in the striatum of awake rats: inhibition of uptake and metabolism, *Acta Physiol Scand* 142, 97-103.
69. Villalobos, V., Suarez, J., Estevez, J., Novo, E., and Bonilla, E. (2001) Effect of chronic manganese treatment on adenosine tissue levels and adenosine A2a receptor binding in diverse regions of mouse brain, *Neurochem Res* 26, 1157-1161.
70. Pazzagli, M., Corsi, C., Fratti, S., Pedata, F., and Pepeu, G. (1995) Regulation of extracellular adenosine levels in the striatum of aging rats, *Brain Res* 684, 103-106.
71. Pazzagli, M., Pedata, F., and Pepeu, G. (1993) Effect of K⁺ depolarization, tetrodotoxin, and NMDA receptor inhibition on extracellular adenosine levels in rat striatum, *Eur J Pharmacol* 234, 61-65.
72. Melani, A., Pantoni, L., Corsi, C., Bianchi, L., Monopoli, A., Bertorelli, R., Pepeu, G., and Pedata, F. (1999) Striatal outflow of adenosine, excitatory amino acids, gamma-aminobutyric acid, and taurine in awake freely moving rats after middle

- cerebral artery occlusion: correlations with neurological deficit and histopathological damage, *Stroke* 30, 2448-2454; discussion 2455.
73. Xu, J. S., Granger, M. C., Chen, Q. Y., Strojek, J. W., Lister, T. E., and Swain, G. M. (1997) Boron-doped diamond thin-film electrodes, *Anal Chem* 69, A591-A597.
 74. Franklin, K. B. J., and Paxinos, G. (1997) *The mouse brain in stereotaxic coordinates*, Academic Press, San Diego.
 75. Lonroth, P., Jansson, P. A., and Smith, U. (1987) A microdialysis method allowing characterization of intercellular water space in humans, *Am J Physiol* 253, E228-231.
 76. Mathews, T. A., Fedele, D. E., Coppelli, F. M., Avila, A. M., Murphy, D. L., and Andrews, A. M. (2004) Gene dose-dependent alterations in extraneuronal serotonin but not dopamine in mice with reduced serotonin transporter expression, *J Neurosci Methods* 140, 169-181.
 77. Acworth, I., and Cunningham, M. L. (1999) The Measurement of Monoamine Neurotransmitters in Microdialysis Perfusates Using HPLC-ECD, *Methods Mol Med* 22, 219-236.
 78. Wu, Q., Reith, M. E., Wightman, R. M., Kawagoe, K. T., and Garris, P. A. (2001) Determination of release and uptake parameters from electrically evoked dopamine dynamics measured by real-time voltammetry, *J Neurosci Methods* 112, 119-133.
 79. Jones, S. R., Garris, P. A., Kilts, C. D., and Wightman, R. M. (1995) Comparison of dopamine uptake in the basolateral amygdaloid nucleus, caudate-putamen, and nucleus accumbens of the rat, *J Neurochem* 64, 2581-2589.

80. Near, J. A., Bigelow, J. C., and Wightman, R. M. (1988) Comparison of uptake of dopamine in rat striatal chopped tissue and synaptosomes, *J Pharmacol Exp Ther* 245, 921-927.
81. Conti, A. C., Lowing, J. L., Susick, L. L., and Bowen, S. E. (2012) Investigation of calcium-stimulated adenylyl cyclases 1 and 8 on toluene and ethanol neurobehavioral actions, *Neurotoxicol Teratol* 34, 481-488.
82. Smith, A. D., and Justice, J. B. (1994) The effect of inhibition of synthesis, release, metabolism and uptake on the microdialysis extraction fraction of dopamine, *J Neurosci Methods* 54, 75-82.
83. Heien, M. L., Phillips, P. E., Stuber, G. D., Seipel, A. T., and Wightman, R. M. (2003) Overoxidation of carbon-fiber microelectrodes enhances dopamine adsorption and increases sensitivity, *Analyst* 128, 1413-1419.
84. Abuse, S., and Administration, M. H. S. (2009) Results from the 2008 national survey on drug use and health: national findings, *Office of Applied Studies (NSDUH Series H-36, HHS Publication No. SMA 09-4434)*.
85. Kuhn, M., Popovic, A., and Pezawas, L. (2013) Neuroplasticity and memory formation in major depressive disorder: An imaging genetics perspective on serotonin and BDNF, *Restor Neurol Neurosci*.
86. Schulte-Herbruggen, O., Vogt, M. A., Hortnagl, H., Gass, P., and Hellweg, R. (2012) Pramipexole is active in depression tests and modulates monoaminergic transmission, but not brain levels of BDNF in mice, *Eur J Pharmacol* 677, 77-86.
87. Singh, M., Setalo, G., Jr., Guan, X., Warren, M., and Toran-Allerand, C. D. (1999) Estrogen-induced activation of mitogen-activated protein kinase in

- cerebral cortical explants: convergence of estrogen and neurotrophin signaling pathways, *J Neurosci* 19, 1179-1188.
88. Gibbs, R. B., Burke, A. M., and Johnson, D. A. (1998) Estrogen replacement attenuates effects of scopolamine and lorazepam on memory acquisition and retention, *Horm Behav* 34, 112-125.
 89. Cavus, I., and Duman, R. S. (2003) Influence of estradiol, stress, and 5-HT_{2A} agonist treatment on brain-derived neurotrophic factor expression in female rats, *Biol Psychiatry* 54, 59-69.
 90. Becker, J. B., and Hu, M. (2008) Sex differences in drug abuse, *Front Neuroendocrinol* 29, 36-47.
 91. Dluzen, D. E., and McDermott, J. L. (2008) Sex differences in dopamine- and vesicular monoamine-transporter functions, *Ann N Y Acad Sci* 1139, 140-150.
 92. Hall, J. N., and Broderick, P. M. (1991) Community networks for response to abuse outbreaks of methamphetamine and its analogs, *NIDA Res Monogr* 115, 109-120.
 93. Dluzen, D. E. (2004) The effect of gender and the neurotrophin, BDNF, upon methamphetamine-induced neurotoxicity of the nigrostriatal dopaminergic system in mice, *Neurosci Lett* 359, 135-138.
 94. Xiao, L., and Becker, J. B. (1998) Effects of estrogen agonists on amphetamine-stimulated striatal dopamine release, *Synapse* 29, 379-391.
 95. Heinzerling, K. G., and Shoptaw, S. (2012) Gender, brain-derived neurotrophic factor Val66Met, and frequency of methamphetamine use, *Gend Med* 9, 112-120.

96. Dluzen, D. E., Gao, X., Story, G. M., Anderson, L. I., Kucera, J., and Walro, J. M. (2001) Evaluation of nigrostriatal dopaminergic function in adult +/+ and +/- BDNF mutant mice, *Exp Neurol* 170, 121-128.
97. Dluzen, D. E. (1996) Effects of testosterone upon MPTP-induced neurotoxicity of the nigrostriatal dopaminergic system of C57/B1 mice, *Brain Res* 715, 113-118.
98. Dluzen, D. E., McDermott, J. L., and Liu, B. (1996) Estrogen as a neuroprotectant against MPTP-induced neurotoxicity in C57/B1 mice, *Neurotoxicol Teratol* 18, 603-606.
99. Dluzen, D. E., McDermott, J. L., and Liu, B. (1996) Estrogen alters MPTP-induced neurotoxicity in female mice: effects on striatal dopamine concentrations and release, *J Neurochem* 66, 658-666.
100. Wilson, J. M., Kalasinsky, K. S., Levey, A. I., Bergeron, C., Reiber, G., Anthony, R. M., Schmunk, G. A., Shannak, K., Haycock, J. W., and Kish, S. J. (1996) Striatal dopamine nerve terminal markers in human, chronic methamphetamine users, *Nat Med* 2, 699-703.
101. Hotchkiss, A. J., and Gibb, J. W. (1980) Long-term effects of multiple doses of methamphetamine on tryptophan hydroxylase and tyrosine hydroxylase activity in rat brain, *J Pharmacol Exp Ther* 214, 257-262.
102. Hotchkiss, A. J., Morgan, M. E., and Gibb, J. W. (1979) The long-term effects of multiple doses of methamphetamine on neostriatal tryptophan hydroxylase, tyrosine hydroxylase, choline acetyltransferase and glutamate decarboxylase activities, *Life Sci* 25, 1373-1378.

103. Woolverton, W. L., Ricaurte, G. A., Forno, L. S., and Seiden, L. S. (1989) Long-term effects of chronic methamphetamine administration in rhesus monkeys, *Brain Res* 486, 73-78.
104. Riddle, E. L., Fleckenstein, A. E., and Hanson, G. R. (2006) Mechanisms of methamphetamine-induced dopaminergic neurotoxicity, *Aaps J* 8, E413-418.
105. Carvalho, M., Carmo, H., Costa, V. M., Capela, J. P., Pontes, H., Remiao, F., Carvalho, F., and Bastos Mde, L. (2012) Toxicity of amphetamines: an update, *Arch Toxicol* 86, 1167-1231.
106. Jones, S. R., Gainetdinov, R. R., Wightman, R. M., and Caron, M. G. (1998) Mechanisms of amphetamine action revealed in mice lacking the dopamine transporter, *J Neurosci* 18, 1979-1986.
107. Segal, D. S., and Kuczenski, R. (1987) Individual differences in responsiveness to single and repeated amphetamine administration: behavioral characteristics and neurochemical correlates, *J Pharmacol Exp Ther* 242, 917-926.
108. Gentry, W. B., Ghafoor, A. U., Wessinger, W. D., Laurenzana, E. M., Hendrickson, H. P., and Owens, S. M. (2004) (+)-Methamphetamine-induced spontaneous behavior in rats depends on route of (+)METH administration, *Pharmacol Biochem Behav* 79, 751-760.
109. Becker, J. B., Perry, A. N., and Westebroek, C. (2012) Sex differences in the neural mechanisms mediating addiction: a new synthesis and hypothesis, *Biol Sex Differ* 3, 14.
110. Schumacher, J., Jamra, R. A., Becker, T., Ohlraun, S., Klopp, N., Binder, E. B., Schulze, T. G., Deschner, M., Schmal, C., Hofels, S., Zobel, A., Illig, T.,

- Propping, P., Holsboer, F., Rietschel, M., Nothen, M. M., and Cichon, S. (2005) Evidence for a relationship between genetic variants at the brain-derived neurotrophic factor (BDNF) locus and major depression, *Biol Psychiatry* 58, 307-314.
111. Becker, J. B. (1999) Gender differences in dopaminergic function in striatum and nucleus accumbens, *Pharmacol Biochem Behav* 64, 803-812.
112. Walker, Q. D., Ray, R., and Kuhn, C. M. (2006) Sex differences in neurochemical effects of dopaminergic drugs in rat striatum, *Neuropsychopharmacology* 31, 1193-1202.
113. Walker, Q. D., Rooney, M. B., Wightman, R. M., and Kuhn, C. M. (2000) Dopamine release and uptake are greater in female than male rat striatum as measured by fast cyclic voltammetry, *Neuroscience* 95, 1061-1070.
114. Yu, L., and Liao, P. C. (2000) Sexual differences and estrous cycle in methamphetamine-induced dopamine and serotonin depletions in the striatum of mice, *J Neural Transm* 107, 419-427.
115. Maina, F. K., Khalid, M., Apawu, A. K., and Mathews, T. A. (2012) Presynaptic dopamine dynamics in striatal brain slices with fast-scan cyclic voltammetry, *J Vis Exp*.
116. Khalid, M., Aoun, R. A., and Mathews, T. A. (2011) Altered striatal dopamine release following a sub-acute exposure to manganese, *J Neurosci Methods* 202, 182-191.
117. Beninger, R. J. (1983) The role of dopamine in locomotor activity and learning, *Brain Res* 287, 173-196.

118. Finch, C. E., and Roth, G. S. (1999) Biochemistry of Aging, in *Basic Neurochemistry: Molecular, Cellular, and Medical Aspects* (Siegel, G. J., Agranoff, Bernard W., Albers, R. Wayne, Fisher, Stephen K., and Uhler, Michael D., Ed.) 6 ed., pp 613-633, Lippincott-Raven, Philadelphia.
119. Thiessen, B., Rajput, A. H., Laverty, W., and Desai, H. (1990) Age, environments, and the number of substantia nigra neurons, *Adv Neurol* 53, 201-206.
120. Adolfsson, R., Gottfries, C. G., Roos, B. E., and Winblad, B. (1979) Post-mortem distribution of dopamine and homovanillic acid in human brain, variations related to age, and a review of the literature, *J Neural Transm* 45, 81-105.
121. Volkow, N. D., Fowler, J. S., Ding, Y. S., Wang, G. J., and Gatley, S. J. (1998) Positron emission tomography radioligands for dopamine transporters and studies in human and nonhuman primates, *Adv Pharmacol* 42, 211-214.
122. Han, Z., Kuyatt, B. L., Kochman, K. A., DeSouza, E. B., and Roth, G. S. (1989) Effect of aging on concentrations of D2-receptor-containing neurons in the rat striatum, *Brain Res* 498, 299-307.
123. Saylor, A. J., Meredith, G. E., Vercillo, M. S., Zahm, D. S., and McGinty, J. F. (2006) BDNF heterozygous mice demonstrate age-related changes in striatal and nigral gene expression, *Exp Neurol* 199, 362-372.
124. Gerhardt, G. A., Cass, W. A., Yi, A., Zhang, Z., and Gash, D. M. (2002) Changes in somatodendritic but not terminal dopamine regulation in aged rhesus monkeys, *J Neurochem* 80, 168-177.

125. Luo, Y., and Roth, G. S. (2000) The roles of dopamine oxidative stress and dopamine receptor signaling in aging and age-related neurodegeneration, *Antioxid Redox Signal* 2, 449-460.
126. Zhang, Z., Andersen, A., Smith, C., Grondin, R., Gerhardt, G., and Gash, D. (2000) Motor slowing and parkinsonian signs in aging rhesus monkeys mirror human aging, *J Gerontol A Biol Sci Med Sci* 55, B473-480.
127. Ziebell, M., Khalid, U., Klein, A. B., Aznar, S., Thomsen, G., Jensen, P., and Knudsen, G. M. (2012) Striatal dopamine transporter binding correlates with serum BDNF levels in patients with striatal dopaminergic neurodegeneration, *Neurobiol Aging* 33, 428 e421-425.
128. Zuccato, C., and Cattaneo, E. (2009) Brain-derived neurotrophic factor in neurodegenerative diseases, *Nat Rev Neurol* 5, 311-322.
129. Saura, J., Richards, J. G., and Mahy, N. (1994) Differential age-related changes of MAO-A and MAO-B in mouse brain and peripheral organs, *Neurobiol Aging* 15, 399-408.
130. Conner, J. M., Lauterborn, J. C., Yan, Q., Gall, C. M., and Varon, S. (1997) Distribution of brain-derived neurotrophic factor (BDNF) protein and mRNA in the normal adult rat CNS: evidence for anterograde axonal transport, *J Neurosci* 17, 2295-2313.
131. Katoh-Semba, R., Semba, R., Takeuchi, I. K., and Kato, K. (1998) Age-related changes in levels of brain-derived neurotrophic factor in selected brain regions of rats, normal mice and senescence-accelerated mice: a comparison to those of nerve growth factor and neurotrophin-3, *Neurosci Res* 31, 227-234.

132. Bosse, K. E., and Mathews, T. A. (2011) Ethanol-induced increases in extracellular dopamine are blunted in brain-derived neurotrophic factor heterozygous mice, *Neurosci Lett* 489, 172-176.
133. He, M., and Shippenberg, T. S. (2000) Strain differences in basal and cocaine-evoked dopamine dynamics in mouse striatum, *J Pharmacol Exp Ther* 293, 121-127.
134. Jones, S. R., Gainetdinov, R. R., Jaber, M., Giros, B., Wightman, R. M., and Caron, M. G. (1998) Profound neuronal plasticity in response to inactivation of the dopamine transporter, *Proc Natl Acad Sci U S A* 95, 4029-4034.
135. Fleckenstein, A. E., Volz, T. J., and Hanson, G. R. (2009) Psychostimulant-induced alterations in vesicular monoamine transporter-2 function: neurotoxic and therapeutic implications, *Neuropharmacology* 56 Suppl 1, 133-138.
136. Rabinovic, A. D., Lewis, D. A., and Hastings, T. G. (2000) Role of oxidative changes in the degeneration of dopamine terminals after injection of neurotoxic levels of dopamine, *Neuroscience* 101, 67-76.
137. Smith, A. D., Castro, S. L., and Zigmond, M. J. (2002) Stress-induced Parkinson's disease: a working hypothesis, *Physiol Behav* 77, 527-531.
138. Baker, S. A., Stanford, L. E., Brown, R. E., and Hagg, T. (2005) Maturation but not survival of dopaminergic nigrostriatal neurons is affected in developing and aging BDNF-deficient mice, *Brain Res* 1039, 177-188.
139. Zhang, L., Doyon, W. M., Clark, J. J., Phillips, P. E., and Dani, J. A. (2009) Controls of tonic and phasic dopamine transmission in the dorsal and ventral striatum, *Mol Pharmacol* 76, 396-404.

140. Saylor, A. J., and McGinty, J. F. (2008) Amphetamine-induced locomotion and gene expression are altered in BDNF heterozygous mice, *Genes Brain Behav* 7, 906-914.
141. Erickson, J. T., Conover, J. C., Borday, V., Champagnat, J., Barbacid, M., Yancopoulos, G., and Katz, D. M. (1996) Mice lacking brain-derived neurotrophic factor exhibit visceral sensory neuron losses distinct from mice lacking NT4 and display a severe developmental deficit in control of breathing, *J Neurosci* 16, 5361-5371.
142. Song, P., Mabrouk, O. S., Hershey, N. D., and Kennedy, R. T. (2012) In vivo neurochemical monitoring using benzoyl chloride derivatization and liquid chromatography-mass spectrometry, *Anal Chem* 84, 412-419.
143. Soblosky, J. S., Colgin, L. L., Parrish, C. M., Davidson, J. F., and Carey, M. E. (1998) Procedure for the sample preparation and handling for the determination of amino acids, monoamines and metabolites from microdissected brain regions of the rat, *J Chromatogr B Biomed Sci Appl* 712, 31-41.
144. Gamache, P., Ryan, E., Svendsen, C., Murayama, K., and Acworth, I. N. (1993) Simultaneous measurement of monoamines, metabolites and amino acids in brain tissue and microdialysis perfusates, *J Chromatogr* 614, 213-220.
145. Clarke, G., O'Mahony, S., Malone, G., and Dinan, T. G. (2007) An isocratic high performance liquid chromatography method for the determination of GABA and glutamate in discrete regions of the rodent brain, *J Neurosci Methods* 160, 223-230.

146. Shah, A. J., de Biasi, V., Taylor, S. G., Roberts, C., Hemmati, P., Munton, R., West, A., Routledge, C., and Camilleri, P. (1999) Development of a protocol for the automated analysis of amino acids in brain tissue samples and microdialysates, *J Chromatogr B Biomed Sci Appl* 735, 133-140.
147. Shah, A. J., Crespi, F., and Heidbreder, C. (2002) Amino acid neurotransmitters: separation approaches and diagnostic value, *J Chromatogr B Analyt Technol Biomed Life Sci* 781, 151-163.
148. Rowley, H. L., Martin, K. F., and Marsden, C. A. (1995) Determination of in vivo amino acid neurotransmitters by high-performance liquid chromatography with o-phthalaldehyde-sulphite derivatisation, *J Neurosci Methods* 57, 93-99.
149. Monge-Acuna, A. A., and Fornaguera-Trias, J. (2009) A high performance liquid chromatography method with electrochemical detection of gamma-aminobutyric acid, glutamate and glutamine in rat brain homogenates, *J Neurosci Methods* 183, 176-181.
150. Halpern, J. M., Xie, S., Schreiber, J. L., Martin, H. B. (2007) Kinetic and Adsorption Studies of Biogenic Amine Neurotransmitters at Polycrystalline Diamond Microelectrodes, *ESC Transactions* 3, 47-57.
151. Suzuki, A., Ivandini, T. A., Yoshimi, K., Fujishima, A., Oyama, G., Nakazato, T., Hattori, N., Kitazawa, S., and Einaga, Y. (2007) Fabrication, characterization, and application of boron-doped diamond microelectrodes for in vivo dopamine detection, *Anal Chem* 79, 8608-8615.

152. Patel, B. A., Galligan, J. J., Swain, G. M., and Bian, X. (2008) Electrochemical monitoring of nitric oxide released by myenteric neurons of the guinea pig ileum, *Neurogastroenterol Motil* 20, 1243-1250.
153. Fierro, S., Yoshikawa, M., Nagano, O., Yoshimi, K., Saya, H., and Einaga, Y. (2012) In vivo assessment of cancerous tumors using boron doped diamond microelectrode, *Sci Rep* 2, 901.
154. Farrar, A. M., Pereira, M., Velasco, F., Hockemeyer, J., Muller, C. E., and Salamone, J. D. (2007) Adenosine A(2A) receptor antagonism reverses the effects of dopamine receptor antagonism on instrumental output and effort-related choice in the rat: implications for studies of psychomotor slowing, *Psychopharmacology (Berl)* 191, 579-586.
155. Farrar, A. M., Segovia, K. N., Randall, P. A., Nunes, E. J., Collins, L. E., Stopper, C. M., Port, R. G., Hockemeyer, J., Muller, C. E., Correa, M., and Salamone, J. D. (2010) Nucleus accumbens and effort-related functions: behavioral and neural markers of the interactions between adenosine A2A and dopamine D2 receptors, *Neuroscience* 166, 1056-1067.
156. Salamone, J. D., Ishiwari, K., Betz, A. J., Farrar, A. M., Mingote, S. M., Font, L., Hockemeyer, J., Muller, C. E., and Correa, M. (2008) Dopamine/adenosine interactions related to locomotion and tremor in animal models: possible relevance to parkinsonism, *Parkinsonism Relat Disord* 14 Suppl 2, S130-134.
157. Boison, D., Singer, P., Shen, H. Y., Feldon, J., and Yee, B. K. (2012) Adenosine hypothesis of schizophrenia--opportunities for pharmacotherapy, *Neuropharmacology* 62, 1527-1543.

158. Cannazza, G., Carrozzo, M. M., Cazzato, A. S., Bretis, I. M., Troisi, L., Parenti, C., Braghiroli, D., Guiducci, S., and Zoli, M. (2012) Simultaneous measurement of adenosine, dopamine, acetylcholine and 5-hydroxytryptamine in cerebral mice microdialysis samples by LC-ESI-MS/MS, *J Pharm Biomed Anal* 71, 183-186.
159. Cvacka, J., Quaiserova, V., Park, J., Show, Y., Muck, A., Jr., and Swain, G. M. (2003) Boron-doped diamond microelectrodes for use in capillary electrophoresis with electrochemical detection, *Anal Chem* 75, 2678-2687.
160. Akula, K. K., Kaur, M., Bishnoi, M., and Kulkarni, S. K. (2008) Development and validation of an RP-HPLC method for the estimation of adenosine and related purines in brain tissues of rats, *J Sep Sci* 31, 3139-3147.
161. Ballarin, M., Herrera-Marschitz, M., Casas, M., and Ungerstedt, U. (1987) Striatal adenosine levels measured 'in vivo' by microdialysis in rats with unilateral dopamine denervation, *Neurosci Lett* 83, 338-344.
162. Chen, L., Cagniard, B., Mathews, T., Jones, S., Koh, H. C., Ding, Y., Carvey, P. M., Ling, Z., Kang, U. J., and Zhuang, X. (2005) Age-dependent motor deficits and dopaminergic dysfunction in DJ-1 null mice, *J Biol Chem* 280, 21418-21426.
163. Dluzen, D. E., McDermott, J. L., and Anderson, L. I. (2001) Tamoxifen diminishes methamphetamine-induced striatal dopamine depletion in intact female and male mice, *J Neuroendocrinol* 13, 618-624.
164. Buczynski, M. W., and Parsons, L. H. (2010) Quantification of brain endocannabinoid levels: methods, interpretations and pitfalls, *Br J Pharmacol* 160, 423-442.

165. Ho, M. C., Cherng, C. G., Tsai, Y. P., Chiang, C. Y., Chuang, J. Y., Kao, S. F., and Yu, L. (2009) Chronic treatment with monoamine oxidase-B inhibitors decreases cocaine reward in mice, *Psychopharmacology (Berl)* 205, 141-149.
166. Anderzhanova, E. A., Bachli, H., Buneeva, O. A., Narkevich, V. B., Medvedev, A. E., Thoeringer, C. K., Wotjak, C. T., and Kudrin, V. S. (2013) Strain differences in profiles of dopaminergic neurotransmission in the prefrontal cortex of the BALB/C vs. C57Bl/6 mice: Consequences of stress and afobazole, *Eur J Pharmacol* 708, 95-104.
167. Li, X., Patel, J. C., Wang, J., Avshalumov, M. V., Nicholson, C., Buxbaum, J. D., Elder, G. A., Rice, M. E., and Yue, Z. (2010) Enhanced striatal dopamine transmission and motor performance with LRRK2 overexpression in mice is eliminated by familial Parkinson's disease mutation G2019S, *J Neurosci* 30, 1788-1797.
168. McDermott, J. L., Liu, B., and Dluzen, D. E. (1994) Sex differences and effects of estrogen on dopamine and DOPAC release from the striatum of male and female CD-1 mice, *Exp Neurol* 125, 306-311.
169. Lowry, O. H., Rosebrough, N. J., Farr, A. L., and Randall, R. J. (1951) Protein measurement with the Folin phenol reagent, *J Biol Chem* 193, 265-275.
170. Ghitza, U. E., Zhai, H., Wu, P., Airavaara, M., Shaham, Y., and Lu, L. (2010) Role of BDNF and GDNF in drug reward and relapse: a review, *Neurosci Biobehav Rev* 35, 157-171.
171. Ferrer, I., Goutan, E., Marin, C., Rey, M. J., and Ribalta, T. (2000) Brain-derived neurotrophic factor in Huntington disease, *Brain Res* 866, 257-261.

172. Corominas-Roso, M., Ramos-Quiroga, J. A., Ribases, M., Sanchez-Mora, C., Palomar, G., Valero, S., Bosch, R., and Casas, M. (2013) Decreased serum levels of brain-derived neurotrophic factor in adults with attention-deficit hyperactivity disorder, *Int J Neuropsychopharmacol*, 1-9.
173. Sohrabji, F., and Lewis, D. K. (2006) Estrogen-BDNF interactions: implications for neurodegenerative diseases, *Front Neuroendocrinol* 27, 404-414.
174. Ferre, S., Fredholm, B. B., Morelli, M., Popoli, P., and Fuxe, K. (1997) Adenosine-dopamine receptor-receptor interactions as an integrative mechanism in the basal ganglia, *Trends Neurosci* 20, 482-487.
175. Svenningsson, P., Le Moine, C., Fisone, G., and Fredholm, B. B. (1999) Distribution, biochemistry and function of striatal adenosine A2A receptors, *Prog Neurobiol* 59, 355-396.
176. Mickley, K. R., and Dluzen, D. E. (2004) Dose-response effects of estrogen and tamoxifen upon methamphetamine-induced behavioral responses and neurotoxicity of the nigrostriatal dopaminergic system in female mice, *Neuroendocrinology* 79, 305-316.

ABSTRACT**INVESTIGATION OF DOPAMINE DYNAMICS IN BDNF^{+/-} MICE USING *IN VIVO*
MICRODIALYSIS
AND
ELECTROCHEMICAL ANALYSIS OF PURINE AND MONOAMINE MOLECULES
USING A BORON-DOPED DIAMOND ELECTRODE**

by

JOHNNA ANN BIRBECK

August 2013

Advisor: Tiffany A. Mathews**Major:** Chemistry (Analytical)**Degree:** Doctor of Philosophy

The goal of the first study was to determine if a reduction in brain-derived neurotrophic factor (BDNF) levels in female mice lead to a dysregulation in their dopaminergic system. Through a series of *in vivo* microdialysis and slice voltammetry experiments, we have discerned that female BDNF^{+/-} mice are hyperdopaminergic similar to their male BDNF^{+/-} counterparts. The *in vivo* microdialysis method zero-net flux highlighted that female BDNF^{+/-} mice had increased extracellular dopamine (DA) levels, while stimulated regional release by high potassium potentiated DA release from vesicular mediated depolarization. Using the complementary technique of fast scan cyclic voltammetry, electrical stimulation evoked greater release in the female BDNF^{+/-} mice, while uptake was not different from female wildtype mice. When the psychostimulant methamphetamine was administered, female BDNF^{+/-} mice had potentiated DA release compared to their wildtype counterparts. Taken together, the DA

release impairments in female mice appears to result in a hyperdopaminergic phenotype with no concomitant alterations in DA uptake.

The aim of the second study was to characterize how lifelong reductions in BDNF affect the striatal dopaminergic system in aged BDNF^{+/-} mice. As BDNF^{+/-} mice aged from 3 to 18 months, their striatal dopamine dynamics, as measured by microdialysis and slice voltammetry, 'normalized' with respect to time. Aged BDNF^{+/-} mice (18 months) had elevated levels of striatal DA metabolites and decreased phasic versus tonic release of DA with time. DA levels in BDNF^{+/-} mice were age-dependent such that low BDNF levels in early adulthood, as previously reported, led to a hyperdopaminergic state while DA dynamics in the aged BDNF^{+/-} mice 'normalized' with no overt alterations in either behavior or neurochemistry.

In the third study we developed a method using a commercially available BDD working electrode for detecting neurotransmitters from two different families with large oxidation potential differences, DA and adenosine (Ado). Hydrodynamic voltammograms were constructed for DA and Ado, and the optimal potential for detection of DA and Ado was determined to be +740 mV and +1200 mV versus a palladium reference electrode, respectively. A working potential of +840 mV was chosen and the detection range achieved with the BDD electrode for DA and Ado was from low nanomolar to high millimolar levels. To determine the practical function of the BDD electrode, tissue content was analyzed for seven monoamines and two purine molecules, which were resolved in a single run in less than 28 min. Our results demonstrate that the BDD electrode is sensitive and robust enough to detect monoamine and purine molecules from frontal cortex and striatal mouse samples.

AUTOBIOGRAPHICAL STATEMENT

Education

2008-2013

Wayne State University (Detroit, Michigan)

Doctor of Philosophy (Ph.D), Chemistry (Analytical)

Dissertation: Investigation of dopamine dynamics in BDNF^{+/-} mice using in vivo microdialysis and electrochemical analysis of purines and monoamines using a boron-doped diamond electrode

2003-2008

Lake Superior State University (Sault Sainte Marie, Michigan)

Bachelor of Science (B.S.) Chemistry

Bachelor of Science (B.S.) Forensic Chemistry

Publications

Birbeck, JA, and Mathews, TA. Simultaneous detection of monoamine and purine neurotransmitters with a boron-doped diamond electrode using high performance liquid chromatography. *Accepted to Analytical Chemistry May 2013.*

Bosse, KE, **Birbeck, JA**, Newman, BE, Mathews, TA. "Analysis of Neurotransmitters and their Metabolites by Liquid Chromatography" *Handbook on Liquid Chromatography.*

Bosse, KE, Maina, FK, **Birbeck, JA**, France, MM, Roberts, JJ, Colombo, ML, Mathews, TA. Aberrant striatal dopamine transmitter dynamics in brain-derived neurotrophic factor-deficient mice, (2012) *Journal of Neurochemistry* 120(3): 385-395.

Keller, BJ, Back, RC, Westrick, J, Werner, M, Evans, B, Moerke, A, Zimmerman, G, Wright, DD, Grenfell, E, **Courneya, J**. Sediment quality at select sites in the St. Marys River Area of Concern, (2011) *Journal of Great Lakes Research* 37: 12-20.

Awards

- Herbert K. Livingston Award for Excellence in Teaching (2013)
- Presentation award Detroit Electrochemistry Society (2012)
- Esther and Stanley Kirschner General Chemistry Teaching Award (2012)
- Summer Dissertation Fellowship (2012)
- Graduate School Professional Travel Award (2012)
- Graduate Assistant Teaching Honor Citation (2009-2010)
- Outstanding Forensic Chemist Award (2008)
- Outstanding Undergraduate Poster Award - Wayne State University (2007)
- Society of Toxicology Undergraduate Toxicology Education Award (Travel; 2006)
- Alpha Chi Honors Society (2005)
- Board of Trustees Academic Excellence Scholarship (2003-2007)
- Michigan Merit Award (2003-2005)
- Michigan Competitive Scholarship (2003-2007)
- Valedictorian Scholarship (2003-2007)